UNIVERSITY OF CALIFORNIA
RIVERSIDE

Functional Domains of Neuron-to-Astrocyte Gq GPCR Communication

A Dissertation submitted in partial satisfaction
of the requirements for the degree of

Doctor of Philosophy

in

Cell, Molecular, and Developmental Biology

by

Min-Yu Sun

June 2012

Dissertation Committee:

Dr. Todd A. Fiacco, Chairperson
Dr. Scott N. Currie
Dr. Devin K. Binder

The Dissertation of Min-Yu Sun is approved:

_____

_____

_____

Committee Chairperson

University of California, Riverside

ACKNOWLEDGEMENTS

I always feel that I am the most fortunate Ph.D. student in the world because of the unique experience I have had at the University of California, Riverside. In the past six years, I was able to pursue things I have been dreaming of doing with help of many lovely people at UCR. Here I would like to express my sincere gratitude to these important ones without whom I would never have such an enjoyable period of time in my life.

Best thanks to my research advisor - Dr. Todd Fiacco - for his support and guidance on my dissertation studies. To me, Dr. Fiacco is the greatest mentor that one could imagine to have. He is always approachable and open to discuss research issues/ideas. One thing I admire the most of Dr. Fiacco is that he is very honest to the experimental results and really tries his best to make things as transparent as possible. He is always encouraging regardless of whether we got positive or negative data. When the results didn't fit our initial expectation, he can always interpret these data in a positive way and help me to figure out a new direction for my research. It is his attitude and faith toward science that has an invaluable impact on me under which I was able to gradually build up self-confidence in doing research. Moreover, I really appreciate the freedom and trust given by Dr. Fiacco, which allows me to maintain a balance between research and life so that I am able to enjoy and take science as my long-term hobby. I also cherish the opportunity to work with members in the Fiacco lab - Prakash, Alison (Xiaoqiao), Tom, Kelli, Tim, Samuel, Emmelyn, Ilona and Taylor. I would like to thank each of them for

making my life in the lab so unforgettable, and for their friendship and encouragements while I was working on my dissertation.

I am also grateful to my dissertation committee members – Dr. Scott Currie and Dr. Devin Binder, for their suggestions on my dissertation research. Dr. Currie has been providing me very helpful advices in my graduate years by being in both my oral qualifying exam and dissertation committees. I also appreciate the support from Dr. Binder on my research in the annual CGNI meeting. Moreover, I would like to thank Dr. Glenn Hatton, my first research mentor. He was such a wise person with a generous mind, and I have benefitted very much from his critical thinking. Furthermore, I really appreciate the tender care from the graduate program in Cell, Molecular, and Developmental Biology. It is the support from Dr. Peter Atkinson – the director of CMDB program, and the timely help from Ms. Kathy Redd, that allows me to complete my degree in a tough financial situation.

I would like to give special thanks to Dr. Iryna Ethell and Dr. Crystal Pontrello for including me as a participant in a collaborative project. The results of this project have been published in PNAS 2012, 109 (7) E442-E451 and the part of my results is included in Chapter 4 of this dissertation with kind permission from PNAS.

Gratefully, in my research years at UCR I was privileged to have the most wonderful dance teacher ever - Ms. Kelli King. I was very blessed to happen to take her classes at a turning point of my research career (when I needed to switch from the Hatton lab to the Fiacco lab), and from that time I have been taking her ballet and modern dance classes for nearly four years. Ms. King has a great personality and a beautiful heart. She

is very kind and considerate and also, always looks at things in a very positive way. Every time when I felt frustrated about my research results, I can always regain the strength and motivation of doing research from her classes. To me, her dance classes function as my spiritual support, especially during the time when I ran into some research difficulties. I would like to sincerely thank Ms. King, my beloved dance teacher, for her companion in the past four years, which makes me never feel lonely even though I came here alone as an international student.

Finally, and most importantly, I would like to thank my parents – Mr. Jyh-Perng Sun and Ms. Hsueh-Fen Chuang, for their endless love and support. It is their faith in me that allows me to freely pursue my academic and career objectives. I am thankful of having a dad who always respects to any of the decisions I have made in my life. Every time when I meet something challenging, his encouraging words are able to strengthen me all the way through. I also appreciate of having a mom who is my best friend and companion and is always there when I need someone to talk to. I enjoy and cherish my life of being loved in such a wonderful family and would like to attribute any of my achievements to my beloved parents.

ABSTRACT OF THE DISSERTATION

Functional Domains of Neuron-to-Astrocyte Gq GPCR Communication

by

Min-Yu Sun

Doctor of Philosophy, Graduate Program in Cell, Molecular, and Developmental Biology
University of California, Riverside, June 2012
Dr. Todd A. Fiacco, Chairperson

The physiological role of astrocytic Gq-protein coupled receptors (Gq GPCRs) has now drawn more attention in the field of neuroscience, as it is now clear that astrocytes sense neuronal signals through activation of their Gq GPCRs. Astrocytes are thus considered excitable and their role in synaptic transmission is under intense investigation. Interestingly, in basal conditions without any user-evoked stimulation, astrocytes exhibit spontaneous Gq GPCR activity driven by mechanisms that still remain mysterious. Understanding the mechanisms underlying these astrocytic Gq GPCR signaling domains in physiological conditions will certainly benefit our knowledge regarding neuron-to-astrocyte communication. Therefore, the main goal of this dissertation is to study the underlying mechanisms of astrocytic Gq GPCR signaling domains in two parts: 1) To identify the factors governing spontaneous astrocytic Gq GPCR activity, and 2) To identify the lowest threshold of neuronal action potential-

mediated synaptic transmission capable of evoking an astrocytic Gq GPCR response, and then to determine if the response occurs as a microdomain or a whole-cell event. In Chapter 2, we demonstrate that spontaneous astrocytic Gq GPCR signaling domains are driven by mechanisms unrelated to action potential-triggered neurotransmitter release, but are dependent on spontaneous miniature neurotransmitter release. It also appears that multiple types of astrocytic Gq GPCRs play essential roles in the generation of spontaneous Gq GPCR activity. In Chapter 3, our results suggest that astrocytes respond to neuronal afferent stimulation at intensities much lower than previously described. Moreover, the evoked Gq GPCR domains are qualitatively different from the spontaneous ones. Consistent with the findings from Chapter 2, the evoked events appear to involve multiple types of astrocytic Gq GPCRs. These data suggest that astrocytes respond to neuronal activity in a manner much more sensitive than previously thought.

We also explored the role of β-Arrestin2 in regulating two forms of synaptic plasticity-long-term potentiation (LTP) and long-term depression (LTD). In Chapter 4, we report normal LTP, but a markedly impaired LTD in β-Arrestin2 knockout mice, suggesting a novel role of β-Arrestin2 in cellular mechanisms of learning and memory. This finding could potentially provide a base for developing treatments for dementia-related disorders such as Alzheimer's disease.

Table of Contents

Chapter 1: Introduction.....1

1.1 Glia: From passive glue to active members of the central nervous system (CNS).....1

1.2 The anatomical organization and physiological properties of protoplasmic astrocytes 2

1.3 Main functions of astrocytes in the CNS.....4

1.4 Neuron-to-astrocyte communication.....8

1.4.1 Astrocytes express numerous neurotransmitter receptors.....8

1.4.2 Mechanisms of Gq GPCR-linked Ca^{2+} elevations in astrocytes.....10

1.4.3 Astrocytes are biochemically excitable cells with Ca^{2+} responses evoked by either neuronal afferent stimulation or exogenously-applied agonists.....11

1.4.4 Astrocytes exhibit spontaneous Ca^{2+} elevations.....13

1.5 Astrocyte-to-neuron communication.....16

1.5.1 Astrocyte to neuron communication under physiological conditions.....16

1.5.2 Astrocyte to neuron communication under pathological conditions.....17

1.6 Role of astrocytic Gq GPCRs in synaptic plasticity.....19

1.7 Role of β-arrestin-2, a scaffolding molecule, in dendritic spine remodeling and synaptic plasticity.....20

1.7.1 Dendritic spine morphology is determined by F-actin dynamics.....20

1.7.2 Regulation of cofilin, an F-actin-binding protein, by NMDA receptor activation and its effects on synaptic plasticity.....22

1.7.3 Spatial distribution of cofilin by β-Arrestin2.....23

1.8 Our hypothesis.....24

1.8.1 Spontaneous astrocytic Gq GPCR microdomain activity can be driven by neuronal activity.....24

1.8.2 Astrocytes can respond to low level Schaffer Collateral (SC) stimulation with microdomain Ca^{2+} elevations.....25

1.8.3 β-Arrestin2 is involved in two forms of NMDAR-dependent synaptic plasticity: LTP and LTD.....26

1.9 References.....27

Chapter 2: Effects of action potential-driven synaptic activity and miniature neurotransmitter release on spontaneous astrocytic Gq GPCR signaling domains 45

2.1 Abstract.....45

2.2 Introduction.....47

2.3 Materials and methods.....51

2.4 Results.....55

2.4.1. Measurement of astrocytic microdomain Ca^{2+} oscillations under increasing laser power intensity.....55

2.4.2. Effects of imaging time at fixed 0.2% laser power on spontaneous astrocyte microdomains.....55

2.4.3 Global increase followed by inhibition of neuronal firing does not result in significant changes in size or frequency of spontaneous astrocytic Gq GPCR activity.....56

2.4.4 Blockade of miniature neurotransmitter release results in significant changes in frequency of spontaneous astrocytic Ca^{2+} activity.....57

2.4.5 Blockade of group I mGluRs does not result in significant changes in frequency of spontaneous astrocytic Ca^{2+} activity.....58

2.5 Discussion.....59

2.6 References.....64

Figure Legends.....67

Chapter 3: Assaying for Gq GPCR signaling domains of neuron-to-astrocyte communication using low intensity Schaffer Collateral stimulation.....82

3.1 Abstract.....82

3.2 Introduction.....84

3.3 Materials and methods.....86

3.4 Results.....91

3.4.1 Astrocytes respond to three pulse SC stimulation with either whole-cell or microdomain Ca^{2+} elevations.....91

3.4.2 Astrocytes do not respond to direct membrane depolarization with Ca^{2+} elevations.....94

3.4.3 Astrocytes respond to single pulse SC stimulation with either whole-cell or microdomain Ca^{2+} elevations.....95

3.4.4 The astrocytic Ca^{2+} elevations evoked by single pulse SC stimulation cannot be fully blocked by group I mGluR antagonists.....97

3.4.5 Determine whether microdomain astrocyte Ca^{2+} elevations can be driven by glutamate release from single identified CA3 synaptic boutons. 97

3.5 Discussion.....99

3.6 References.....104

Figure Legends.....105

Chapter 4: Exploring the role for β-Arrestin2 in NMDA receptor-dependent long-term potentiation (LTP) and long-term depression (LTD).....125

4.1 Abstract.....125

4.2 Introduction.....126

4.3 Materials and methods.....127

4.4 Results.....129

4.5 Discussion.....130

4.6 References.....132

Figure Legends.....134

Chapter 5: Discussion and Perspective.....136

5.1 The function of astrocyte Gq GPCR activity in neurophysiology.....136

5.2 Effects of miniature neurotransmitter release on spontaneous astrocytic Ca^{2+} elevations.....140

5.3 Plasticity of astrocytic Gq GPCRs.....141

5.4 References.....143

Figure Legend.....146

List of Figures

Figure 2.1 Determining Gq GPCR signaling domains in an astrocyte

Figure 2.2 Effects of increasing laser output power on spontaneous astrocytic Ca^{2+} elevations

Figure 2.3 Effects of exposure to 0.2% confocal laser light over time on astrocytic Ca^{2+} activity

Figure 2.4 Microdomain astrocyte Ca^{2+} activity under conditions of 2.5 mM K^{+} (control), 5 mM K^{+} and 5 mM K^{+}+TTX

Figure 2.5 Frequency and size distribution of spontaneous astrocytic Ca^{2+} elevations following elevated or blocked neuronal firing

Figure 2.6 Spontaneous astrocytic Ca^{2+} elevations following blockade of quantal vesicular release of neurotransmitter

Figure 2.7 Spontaneous astrocytic Ca^{2+} activity before and after block of group I mGluRs

Figure. 3.1 Astrocyte Ca^{2+}elevations following three pulse SC stimulation.

Figure 3.2 Quantitative analysis of astrocyte Ca^{2+}elevations following three pulse SC stimulation

Figure 3.3 Recording of astrocytic Ca^{2+} activity following direct cell membrane depolarization

Figure 3.4 Astrocyte Ca^{2+}elevations following single pulse SC stimulation

Figure 3.5 Quantitative analysis of astrocyte Ca^{2+}elevations following single pulse SC stimulation

Figure 3.6 Effects of group I mGluR antagonists on astrocytic Ca^{2+} responses following single pulse SC stimulation

Figure 3.7 Microdomain astrocytic Ca^{2+} elevations evoked by action potentials in single CA3 pyramidal neurons

Figure 3.8 4-AP effects on microdomain astrocytic Ca^{2+} elevations evoked by single neuronal action potentials

Figure 3.9 Potential problems associated with 4-AP to study astrocytic Ca^{2+} elevations evoked by single neuronal action potentials

Figure 4 β-Arrestin2 KO mice exhibit normal baseline synaptic function and LTP, but significantly impaired LTD compared to wild-type mice

Figure 5 Experimental design for simultaneous recording of astrocytic glutamate transporter currents and Ca^{2+} elevations following high frequency SC stimulation

Chapter 1: Introduction

1.1 Glia: From passive glue to active members of the central nervous system (CNS)

Given the fact that neurons are the only cell type in the central nervous system (CNS) capable of firing action potentials, the role of glia in CNS physiology and function has been largely neglected for nearly a century since their cell identity was confirmed in the late 1800s (Agulhon et al., 2008). Researchers had considered glia as a passive connective tissue filling in space unoccupied by neurons and thus not important in the transmission of information in the brain. This concept, however, has been revised lately since various types of G protein-coupled receptors (GPCRs) were identified in glial cells in cell culture (McCarthy and de Vellis, 1978; Van Calker et al., 1978), as well as in acute tissue slices and *in vivo* (Porter and McCarthy, 1997). As the GPCRs expressed by glial cells are similar to those expressed by neurons, it is now generally accepted that glial cells are biochemically excitable and can respond to released neurotransmitters in various forms, one of which is increased cytoplasmic Ca^{2+} concentration (Agulhon et al., 2008).

Based on morphology and function, glial cells can be divided into four major groups: 1) oligodendrocytes and Schwann cells, 2) microglia, 3) nerve/glial antigen 2 (NG-2) positive cells, and 4) astrocytes (Agulhon et al., 2008). Among these groups, astrocytes are the predominant cell type that comprises nearly one-third of the cells in the mouse brain and approximately half of the cells in the human brain (Cahoy et al., 2008).

1.2 The anatomical organization and physiological properties of protoplasmic astrocytes

Being as heterogeneous as neurons in terms of morphology, antigenic phenotype, location and function, astrocytes can be classified into at least two main categories: protoplasmic and fibrillary (or fibrous) astrocytes. Protoplasmic astrocytes distribute mainly in gray matter with their ramified processes heavily enwrapping synapses and blood vessels, whereas fibrillary astrocytes, the major type of astrocytes located in white matter, have long processes that run between myelinated fibers to contact nodes of Ranvier as well as to produce end feet for vascular attachment (Walz, 2000; Barres, 2008). However, protoplasmic and fibrillary astrocytes can both be recognized by their expression of glial fibrillary acidic protein (GFAP), an intermediate filament exclusively expressed by astrocytes in the CNS (Eng et al., 1971; Bignami et al., 1972; Bushong et al., 2002). Moreover, specialized astrocytes that exhibit similarity to protoplasmic astrocytes are also found in certain brain areas, including Müller glia in the retina and Bergmann glia in the cerebellum and radial glia in the developing cortex (Walz, 2000; Barres, 2008).

Studies over the past few years have proposed that protoplasmic astrocytes, with their unique spatial distribution and extensive interaction with neuronal elements, could be critical members that take part in synaptic transmission (Bushong et al., 2002; Agulhon et al., 2008; Barres, 2008). With the aid of three-dimensional (3D) confocal analysis and electron microscopy, Bushong et al. in 2002 indicated that protoplasmic astrocytes establish primarily exclusive territories with only a limited degree of overlap with neighboring astrocytes. This segregated anatomical organization suggests that each

protoplasmic astrocyte has its own distinct domain to interact with blood vessels or synapses, and these clusters of elements can be differentially influenced by the activity of this particular astrocyte (Bushong et al., 2002). In adult rat hippocampal CA1, a single astrocyte has a soma diameter of 7-9 μm. However, when its processes are taken into account, the astrocyte could have a volume up to nearly 66,000 μm^3 and would influence approximately 140,000 synapses (Bushong et al., 2002). In fact, discrete astrocytic "microdomains" have been revealed by Grosche et al. as small compartments on the spongiform processes of Bergmann glia that are capable of limiting the propagation of glial Ca^{2+} responses evoked by neuronal activity (Grosche et al., 1999), suggesting protoplasmic astrocytes in CA1 would have this similar organization and be able to separate the neuropil on multiple levels (Bushong et al., 2002). Interestingly, astrocyte processes have been shown preferentially surrounding the perimeter of the axon-dendritic spine interface that have more glutamate escaping from the synaptic cleft (Ventura and Harris, 1999), implying an essential role for astrocytes in synaptic transmission.

The physiological properties of protoplasmic astrocytes have been investigated. Whole cell currents were recorded from astrocytes for the first time in slices from newborn animals (Steinhauser et al., 1992). In this study, at least two forms of membrane current patterns were identified that differentiate astrocytes into "passive" and "complex" cells. Passive astrocytes have high levels of GFAP expression and display a linear current-voltage relationship while their holding membrane potential was switched from -80 mV to both hyperpolarizing and depolarizing potentials (-160 mV to +20 mV) in 10 mV increments. Complex astrocytes, on the other hand, have low or negligible GFAP

expression and exhibit both inwardly and outwardly rectifying currents following the voltage-step protocol (Steinhauser et al., 1992; Zhou et al., 2006). Similar patterns were found in adult tissue as well, suggesting this phenomenon is preserved after development (Kressin et al., 1995). However, approximately 90% of mature astrocytes in the hippocampal CA1 region are electrophysiologically passive and GFAP positive ($GFAP^+$) whereas the remaining 10% appear to have voltage-gated channels, are GFAP negative ($GFAP^-$), and are called NG2 glia due to their exclusive NG2 expression (Zhou et al., 2006). Other differences between $GFAP^+$ astrocytes and NG2 glia include gap junction coupling present solely among $GFAP^+$ astrocytes, whereas NG2 glia do not exhibit coupling. Moreover, NG2 glia have relatively high membrane resistances of more than 200 MΩ (range 200-400 MΩ) compared to the low membrane resistance of 10MΩ or less recorded in $GFAP^+$ astrocytes (Lin and Bergles, 2002; Zhou et al., 2006).

1.3 Main functions of astrocytes in the CNS

Astrocytes exhibit various functions in the CNS. One of the most well-established functions is to regulate extracellular potassium ($[K^+]_o$) homeostasis. Due to their abundant expression of K^+ channels, astrocytes have a very dominant K^+ conductance, resulting in their negative resting membrane potential being close to the K^+ equilibrium potential. Astrocytes have been shown to take up excess K^+ ions from the extracellular space via three mechanisms: The Na^+/K^+ pump (Walz and Hinks, 1985; Ballanyi et al., 1987; Rose and Ransom, 1996; Ransom et al., 2000), an anion transporter that co-transports K^+ and Na^+ with Cl^- (Walz and Hinks, 1985), and K^+ channels (Ballanyi et al., 1987). Following K^+ uptake, astrocytes transport these ions via gap junctions and release

them in locations where the extracellular K^+ concentration is low, a process known as "K^+ spatial buffering" (Kuffler and Nicholls, 1966; Orkand et al., 1966; Djukic et al., 2007). The first identified inwardly-rectifying K^+ (K_{ir}) channel expressed by astrocytes, $K_{ir}4.1$, plays a critical role in K^+ spatial buffering (Takumi et al., 1995; Poopalasundaram et al., 2000), as conditional knock-out of $K_{ir}4.1$ resulted in a marked impairment of K^+ uptake and early postnatal mortality (Djukic et al., 2007). Since the extracellular K^+ concentration critically influences cellular resting membrane potential, it can potentially influence rates of neuronal firing and neurotransmitter release (Baylor and Nicholls, 1969; Balestrino et al., 1986). Failure of removing excess K^+ ions from the extracellular space could increase the overall neuronal excitability through a positive feedback loop (Magistretti and Ransom, 2002), thereby increasing the likelihood of seizure occurrence. Indeed, $K_{ir}4.1$ has been shown to be a putative seizure susceptibility gene in mice (Ferraro et al., 2004), as well as in humans (Buono et al., 2004).

Another important function of astrocytes is their involvement in glutamate uptake and metabolism. Glutamate is the predominant excitatory neurotransmitter in the CNS (Fortnum, 1984). After being released from presynaptic terminals, glutamate is mainly taken up by astrocytes and is converted into glutamine via glutamine synthetase, an ATP-dependent enzyme exclusively expressed by astrocytes (Martinez-Hernandez et al., 1977). Glutamine is then delivered to presynaptic neurons where it is converted to glutamate and stored in vesicles to initiate a new cycle of neurotransmitter release. Being a critical part of this "glutamate-glutamine cycle", astrocytes remove excess glutamate from the extracellular space through glutamate transporters, thus preventing neuronal

excitotoxicity (Rosenberg and Aizenman, 1989). There are two types of glutamate transporters expressed by astrocytes: GLT-1 and GLAST (Rothstein et al., 1994). The essential role of astrocyte glutamate transporters in maintaining extracellular levels of glutamate was reinforced by a previous finding, where Rothstein et al. showed that genetic down-regulation of GLAST or GLT-1, but not the neuronal subtype EAAC1, caused elevated extracellular levels of glutamate and neurotoxicity (Rothstein et al., 1996).

Astrocytes also appear to express the water channel aquaporin 4 (AQP4) and play an important role in water homeostasis (Amiry-Moghaddam and Ottersen, 2003; Kimelberg, 2007). AQP4 is the predominant aquaporin in the brain, which is primarily present on the plasma membrane of astrocytes (Jung et al., 1994) but with lower expression levels in ependymal cells (Kobayashi et al., 2001; Amiry-Moghaddam et al., 2003). Its expression is absent from neurons, oligodendrocytes and microglia (Amiry-Moghaddam and Ottersen, 2003). AQP4 is particularly concentrated in astrocyte processes that are in contact with blood vessels and the pia. These astrocyte processes are part of the perivascular and subpial endfeet, with AQP4 distribution about one order of magnitude higher than in non-endfeet membranes including those near synapses (Amiry-Moghaddam and Ottersen, 2003). Immunolocalization experiments have shown a strict overlap between AQP4 and $K_{ir}4.1$ distribution, suggesting that these two molecules function together. This hypothesis was tested in acute cortical slices following evoked neuronal activity in layer IV. In this study, water flux was monitored by optical signals which were generated or diminished when the extracellular space increased or decreased,

respectively. The results demonstrated that water transport is neuronal activity-dependent, and is coupled to flux of K^+ (Niermann et al., 2001). Similarly, another study revealed impaired K^+ clearance following stimulation of Schaffer Collaterals and perforant path fibers in hippocampal slices from mice lacking perivascular AQP4. The excessive amounts of extracellular K^+ could potentially facilitate the generation of epileptiform discharges by depolarizing neurons. Indeed, these mice were shown to have more pronounced epileptic seizures induced by hyperthermia, even though the threshold to induce seizures was the same as that of wild-type mice. Taken together, these findings suggest that water flux through perivascular AQP4 is coupled to efficient K^+ removal and that deficits in water transport could enhance neuronal excitability and seizure severity (Amiry-Moghaddam et al., 2003). The correlation between AQP4 and seizure severity gives rise to essential roles played by AQP4 and astrocytes in pathological conditions, which also includes the development of brain edema. It has been shown that expression of AQP4 on the perivascular endfeet of astrocytes contributes to brain edema formation (Nielsen et al., 1997; Amiry-Moghaddam et al., 2003), and a delayed onset of hyponatremic edema was also observed in mice lacking AQP4 at the interface between brain and blood/CSF (Vajda et al., 2002).

Other critical functions of astrocytes include their contribution to CNS development. They promote synaptogenesis by releasing thrombospondin (TSP), a large matrix-associated protein. A significant reduction in synapse number was found in Thrombospondin-1/2 knockout mouse brain, suggesting the involvement of astrocytes in facilitating synapse formation *in vivo* (Christopherson et al., 2005; Barres, 2008).

1.4 Neuron-to-astrocyte communication

1.4.1 Astrocytes express numerous neurotransmitter receptors

It is now widely accepted that astrocytes are capable of responding to neuronal signaling due to their expression of numerous neurotransmitter receptor types (Bowman and Kimelberg, 1984; Kettenmann et al., 1984). To date, there are at least twelve types of neurotransmitter receptors identified in astrocytes (including protoplasmic and fibrillary astrocytes as well as Bergmann and Müller glia) : 1) glutamate receptors, 2) γ-amino-butyric-acid (GABA) receptors, 3) purinoreceptors (ATP receptors), 4) histamine receptors, 5) cholinergic receptors, 6) adrenergic receptors, 7) serotonergic receptors, 8) substance P receptors, 9) opioid receptors, 10) dopaminergic receptors, 11) atrial natriuretic factor receptors, and 12) cannabinoid receptors (CB1R) (Porter and McCarthy, 1997; Navarrete and Araque, 2008). Astrocytes exhibit both ionotropic receptors and metabotropic receptors to glutamate, GABA and ATP. However, whether passive astrocytes express ionotropic neurotransmitter receptors is not clear, and the functional importance of ionotropic receptors present in astrocytes remains largely unresolved. Due to their expression of these various types of neurotransmitter receptors, astrocytes have been shown to respond to neuronal activity with increases in intracellular Ca^{2+} concentration (Porter and McCarthy, 1996, 1997; Agulhon et al., 2008). This intracellular Ca^{2+} elevation results mainly, if not exclusively, from Gq subtype G protein coupled receptors (Gq GPCRs), and not from a Ca^{2+} influx through voltage-gated calcium channels (VGCCs) or ionotropic receptors permeable to extracellular Ca^{2+} (Duffy and MacVicar, 1994; Jabs et al., 1994; Porter and McCarthy, 1995; Carmignoto et al., 1998;

Nett et al., 2002; Parri and Crunelli, 2003; Beck et al., 2004; Straub et al., 2006; Agulhon et al., 2008).

The most abundant type of metabotropic glutamate Gq GPCR found in astrocytes is $mGluR_5$ (Romano et al., 1995; van den Pol et al., 1995). There is only very little evidence showing $mGluR_1$ expression in astrocytes *in situ* (Shigemoto et al., 1992; Baude et al., 1993; van den Pol et al., 1995; Mudo et al., 2007). Activation of $mGluR_5$ upon glutamate binding results in increased cytoplasmic Ca^{2+} concentration that can be blocked by inhibitors of store-specific Ca^{2+}-ATPases such as thapsigargin. Also, Ca^{2+} elevations were inhibited following the application of heparin, an inositol 1,4,5-trisphosphate (IP_3) receptor blocker (Kirischuk et al., 1999). These results provide strong evidence that activation of astrocyte Gq GPCRs upon binding neurotransmitters is coupled to intracellular Ca^{2+} elevations triggered by IP_3-induced Ca^{2+} release from internal stores. This mechanism is utilized by other Gq GPCRs in astrocytes including the metabotropic GABA receptors-$GABA_BRs$ (Nielsen et al., 1997; Kang et al., 1998), the P2Y receptors, which are activated upon binding to ATP (Kirischuk et al., 1995; Verkhratsky et al., 1998), the metabotropic cholinoreceptors (muscarinic receptors, mAChRs) activated by acetylcholine (Catlin et al., 2000; Shelton and McCarthy, 2000; Araque et al., 2002), the α1-adrenergic receptors (Shao and McCarthy, 1993; Kirischuk et al., 1996), the H_1 histamine receptors (Kirischuk et al., 1996), the A1 adenosine receptors (Porter and McCarthy, 1995), and the CB1Rs activated by endocannabinoids released from postsynaptic neurons upon sufficient depolarization (Navarrete and Araque, 2008).

1.4.2 Mechanisms of Gq GPCR-linked Ca^{2+} elevations in astrocytes

Given that the Gq GPCR-triggered intracellular Ca^{2+} elevation is the most well-established astrocyte response to neuronal activity, mechanisms underlying Gq GPCR activation have also been heavily investigated (Agulhon et al., 2008). It is generally thought that Gq GPCR activation is linked to phospholipase C (PLC)/IP_3 pathway (Waldo et al., 2010). Following Gq GPCR activation, PLC is activated and cleaves the membrane-bound phosphatidylinositol 4, 5-bisphosphate (PIP_2) into diacylglycerol (DAG) and IP_3. These newly-generated IP_3 molecules are mobile and bind IP_3 receptors (IP_3R) located on the membrane of endoplasmic reticulum (ER), triggering Ca^{2+} release from ER (Scemes, 2000; Parri and Crunelli, 2003; Volterra and Steinhauser, 2004; Fiacco and McCarthy, 2006; Scemes and Giaume, 2006). Moreover, functional IP_3Rs that are exclusively expressed by hippocampal astrocytes have been identified as type 2 IP_3Rs (IP_3R2), which are not found in neurons or other types of glia (Sheppard et al., 1997; Holtzclaw et al., 2002; Hertle and Yeckel, 2007; Weerth et al., 2007; Petravicz et al., 2008). Activation of IP_3R can be positively modulated by the store-released Ca^{2+}, which functions as a co-agonist on these receptors. Moreover, the store-released Ca^{2+} also enhances PLC activation and results in more IP_3 generation (Foskett et al., 2007). Both of these actions most likely contribute to Ca^{2+} propagation across a variable volume of cytoplasm–the so called “intracellular Ca^{2+} wave”. Another molecule generated from PIP_2 cleavage, DAG, has been shown to participate in the termination of the astrocytic Ca^{2+} transients via activation of its downstream molecule—protein kinase C (PKC) (Codazzi et al., 2001; Parri and Crunelli, 2003).

1.4.3 Astrocytes are biochemically excitable cells with Ca^{2+} responses evoked by either neuronal afferent stimulation or exogenously-applied agonists

There is accumulating evidence indicating that elevated neuronal activity evokes astrocytic Ca^{2+} responses in brain areas including the hippocampus, cerebellum, and retina. Electrical stimulation of neuronal afferents in hippocampal slices triggers hippocampal astrocytic Ca^{2+} elevations via activation of astrocytic mGluRs (Porter and McCarthy, 1996; Pasti et al., 1997; Fellin et al., 2004; Perea and Araque, 2005), $GABA_B$ receptors (Kang et al., 1998); muscarinic acetylcholine receptors (Araque et al., 2002; Perea and Araque, 2005), as well as endocannabinoid receptors (Navarrete and Araque, 2008). The Bergmann glial cells in the cerebellum *in situ* were also shown able to respond to electrical stimulation of parallel fibers or neurons with Ca^{2+} elevations. These responses most likely result from activation of α-adrenergic, purinergic, $mGluR_1$ and/or AMPA receptors (Kulik et al., 1999; Matyash et al., 2001; Grosche et al., 2002; Matsui and Jahr, 2004; Matsui et al., 2005; Beierlein and Regehr, 2006; Piet and Jahr, 2007). The Müller glial cells in the isolated rat retina appear to respond to light flashes (physiological stimuli) with Ca^{2+} increases mediated by glial purinergic receptor activation (Newman, 2005). The occurrence of neuronal activity-evoked astrocytic Ca^{2+} responses are further proven from the *in vivo* studies (Hirase et al., 2004; Wang et al., 2006; Dombeck et al., 2007; Gobel et al., 2007; Bekar et al., 2008; Schummers et al., 2008). By applying whisker stimulation to anesthetized adult mice, Wang et al. in 2006 were able to elicit Ca^{2+} elevations in both soma and processes of astrocytes in the barrel cortex. These astrocytic Ca^{2+} elevations were reduced in the presence of the group I mGluR antagonists

MPEP and LY367385, implying the involvement of astrocytic Gq mGluRs activated by synaptically-released glutamate (Wang et al., 2006). Another *in vivo* study also demonstrated that in the adult ferret visual cortex, astrocytes respond to visual stimuli with robust Ca^{2+} responses detected in the cell bodies (Schummers et al., 2008). Moreover, astrocytes in the somatosensory cortex of anaesthetized mice respond to foot shock with activation of α-adrenergic receptors following the release of norepinephrine from the locus coeruleus (Bekar et al., 2008). Calcium transients measured in astrocytes in the somatosensory cortex correspond to running behavior in awake adolescent mice (Dombeck et al., 2007). Taken together, both *in situ* and *in vivo* studies have indicated a neuron-to-astrocyte communication via activation of astrocytic Gq GPCRs (Agulhon et al., 2008).

Astrocytic Ca^{2+} transients can also be evoked following application of exogenous Gq GPCR agonists (Yagodin et al., 1994; Yagodin et al., 1995; Sheppard et al., 1997; Zur Nieden and Deitmer, 2006; Fiacco et al., 2007). Interestingly, agonist-evoked astrocytic Ca^{2+} transients tend to have a specific initiation site, or "Ca^{2+} hotspot", located in one of the processes. These Ca^{2+} signals then propagate to other regions of the cell as an intracellular wave. The proposed mechanism underlying the intracellular Ca^{2+} wave is thought to be Ca^{2+}-induced Ca^{2+} release via the coordinated activity of Ca^{2+} functioning as a co-agonist with IP_3, and IP_3R clustering on the ER membrane (Roth et al., 1995; Sheppard et al., 1997; Simpson and Russell, 1997; Thomas et al., 2000; Shuai and Jung, 2003; Weerth et al., 2007). Interestingly, activation of different astrocytic Gq GPCRs following exogenous Gq GPCR agonist application results in the same pattern of Ca^{2+}

initiation sites, implying that different Gq GPCRs share the same machinery that drives these intracellular Ca^{2+} waves. Moreover, individual astrocytes have their own "Ca^{2+} signature" (Yagodin et al., 1994; Fiacco et al., 2007). The functional implications for these signatures and shared patterns of signaling among various Gq GPCRs is still not fully elucidated, but it may indicate participation of multiple astrocytic Gq GPCRs in the same cellular functions. Hotspots of Gq GPCR signaling machinery in astrocytes also opens the possibility for use-dependent plasticity with higher densities of Gq GPCR expression in astrocyte microdomains neighboring more active or potentiated synapses. This would allow an astrocyte to fine tune its Gq GPCR distribution and function in correlation with local synaptic strength (Agulhon et al., 2008).

1.4.4 Astrocytes exhibit spontaneous Ca^{2+} elevations

Spontaneous astrocyte Ca^{2+} activity is readily observed under basal conditions without any user-evoked stimulation in slices from hippocampus, cortex, and thalamus (Parri et al., 2001; Aguado et al., 2002; Nett et al., 2002). This phenomenon exists not only in acute slice models, but also *in vivo* with similar magnitudes, frequencies, and patterns of activity (Hirase et al., 2004; Nimmerjahn et al., 2004; Wang et al., 2006). Spontaneous Ca^{2+} elevations are present in both astrocyte cell bodies as well as in isolated processes and vary in size. Some astrocyte Ca^{2+} transients occupy an area that spans nearly the entire cell volume, whereas others are confined to very restricted territories of fine processes. Interestingly, these local "microdomain" Ca^{2+} elevations usually appear asynchronously, suggesting their independence from one another. The mechanisms underlying the generation of these astrocytic Ca^{2+} events, however, are still

not fully elucidated. It has been shown that interfering with IP_3 binding to IP_3R using the IP_3R antagonist heparin significantly reduces astrocytic spontaneous Ca^{2+} elevations (Nett et al., 2002), providing evidence that the spontaneous Ca^{2+} elevations are mainly due to Ca^{2+} release from internal stores and have very little to do with extracellular Ca^{2+} influx. This suggestion was further confirmed from findings showing that hippocampal astrocytes in mice lacking IP_3R2 expression do not exhibit spontaneous Ca^{2+} elevations (Petravicz et al., 2008). The spontaneous astrocytic Ca^{2+} elevations also appear independent of neuronal activity, as they remain present when miniature or action potential-driven neurotransmitter release is blocked (Parri et al., 2001; Nett et al., 2002; Parri and Crunelli, 2003). These results suggest that spontaneous astrocytic Ca^{2+} elevations are driven by intrinsic mechanisms such as constitutive Gq GPCR activity, which facilitates the activation of G-proteins by exchanging guanosine diphosphate (GDP) to guanosine triphosphate (GTP) in the absence of agonist (de Ligt et al., 2000; Hermans and Challiss, 2001). Interestingly, in recombinant model cell systems, type 1a metabotropic glutamate receptors ($mGluR_{1a}$) exhibit constitutive activity proportional to the level of the receptor expression (Prezeau et al., 1996), implying that any constitutive Gq GPCR activity that is restricted to local areas could originate from local Gq GPCR clustering “hotspots”. This theory was supported by the identification of Homer, a family of proteins involved in regulating mGluR cell surface expression in neurons (Brakeman et al., 1997; Kato et al., 1998; Ciruela et al., 1999; Roche et al., 1999), as well as coupling group I mGluRs to IP_3Rs and thus being able to cooperate with IP_3 generation and Ca^{2+} release from the internal stores (Tu et al., 1998). Moreover, the physical

interaction between mGluRs and Homer was also shown in hypothalamic astrocytes (Dziedzic et al., 2003). Taken together, these findings suggest that the spontaneous microdomain astrocytic Ca^{2+} signaling domains could result from constitutive Gq GPCR activity and depend on the local levels of Gq GPCR cell surface expression. Even though they can occur in the absence of neuronal activity, previous work also showed that spontaneous whole-cell astrocytic Ca^{2+} elevations are synchronized by neuronal action potentials (Aguado et al., 2002).

What types of Gq GPCRs are involved in the generation of spontaneous astrocytic Ca^{2+} elevations? Given that group I mGluRs (particular $mGluR_5$) plays a major role in astrocytic Ca^{2+} responses evoked by elevating neuronal activity *in situ* and *in vivo* (Porter and McCarthy, 1996; Wang et al., 2006), it is logical to assume that group I mGluRs could be essential for the generation of spontaneous astrocytic Ca^{2+} elevations. This hypothesis was tested and supported based on zur Nieden and Deitmer's finding that spontaneous astrocytic Ca^{2+} transients were largely abolished in the presence of (+)-α-methyl-4-carboxyphenylglycine (MCPG), a group I and II mGluR antagonist (Zur Nieden and Deitmer, 2006). However, results from other research groups suggest that mGluRs do not play a significant role in spontaneous astrocyte Ca^{2+} events. Aguado et al. observed no significant effects of MCPG on the spontaneous astrocytic Ca^{2+} transients (Aguado et al., 2002). Approximately at the same time, Nett et al. published their work showing that application of an antagonist cocktail containing antagonists for mGluR1a (AIDA), mGluR5 (MPEP), group II/III mGluRs (CPPG) and P2YRs (PPADS and suramin), did not affect spontaneous astrocytic Ca^{2+} transients while completely blocking mGluR

agonist trans-1-amino-cyclopentane-1,3-dicarboxylic acid (tACPD) as well as ATP-evoked astrocytic Ca^{2+} responses (Nett et al., 2002). These findings together suggest that other types of astrocytic Gq GPCRs could play more essential roles in the generation of spontaneous astrocytic Ca^{2+} activity.

1.5 Astrocyte-to-neuron communication

1.5.1 Astrocyte to neuron communication under physiological conditions

Astrocytes have been shown able to release transmitters, a phenomenon suggesting that communication between astrocytes and neurons could be bidirectional (Agulhon et al., 2008; Hamilton and Attwell, 2010). Studies applying paired recordings and Ca^{2+} imaging have identified a slow inward current (SIC) in the postsynaptic neurons while the intracellular Ca^{2+}concentration of a nearby astrocyte is elevated (Parri et al., 2001; Angulo et al., 2004; Fellin et al., 2004; Perea and Araque, 2005; D'Ascenzo et al., 2007). SICs are thought to be generated by astrocyte glutamate acting on extrasynaptic NMDA receptors (Hamilton and Attwell, 2010). In fact, being in contact with multiple synapses allows single astrocytes to trigger SICs in several (~5-8) neurons, thus enhancing synchronized neuronal firing patterns. (Parri et al., 2001; Angulo et al., 2004; Fellin et al., 2004).

In addition to releasing glutamate, astrocytes have been reported to release other transmitters including ATP and D-serine. Serrano et al. in 2006 indicated that in response to repetitive stimulation of hippocampal excitatory neurons, there is a depression of transmitter release from adjacent unactivated synapses. This inhibitory effect results from

activation of presynaptic $GABA_B$ receptors by interneuron-released GABA. Moreover, $GABA_B$ receptors in the nearby astrocytes are also activated and followed by astrocyte Ca^{2+} increases, leading to release of ATP from astrocytes which is then broken down into adenosine in the extracellular space. Adenosine binds and activates A1 receptors on excitatory presynaptic terminals which inhibits presynaptic neurotransmitter release (Pascual et al., 2005; Serrano et al., 2006). Furthermore, adenosine also activates postsynaptic A1 receptors coupled to K^+ channels, resulting in neuronal hyperpolarization and reduced excitability (Newman, 2003). These processes together could be the underlying mechanisms for sleep regulation (Halassa et al., 2009).

Another transmitter that could possibly be released from astrocytes is D-serine, which is synthesized in astrocytes from L-serine by the glial enzyme serine racemase (Wolosker et al., 1999). A previous study done in cell culture has shown that activation of astrocytic GluRs upon binding exogenously-applied glutamate triggers Ca^{2+} dependent release of D-serine (Mothet et al., 2005). D-serine can then function as a co-agonist of synaptic NMDA receptors and can potentially promote the induction of long-term potentiation (LTP), as breaking down D-serine by the enzyme D-amino acid oxidase decreased postsynaptic NMDA currents and prevented LTP (Yang et al., 2003; Panatier et al., 2006).

1.5.2 Astrocyte to neuron communication under pathological conditions

The possibility that astrocytes release transmitters under pathological conditions has also been studied (Hamilton and Attwell, 2010). Large amounts of glutamate are released from cortical astrocytes in a model of epilepsy, and this phenomenon is

considered a putative cause for seizure initiation (Tian et al., 2005). However, this idea is still controversial as another study has come up with observations conflicting with the previous findings (Fellin et al., 2006). Moreover, Astrocytes were also found able to release transmitters in response to hypotonic treatments (Kimelberg et al., 1990). These transmitters are thought to be released via volume-regulated anion channels (VRACs) expressed by astrocytes. The release of excitatory transmitters such as glutamate could lead to neuronal excitotoxicity and has been suggested to promote the progress of acute pathologies where astrocytic swelling occurs rapidly, including stroke and trauma (Kimelberg et al., 1995; 2005; 2006; Mongin and Kimelberg, 2005). In addition to releasing transmitters via VRACs, it has been shown that cultured astrocytes release transmitters through multiple mechanisms such as connexin hemichannels (Stout et al., 2002; Ye et al., 2003; Kang et al., 2008), pore-forming P2X7 purinergic receptors (Duan et al., 2003; Fellin et al., 2006), and reversal of glutamate transporters (Anderson and Swanson, 2000), each of which is Ca^{2+}-independent and would likely happen under pathological conditions (Agulhon et al., 2008).

Astrocytes have also been shown able to release prostaglandin E_2 (PGE_2) in pathological conditions such as Alzheimer's disease, HIV infection and stroke. The astrocyte-released PGE_2 together with tumor necrosis factor α (TNF-α) generated from activated microglia leads to astrocytic Ca^{2+} elevations, thus enhancing astrocytic exocytotic release of glutamate (Bezzi et al., 1998; 2001). By over-activating neuronal NMDA receptors, this astrocyte-released glutamate can increase overall neuronal excitability and contribute to neuronal death (Hamilton and Attwell, 2010).

1.6 Role of astrocytic Gq GPCRs in synaptic plasticity

Given that astrocytes are able to talk to neurons by stimulating extrasynaptic NMDRs, it raises the possibility that astrocytes might be involved in two types of NMDA receptor-dependent synaptic plasticity: long-term potentiation (LTP) and long-term depression (LTD) (Malenka and Nicoll, 1999). Consistent with this hypothesis, previous work has reported a modified strength of LTP in the hippocampus from mice lacking astrocyte-specific GFAP or S100B (a calcium-binding protein) expression, suggesting an essential role of astrocytes in synaptic plasticity (McCall et al., 1996; Nishiyama et al., 2002). Furthermore, studies have indicated that in both the hypothalamus and hippocampus, astrocytes impact LTP induction through the release of D-serine (Yang et al., 2003; Panatier et al., 2006). However, it was not clear whether D-serine was released from astrocytes through a Ca^{2+}-dependent mechanism, or whether astrocytic Gq GPCRs were involved in modulating hippocampal LTP. To elucidate this issue, Henneberger et al. (2010) clamped astrocyte Ca^{2+} to prevent Gq GPCR-mediated Ca^{2+} rises in astrocytes. This manipulation abolished LTP induction, while bath-applying D-serine reversed this blockade. These results suggested that release of D-serine from astrocytes relies on intracellular astrocytic Ca^{2+} elevations, which are known to normally result from Gq GPCR activation (Henneberger et al., 2010). However, at about the same time another published study reported conflicting results. Agulhon et al. found unaltered LTP in mice lacking IP_3R2 expression, which fully prevented Gq GPCR-mediated astrocyte Ca^{2+} elevations (Agulhon et al., 2010). Due to this controversy, the involvement of astrocytic Gq GPCRs in hippocampal LTP induction is still under dispute.

1.7 Role of β-arrestin-2, a scaffolding molecule, in dendritic spine remodeling and synaptic plasticity

1.7.1 Dendritic spine morphology is determined by F-actin dynamics

Dendritic spines are small protrusions located on excitatory postsynaptic neuronal dendrites, and their morphogenesis is highly correlated to functional development of excitatory synapses (Pontrello and Ethell, 2009). Dendritic spines can be classified into three groups based on their morphology: thin, mushroom, and stubby (Lippman and Dunaevsky, 2005; Matus, 2005; Tada and Sheng, 2006), all of which originate from filopodia-like protrusions observed in both *in vitro* and in *vivo* (Dailey and Smith, 1996; Ziv and Smith, 1996; Maletic-Savatic et al., 1999; Marrs et al., 2001; Okabe et al., 2001; Trachtenberg et al., 2002; Ziv and Garner, 2004; Knott et al., 2006). In the adult brain, spines are plastic and can undergo dynamic reconstruction in response to changes in synaptic efficacy, thus being implicated in processes of learning and memory (Segal, 2005; Newpher and Ehlers, 2009). Spine head enlargement has been found under conditions of LTP (Lang et al., 2004; Matsuzaki et al., 2004), whereas spine head shrinkage or spine elimination can be induced under conditions of LTD (Zhou et al., 2004). Moreover, in developing rat barrel cortex (Lendvai et al., 2000), motor cortex (Kleim et al., 1998), and hippocampus (Geinisman et al., 2000; Leuner et al., 2003), spines were shown to undergo experience-dependent structural remodeling following application of various learning protocols. Loss of dendritic spines has been shown to have detrimental effects on brain function in several neurodegenerative diseases (Halpain et al., 2005), and their rapid remodeling can contribute to recovery from stressors such as sleep

deprivation (Chen et al., 2009), as well as from damage to neurons (Cotman and Nieto-Sampedro, 1984; Pontrello and Ethell, 2009).

Changes in spine structure and morphology are largely driven by actin filament (F-actin) dynamics (Ethell and Pasquale, 2005). Actin dynamics have been shown to control cell locomotion (Pollard et al., 2001) and axon pathfinding (Lowery and Van Vactor, 2009) in motile cells and in growth cones, respectively. When it comes to spine remodeling, F-actin turnover triggers new spine formation as well as elimination of existing spines, and is considered the underlying mechanism for morphological spine plasticity (Smart and Halpain, 2000; Kolb et al., 2008). F-action is made from assembly of globular action (G-action) monomers, and this polymerization is bidirectional with one end growing faster (the so called barbed or plus end) whereas the other end elongates more slowly (the pointed or minus end) (Pontrello and Ethell, 2009). F-action dynamics can be regulated by various actin-binding proteins including Action-Related Protein (Arp) 2/3 complex (Pantaloni et al., 2000; Amann and Pollard, 2001), cortactin (Wu and Parsons, 1993; Ammer and Weed, 2008), α-Actinin (Sjoblom et al., 2008), drebrin (Shirao et al., 1994), profilin (Carlsson et al., 1977), spinophilin (Neurabin II) and Neurabin I (Allen et al., 1997; Nakanishi et al., 1997), cofilin (Bamburg, 1999; Condeelis, 2001; Sarmiere and Bamburg, 2004), gelsolin (Yin and Stossel, 1979), and myosins (Morales and Fifkova, 1989).

1.7.2 Regulation of cofilin, an F-actin-binding protein, by NMDA receptor activation and its effects on synaptic plasticity

Among the action-binding proteins, cofilin is a member of the ADF/cofilin family of actin-depolymerizing proteins that sever filaments and generate free barbed ends (Bamburg, 1999; Condeelis, 2001; Sarmiere and Bamburg, 2004). In resting cells, low levels of cofilin activity facilitate F-actin depolymerization at the pointed ends and polymerization at the barbed ends, resulting in a slow F-actin turnover rate (Bamburg and Wiggan, 2002). Elevated cofilin activity, however, triggers fast F-actin dynamics at the leading edge of migrating cells and in neuronal growth cones (Gungabissoon and Bamburg, 2003; Gehler et al., 2004; DesMarais et al., 2005). Cofilin activity is determined by its phosphorylation status. LIM kinase (LIMK) phosphorylates cofilin at Serine 3 and inactivates it, thus inhibiting its binding to F-actin (Arber et al., 1998; Yang et al., 1998). On the other hand, cofilin is activated through its dephosphorylation by phosphatases slingshot (SSH) and chronophin (CIN) (Niwa et al., 2002; Gohla et al., 2005; Huang et al., 2006).

Regulation of cofilin activity has been reported to be critical for LTP induction due to its effects on synaptic structural plasticity. The inactive phosphomimetic cofilin^{S3D} mutant was reported to have protective effects against Aβ-induced spine loss (Chen et al., 2007; Shankar et al., 2007). Moreover, spine remodeling and new filopodia-like protrusions became dominant under the effects of constitutively-active cofilin^{S3A}, whereas overexpressing inactive cofilin^{S3D} enhanced stabilization of mature dendritic spines (Shi et al., 2009). The underlying mechanisms that regulate cofilin activity have

been proposed, one of which is NMDA receptor-mediated dephosphorylation of cofilin (Carlisle et al., 2008). Activation of NMDA receptors triggers Ca^{2+} influx, which in turn activates calcineurin and leads to upregulation of SSH activity, thereby resulting in dephosphorylation and activation of cofilin (Wang et al., 2005). In acute hippocampal slices, the induction of LTD by low-frequency stimulation is followed by activation of the NMDA receptor calcineurin pathway, which was shown to mediate spine shrinkage via regulation of cofilin activity (Zhou et al., 2004). Another previous study revealed significantly altered LTD in mice lacking cofilin expression in forebrain neurons while the level of LTP was unchanged (Rust et al., 2010). These results together suggest an essential role of cofilin in regulating synaptic plasticity under the control of its phosphorylation status (Pontrello and Ethell, 2009).

1.7.3 Spatial distribution of cofilin by β-Arrestin2

It has been reported that cofilin tends to accumulate in the "shell" area of dendritic spines with a dynamic F-actin pool, and is less abundant in the "core" area with a stable F-actin pool (Racz and Weinberg, 2006). The mechanisms underlying the spatial distribution of cofilin in dendritic spines, however, have not been fully elucidated. One group of potential candidates that might be involved in this process is β-Arrestins. In addition to their roles in controlling GPCR desensitization and internalization (Luttrell and Lefkowitz, 2002; DeWire et al., 2007; Defea, 2008), the ability of β-Arrestins to regulate F-actin dynamics via scaffolding actin-binding proteins has also been reported (Barlic et al., 2000; Bhattacharya et al., 2002; Wang and DeFea, 2006). Given that β-Arrestins were shown to mediate cofilin translocation in migrating cells (Xiao et al., 2010;

Zoudilova et al., 2010), a study done by Pontrello and colleagues investigated the ability of β-Arrestin2 to regulate cofilin translocation in correlation with NMDA-induced dendritic spine remodeling (Pontrello, 2011). For neurons lacking β-Arrestin2, there was failure of translocation of constitutively active cofilin^{S3A} into dendritic spines following activation of NMDA receptors, implying that activation of cofilin alone is not sufficient for its trafficking into dendritic spines. Moreover, mature spines appear to have a normal morphology in β-Arrestin2-deficient neurons but lose the ability to undergo remodeling in response to NMDA treatment or over-expression of constitutively active cofilin^{S3A}. This phenomenon was rescued when β-Arrestin2 was overexpressed in these neurons, suggesting that β-Arrestin2 is involved in cofilin-mediated spine remodeling and is required for regulating spatial distribution of active cofilin following NMDA receptor activation (Pontrello, 2011).

1.8 Our hypothesis

1.8.1 Spontaneous astrocytic Gq GPCR microdomain activity can be driven by neuronal activity

Spontaneous astrocytic Ca^{2+} activity is a phenomenon that has been observed in cell culture (Fatatis and Russell, 1992; Charles, 1994; Harris-White et al., 1998), *in situ* (Parri et al., 2001; Aguado et al., 2002; Nett et al., 2002) and *in vivo* (Hirase et al., 2004; Nimmerjahn et al., 2004; Wang et al., 2006). However, the mechanisms underlying these events as well as their physiological implications have remained a mystery. As Ca^{2+} events in the astrocyte cell bodies persist when action potentials and miniature vascular

release of neurotransmitters were blocked by TTX and bafilomycin, respectively (Parri et al., 2001; Aguado et al., 2002; Nett et al., 2002; Parri and Crunelli, 2003), it has been suggested that spontaneous astrocytic Ca^{2+} transients occur independent of neuronal activity. Another study, however, observed increased frequency of astrocytic microdomain Ca^{2+} elevations following application of mGluR agonists at low concentrations (Zur Nieden and Deitmer, 2006), giving rise to the possibility that local glutamate spillover from neuronal synaptic transmission is what triggers astrocytic microdomain Ca^{2+} activity. A primary goal of my dissertation research is to clarify the mechanisms controlling spontaneous microdomain astrocytic Gq GPCR activity, which is the subject of Chapter 2.

1.8.2 Astrocytes can respond to low level Schaffer Collateral (SC) stimulation with microdomain Ca^{2+} elevations

It is very well established that high-frequency stimulation of neuronal afferents results in activation of astrocytic Gq GPCRs with somatic Ca^{2+} elevations in hippocampal slices (Porter and McCarthy, 1996; Pasti et al., 1997; Kang et al., 1998; Araque et al., 2002; Fellin et al., 2004; Perea and Araque, 2005; Navarrete and Araque, 2008). Moreover, astrocytes *in vivo* also respond with Ca^{2+} elevations in the soma and/or processes to whisker stimulation (Wang et al., 2006), visual stimuli (Schummers et al., 2008), robust foot stimulation (Bekar et al., 2008), and running behavior (Dombeck et al., 2007). However, the possibility that astrocytes respond to low intensity stimulation with microdomain Ca^{2+} elevations still remains undetermined. The subject of Chapter 3 of this dissertation is to provide evidence that identifies how astrocytes respond to low levels of

excitatory afferent stimulation in the hippocampus including the threshold of neuronal activity necessary for evoking astrocytic Ca^{2+} elevations as well as the astrocytic Gq GPCR response characteristics and receptors involved.

1.8.3 β-Arrestin2 is involved in two forms of NMDAR-dependent synaptic plasticity: LTP and LTD

Previous studies suggested that cofilin activity is determined by its phosphorylation status and is upregulated by NMDA receptor activation (Wang et al., 2005; Pontrello and Ethell, 2009). Moreover, translocation of cofilin to dendritic spines is required for functional spine turnover and synaptic plasticity, and is thought to be controlled by β-Arrestin2 (Zoudilova et al., 2010). The correlation between β-Arrestin2 and NMDA receptor-mediated spine structural plasticity was supported based on findings showing impaired spine remodeling upon exposure to NMDA (Pontrello, 2011). Due to the involvement of β-Arrestin2 in NMDA receptor-mediated spine structural plasticity, it is likely that β-Arrestin2 impacts the strength of LTP and LTD, two forms of synaptic plasticity that are NMDA receptor-dependent. This is the subject of Chapter 4 of this dissertation.

1.9 References

Aguado F, Espinosa-Parrilla JF, Carmona MA, Soriano E (2002) Neuronal activity regulates correlated network properties of spontaneous calcium transients in astrocytes in situ. J Neurosci 22:9430-9444.

Agulhon C, Fiacco TA, McCarthy KD (2010) Hippocampal short- and long-term plasticity are not modulated by astrocyte Ca2+ signaling. Science 327:1250-1254.

Agulhon C, Petravicz J, McMullen AB, Sweger EJ, Minton SK, Taves SR, Casper KB, Fiacco TA, McCarthy KD (2008) What is the role of astrocyte calcium in neurophysiology? Neuron 59:932-946.

Allen PB, Ouimet CC, Greengard P (1997) Spinophilin, a novel protein phosphatase 1 binding protein localized to dendritic spines. Proc Natl Acad Sci U S A 94:9956-9961.

Amann KJ, Pollard TD (2001) The Arp2/3 complex nucleates actin filament branches from the sides of pre-existing filaments. Nat Cell Biol 3:306-310.

Amiry-Moghaddam M, Ottersen OP (2003) The molecular basis of water transport in the brain. Nat Rev Neurosci 4:991-1001.

Amiry-Moghaddam M, Otsuka T, Hurn PD, Traystman RJ, Haug FM, Froehner SC, Adams ME, Neely JD, Agre P, Ottersen OP, Bhardwaj A (2003) An alpha-syntrophin-dependent pool of AQP4 in astroglial end-feet confers bidirectional water flow between blood and brain. Proc Natl Acad Sci U S A 100:2106-2111.

Ammer AG, Weed SA (2008) Cortactin branches out: roles in regulating protrusive actin dynamics. Cell Motil Cytoskeleton 65:687-707.

Anderson CM, Swanson RA (2000) Astrocyte glutamate transport: review of properties, regulation, and physiological functions. Glia 32:1-14.

Angulo MC, Kozlov AS, Charpak S, Audinat E (2004) Glutamate released from glial cells synchronizes neuronal activity in the hippocampus. J Neurosci 24:6920-6927.

Araque A, Martin ED, Perea G, Arellano JI, Buno W (2002) Synaptically released acetylcholine evokes Ca^{2+} elevations in astrocytes in hippocampal slices. J Neurosci 22:2443-2450.

Arber S, Barbayannis FA, Hanser H, Schneider C, Stanyon CA, Bernard O, Caroni P (1998) Regulation of actin dynamics through phosphorylation of cofilin by LIM-kinase. Nature 393:805-809.

Balestrino M, Aitken PG, Somjen GG (1986) The effects of moderate changes of extracellular K^+ and Ca^{2+} on synaptic and neural function in the CA1 region of the hippocampal slice. Brain Res 377:229-239.

Ballanyi K, Grafe P, ten Bruggencate G (1987) Ion activities and potassium uptake mechanisms of glial cells in guinea-pig olfactory cortex slices. J Physiol 382:159-174.

Bamburg JR (1999) Proteins of the ADF/cofilin family: essential regulators of actin dynamics. Annu Rev Cell Dev Biol 15:185-230.

Bamburg JR, Wiggan OP (2002) ADF/cofilin and actin dynamics in disease. Trends Cell Biol 12:598-605.

Barlic J, Andrews JD, Kelvin AA, Bosinger SE, DeVries ME, Xu L, Dobransky T, Feldman RD, Ferguson SS, Kelvin DJ (2000) Regulation of tyrosine kinase activation and granule release through beta-arrestin by CXCRI. Nat Immunol 1:227-233.

Barres BA (2008) The mystery and magic of glia: a perspective on their roles in health and disease. Neuron 60:430-440.

Baude A, Nusser Z, Roberts JD, Mulvihill E, McIlhinney RA, Somogyi P (1993) The metabotropic glutamate receptor (mGluR1 alpha) is concentrated at perisynaptic membrane of neuronal subpopulations as detected by immunogold reaction. Neuron 11:771-787.

Baylor DA, Nicholls JG (1969) Changes in extracellular potassium concentration produced by neuronal activity in the central nervous system of the leech. J Physiol 203:555-569.

Beck A, Nieden RZ, Schneider HP, Deitmer JW (2004) Calcium release from intracellular stores in rodent astrocytes and neurons in situ. Cell Calcium 35:47-58.

Beierlein M, Regehr WG (2006) Brief bursts of parallel fiber activity trigger calcium signals in bergmann glia. J Neurosci 26:6958-6967.

Bekar LK, He W, Nedergaard M (2008) Locus coeruleus alpha-adrenergic-mediated activation of cortical astrocytes in vivo. Cereb Cortex 18:2789-2795.

Bezzi P, Carmignoto G, Pasti L, Vesce S, Rossi D, Rizzini BL, Pozzan T, Volterra A (1998) Prostaglandins stimulate calcium-dependent glutamate release in astrocytes. Nature 391:281-285.

Bezzi P, Domercq M, Brambilla L, Galli R, Schols D, De Clercq E, Vescovi A, Bagetta G, Kollias G, Meldolesi J, Volterra A (2001) CXCR4-activated astrocyte glutamate release via TNFalpha: amplification by microglia triggers neurotoxicity. Nat Neurosci 4:702-710.

Bhattacharya M, Anborgh PH, Babwah AV, Dale LB, Dobransky T, Benovic JL, Feldman RD, Verdi JM, Rylett RJ, Ferguson SS (2002) Beta-arrestins regulate a Ral-GDS Ral effector pathway that mediates cytoskeletal reorganization. Nat Cell Biol 4:547-555.

Bignami A, Eng LF, Dahl D, Uyeda CT (1972) Localization of the glial fibrillary acidic protein in astrocytes by immunofluorescence. Brain Res 43:429-435.

Bowman CL, Kimelberg HK (1984) Excitatory amino acids directly depolarize rat brain astrocytes in primary culture. Nature 311:656-659.

Brakeman PR, Lanahan AA, O'Brien R, Roche K, Barnes CA, Huganir RL, Worley PF (1997) Homer: a protein that selectively binds metabotropic glutamate receptors. Nature 386:284-288.

Buono RJ, Lohoff FW, Sander T, Sperling MR, O'Connor MJ, Dlugos DJ, Ryan SG, Golden GT, Zhao H, Scattergood TM, Berrettini WH, Ferraro TN (2004) Association between variation in the human KCNJ10 potassium ion channel gene and seizure susceptibility. Epilepsy Res 58:175-183.

Bushong EA, Martone ME, Jones YZ, Ellisman MH (2002) Protoplasmic astrocytes in CA1 stratum radiatum occupy separate anatomical domains. J Neurosci 22:183-192.

Cahoy JD, Emery B, Kaushal A, Foo LC, Zamanian JL, Christopherson KS, Xing Y, Lubischer JL, Krieg PA, Krupenko SA, Thompson WJ, Barres BA (2008) A transcriptome database for astrocytes, neurons, and oligodendrocytes: a new resource for understanding brain development and function. J Neurosci 28:264-278.

Carlisle HJ, Manzerra P, Marcora E, Kennedy MB (2008) SynGAP regulates steady-state and activity-dependent phosphorylation of cofilin. J Neurosci 28:13673-13683.

Carlsson L, Nystrom LE, Sundkvist I, Markey F, Lindberg U (1977) Actin polymerizability is influenced by profilin, a low molecular weight protein in non-muscle cells. J Mol Biol 115:465-483.

Carmignoto G, Pasti L, Pozzan T (1998) On the role of voltage-dependent calcium channels in calcium signaling of astrocytes in situ. J Neurosci 18:4637-4645.

Catlin MC, Guizzetti M, Costa LG (2000) Effect of ethanol on muscarinic receptor-induced calcium responses in astroglia. J Neurosci Res 60:345-355.

Charles AC (1994) Glia-neuron intercellular calcium signaling. Dev Neurosci 16:196-206.

Chen JR, Wang TJ, Huang HY, Chen LJ, Huang YS, Wang YJ, Tseng GF (2009) Fatigue reversibly reduced cortical and hippocampal dendritic spines concurrent with compromise of motor endurance and spatial memory. Neuroscience 161:1104-1113.

Chen LY, Rex CS, Casale MS, Gall CM, Lynch G (2007) Changes in synaptic morphology accompany actin signaling during LTP. J Neurosci 27:5363-5372.

Christopherson KS, Ullian EM, Stokes CC, Mullowney CE, Hell JW, Agah A, Lawler J, Mosher DF, Bornstein P, Barres BA (2005) Thrombospondins are astrocyte-secreted proteins that promote CNS synaptogenesis. Cell 120:421-433.

Ciruela F, Soloviev MM, McIlhinney RA (1999) Co-expression of metabotropic glutamate receptor type 1alpha with homer-1a/Vesl-1S increases the cell surface expression of the receptor. Biochem J 341 (Pt 3):795-803.

Codazzi F, Teruel MN, Meyer T (2001) Control of astrocyte Ca^{2+} oscillations and waves by oscillating translocation and activation of protein kinase C. Curr Biol 11:1089-1097.

Condeelis J (2001) How is actin polymerization nucleated in vivo? Trends Cell Biol 11:288-293.

Cotman CW, Nieto-Sampedro M (1984) Cell biology of synaptic plasticity. Science 225:1287-1294.

D'Ascenzo M, Fellin T, Terunuma M, Revilla-Sanchez R, Meaney DF, Auberson YP, Moss SJ, Haydon PG (2007) mGluR5 stimulates gliotransmission in the nucleus accumbens. Proc Natl Acad Sci U S A 104:1995-2000.

Dailey ME, Smith SJ (1996) The dynamics of dendritic structure in developing hippocampal slices. J Neurosci 16:2983-2994.

de Ligt RA, Kourounakis AP, AP IJ (2000) Inverse agonism at G protein-coupled receptors: (patho)physiological relevance and implications for drug discovery. Br J Pharmacol 130:1-12.

Defea K (2008) Beta-arrestins and heterotrimeric G-proteins: collaborators and competitors in signal transduction. Br J Pharmacol 153 Suppl 1:S298-309.

DesMarais V, Ghosh M, Eddy R, Condeelis J (2005) Cofilin takes the lead. J Cell Sci 118:19-26.

DeWire SM, Ahn S, Lefkowitz RJ, Shenoy SK (2007) Beta-arrestins and cell signaling. Annu Rev Physiol 69:483-510.

Djukic B, Casper KB, Philpot BD, Chin LS, McCarthy KD (2007) Conditional knock-out of Kir4.1 leads to glial membrane depolarization, inhibition of potassium and glutamate uptake, and enhanced short-term synaptic potentiation. J Neurosci 27:11354-11365.

Dombeck DA, Khabbaz AN, Collman F, Adelman TL, Tank DW (2007) Imaging large-scale neural activity with cellular resolution in awake, mobile mice. Neuron 56:43-57.

Duan S, Anderson CM, Keung EC, Chen Y, Swanson RA (2003) P2X7 receptor-mediated release of excitatory amino acids from astrocytes. J Neurosci 23:1320-1328.

Duffy S, MacVicar BA (1994) Potassium-dependent calcium influx in acutely isolated hippocampal astrocytes. Neuroscience 61:51-61.

Dziedzic B, Prevot V, Lomniczi A, Jung H, Cornea A, Ojeda SR (2003) Neuron-to-glia signaling mediated by excitatory amino acid receptors regulates ErbB receptor function in astroglial cells of the neuroendocrine brain. J Neurosci 23:915-926.

Eng LF, Vanderhaeghen JJ, Bignami A, Gerstl B (1971) An acidic protein isolated from fibrous astrocytes. Brain Res 28:351-354.

Ethell IM, Pasquale EB (2005) Molecular mechanisms of dendritic spine development and remodeling. Prog Neurobiol 75:161-205.

Fatatis A, Russell JT (1992) Spontaneous changes in intracellular calcium concentration in type I astrocytes from rat cerebral cortex in primary culture. Glia 5:95-104.

Fellin T, Gomez-Gonzalo M, Gobbo S, Carmignoto G, Haydon PG (2006) Astrocytic glutamate is not necessary for the generation of epileptiform neuronal activity in hippocampal slices. J Neurosci 26:9312-9322.

Fellin T, Pascual O, Gobbo S, Pozzan T, Haydon PG, Carmignoto G (2004) Neuronal synchrony mediated by astrocytic glutamate through activation of extrasynaptic NMDA receptors. Neuron 43:729-743.

Ferraro TN, Golden GT, Smith GG, Martin JF, Lohoff FW, Gieringer TA, Zamboni D, Schwebel CL, Press DM, Kratzer SO, Zhao H, Berrettini WH, Buono RJ (2004)

Fine mapping of a seizure susceptibility locus on mouse Chromosome 1: nomination of Kcnj10 as a causative gene. Mamm Genome 15:239-251.

Fiacco TA, McCarthy KD (2006) Astrocyte calcium elevations: properties, propagation, and effects on brain signaling. Glia 54:676-690.

Fiacco TA, Agulhon C, Taves SR, Petravicz J, Casper KB, Dong X, Chen J, McCarthy KD (2007) Selective stimulation of astrocyte calcium in situ does not affect neuronal excitatory synaptic activity. Neuron 54:611-626.

Foskett JK, White C, Cheung KH, Mak DO (2007) Inositol trisphosphate receptor Ca2+ release channels. Physiol Rev 87:593-658.

Gehler S, Shaw AE, Sarmiere PD, Bamburg JR, Letourneau PC (2004) Brain-derived neurotrophic factor regulation of retinal growth cone filopodial dynamics is mediated through actin depolymerizing factor/cofilin. J Neurosci 24:10741-10749.

Geinisman Y, Disterhoft JF, Gundersen HJ, McEchron MD, Persina IS, Power JM, van der Zee EA, West MJ (2000) Remodeling of hippocampal synapses after hippocampus-dependent associative learning. J Comp Neurol 417:49-59.

Gobel W, Kampa BM, Helmchen F (2007) Imaging cellular network dynamics in three dimensions using fast 3D laser scanning. Nat Methods 4:73-79.

Gohla A, Birkenfeld J, Bokoch GM (2005) Chronophin, a novel HAD-type serine protein phosphatase, regulates cofilin-dependent actin dynamics. Nat Cell Biol 7:21-29.

Grosche J, Kettenmann H, Reichenbach A (2002) Bergmann glial cells form distinct morphological structures to interact with cerebellar neurons. J Neurosci Res 68:138-149.

Grosche J, Matyash V, Moller T, Verkhratsky A, Reichenbach A, Kettenmann H (1999) Microdomains for neuron-glia interaction: parallel fiber signaling to Bergmann glial cells. Nat Neurosci 2:139-143.

Gungabissoon RA, Bamburg JR (2003) Regulation of growth cone actin dynamics by ADF/cofilin. J Histochem Cytochem 51:411-420.

Halassa MM, Florian C, Fellin T, Munoz JR, Lee SY, Abel T, Haydon PG, Frank MG (2009) Astrocytic modulation of sleep homeostasis and cognitive consequences of sleep loss. Neuron 61:213-219.

Halpain S, Spencer K, Graber S (2005) Dynamics and pathology of dendritic spines. Prog Brain Res 147:29-37.

Hamilton NB, Attwell D (2010) Do astrocytes really exocytose neurotransmitters? Nat Rev Neurosci 11:227-238.

Harris-White ME, Zanotti SA, Frautschy SA, Charles AC (1998) Spiral intercellular calcium waves in hippocampal slice cultures. J Neurophysiol 79:1045-1052.

Henneberger C, Papouin T, Oliet SH, Rusakov DA (2010) Long-term potentiation depends on release of D-serine from astrocytes. Nature 463:232-236.

Hermans E, Challiss RA (2001) Structural, signalling and regulatory properties of the group I metabotropic glutamate receptors: prototypic family C G-protein-coupled receptors. Biochem J 359:465-484.

Hertle DN, Yeckel MF (2007) Distribution of inositol-1,4,5-trisphosphate receptor isotypes and ryanodine receptor isotypes during maturation of the rat hippocampus. Neuroscience 150:625-638.

Hirase H, Qian L, Bartho P, Buzsaki G (2004) Calcium dynamics of cortical astrocytic networks in vivo. PLoS Biol 2:E96.

Holtzclaw LA, Pandhit S, Bare DJ, Mignery GA, Russell JT (2002) Astrocytes in adult rat brain express type 2 inositol 1,4,5-trisphosphate receptors. Glia 39:69-84.

Huang TY, DerMardirossian C, Bokoch GM (2006) Cofilin phosphatases and regulation of actin dynamics. Curr Opin Cell Biol 18:26-31.

Jabs R, Kirchhoff F, Kettenmann H, Steinhauser C (1994) Kainate activates Ca^{2+}-permeable glutamate receptors and blocks voltage-gated K+ currents in glial cells of mouse hippocampal slices. Pflugers Arch 426:310-319.

Jung JS, Bhat RV, Preston GM, Guggino WB, Baraban JM, Agre P (1994) Molecular characterization of an aquaporin cDNA from brain: candidate osmoreceptor and regulator of water balance. Proc Natl Acad Sci U S A 91:13052-13056.

Kang J, Jiang L, Goldman SA, Nedergaard M (1998) Astrocyte-mediated potentiation of inhibitory synaptic transmission. Nat Neurosci 1:683-692.

Kang J, Kang N, Lovatt D, Torres A, Zhao Z, Lin J, Nedergaard M (2008) Connexin 43 hemichannels are permeable to ATP. J Neurosci 28:4702-4711.

Kato A, Ozawa F, Saitoh Y, Fukazawa Y, Sugiyama H, Inokuchi K (1998) Novel members of the Vesl/Homer family of PDZ proteins that bind metabotropic glutamate receptors. J Biol Chem 273:23969-23975.

Kettenmann H, Backus KH, Schachner M (1984) Aspartate, glutamate and gamma-aminobutyric acid depolarize cultured astrocytes. Neurosci Lett 52:25-29.

Kimelberg HK (2005) Astrocytic swelling in cerebral ischemia as a possible cause of injury and target for therapy. Glia 50:389-397.

Kimelberg HK (2007) Supportive or information-processing functions of the mature protoplasmic astrocyte in the mammalian CNS? A critical appraisal. Neuron Glia Biol 3:181-189.

Kimelberg HK, Macvicar BA, Sontheimer H (2006) Anion channels in astrocytes: biophysics, pharmacology, and function. Glia 54:747-757.

Kimelberg HK, Rutledge E, Goderie S, Charniga C (1995) Astrocytic swelling due to hypotonic or high K^+ medium causes inhibition of glutamate and aspartate uptake and increases their release. J Cereb Blood Flow Metab 15:409-416.

Kimelberg HK, Goderie SK, Higman S, Pang S, Waniewski RA (1990) Swelling-induced release of glutamate, aspartate, and taurine from astrocyte cultures. J Neurosci 10:1583-1591.

Kirischuk S, Scherer J, Kettenmann H, Verkhratsky A (1995) Activation of P2-purinoreceptors triggered Ca2+ release from InsP3-sensitive internal stores in mammalian oligodendrocytes. J Physiol 483 (Pt 1):41-57.

Kirischuk S, Tuschick S, Verkhratsky A, Kettenmann H (1996) Calcium signalling in mouse Bergmann glial cells mediated by alpha1-adrenoreceptors and H1 histamine receptors. Eur J Neurosci 8:1198-1208.

Kirischuk S, Kirchhoff F, Matyash V, Kettenmann H, Verkhratsky A (1999) Glutamate-triggered calcium signalling in mouse bergmann glial cells in situ: role of inositol-1,4,5-trisphosphate-mediated intracellular calcium release. Neuroscience 92:1051-1059.

Kleim JA, Pipitone MA, Czerlanis C, Greenough WT (1998) Structural stability within the lateral cerebellar nucleus of the rat following complex motor learning. Neurobiol Learn Mem 69:290-306.

Knott GW, Holtmaat A, Wilbrecht L, Welker E, Svoboda K (2006) Spine growth precedes synapse formation in the adult neocortex in vivo. Nat Neurosci 9:1117-1124.

Kobayashi H, Minami S, Itoh S, Shiraishi S, Yokoo H, Yanagita T, Uezono Y, Mohri M, Wada A (2001) Aquaporin subtypes in rat cerebral microvessels. Neurosci Lett 297:163-166.

Kolb B, Cioe J, Comeau W (2008) Contrasting effects of motor and visual spatial learning tasks on dendritic arborization and spine density in rats. Neurobiol Learn Mem 90:295-300.

Kressin K, Kuprijanova E, Jabs R, Seifert G, Steinhauser C (1995) Developmental regulation of Na^+ and K^+ conductances in glial cells of mouse hippocampal brain slices. Glia 15:173-187.

Kuffler SW, Nicholls JG (1966) The physiology of neuroglial cells. Ergeb Physiol 57:1-90.

Kulik A, Haentzsch A, Luckermann M, Reichelt W, Ballanyi K (1999) Neuron-glia signaling via alpha(1) adrenoceptor-mediated Ca^{2+} release in Bergmann glial cells in situ. J Neurosci 19:8401-8408.

Lang C, Barco A, Zablow L, Kandel ER, Siegelbaum SA, Zakharenko SS (2004) Transient expansion of synaptically connected dendritic spines upon induction of hippocampal long-term potentiation. Proc Natl Acad Sci U S A 101:16665-16670.

Lendvai B, Stern EA, Chen B, Svoboda K (2000) Experience-dependent plasticity of dendritic spines in the developing rat barrel cortex in vivo. Nature 404:876-881.

Leuner B, Falduto J, Shors TJ (2003) Associative memory formation increases the observation of dendritic spines in the hippocampus. J Neurosci 23:659-665.

Lin SC, Bergles DE (2002) Physiological characteristics of NG2-expressing glial cells. J Neurocytol 31:537-549.

Lippman J, Dunaevsky A (2005) Dendritic spine morphogenesis and plasticity. J Neurobiol 64:47-57.

Lowery LA, Van Vactor D (2009) The trip of the tip: understanding the growth cone machinery. Nat Rev Mol Cell Biol 10:332-343.

Luttrell LM, Lefkowitz RJ (2002) The role of beta-arrestins in the termination and transduction of G-protein-coupled receptor signals. J Cell Sci 115:455-465.

Malenka RC, Nicoll RA (1999) Long-term potentiation--a decade of progress? Science 285:1870-1874.

Maletic-Savatic M, Malinow R, Svoboda K (1999) Rapid dendritic morphogenesis in CA1 hippocampal dendrites induced by synaptic activity. Science 283:1923-1927.

Marrs GS, Green SH, Dailey ME (2001) Rapid formation and remodeling of postsynaptic densities in developing dendrites. Nat Neurosci 4:1006-1013.

Martinez-Hernandez A, Bell KP, Norenberg MD (1977) Glutamine synthetase: glial localization in brain. Science 195:1356-1358.

Matsui K, Jahr CE (2004) Differential control of synaptic and ectopic vesicular release of glutamate. J Neurosci 24:8932-8939.

Matsui K, Jahr CE, Rubio ME (2005) High-concentration rapid transients of glutamate mediate neural-glial communication via ectopic release. J Neurosci 25:7538-7547.

Matsuzaki M, Honkura N, Ellis-Davies GC, Kasai H (2004) Structural basis of long-term potentiation in single dendritic spines. Nature 429:761-766.

Matus A (2005) Growth of dendritic spines: a continuing story. Curr Opin Neurobiol 15:67-72.

Matyash V, Filippov V, Mohrhagen K, Kettenmann H (2001) Nitric oxide signals parallel fiber activity to Bergmann glial cells in the mouse cerebellar slice. Mol Cell Neurosci 18:664-670.

McCall MA, Gregg RG, Behringer RR, Brenner M, Delaney CL, Galbreath EJ, Zhang CL, Pearce RA, Chiu SY, Messing A (1996) Targeted deletion in astrocyte intermediate filament (Gfap) alters neuronal physiology. Proc Natl Acad Sci U S A 93:6361-6366.

McCarthy KD, de Vellis J (1978) Alpah-adrenergic receptor modulation of beta-adrenergic, adenosine and prostaglandin E1 increased adenosine 3':5'-cyclic monophosphate levels in primary cultures of glia. J Cyclic Nucleotide Res 4:15-26.

Mongin AA, Kimelberg HK (2005) ATP regulates anion channel-mediated organic osmolyte release from cultured rat astrocytes via multiple Ca2+-sensitive mechanisms. Am J Physiol Cell Physiol 288:C204-213.

Morales M, Fifkova E (1989) In situ localization of myosin and actin in dendritic spines with the immunogold technique. J Comp Neurol 279:666-674.

Mothet JP, Pollegioni L, Ouanounou G, Martineau M, Fossier P, Baux G (2005) Glutamate receptor activation triggers a calcium-dependent and SNARE protein-dependent release of the gliotransmitter D-serine. Proc Natl Acad Sci U S A 102:5606-5611.

Mudo G, Trovato-Salinaro A, Caniglia G, Cheng Q, Condorelli DF (2007) Cellular localization of mGluR3 and mGluR5 mRNAs in normal and injured rat brain. Brain Res 1149:1-13.

Nakanishi H, Obaishi H, Satoh A, Wada M, Mandai K, Satoh K, Nishioka H, Matsuura Y, Mizoguchi A, Takai Y (1997) Neurabin: a novel neural tissue-specific actin filament-binding protein involved in neurite formation. J Cell Biol 139:951-961.

Navarrete M, Araque A (2008) Endocannabinoids mediate neuron-astrocyte communication. Neuron 57:883-893.

Nett WJ, Oloff SH, McCarthy KD (2002) Hippocampal astrocytes in situ exhibit calcium oscillations that occur independent of neuronal activity. J Neurophysiol 87:528-537.

Newman EA (2003) Glial cell inhibition of neurons by release of ATP. J Neurosci 23:1659-1666.

Newman EA (2005) Calcium increases in retinal glial cells evoked by light-induced neuronal activity. J Neurosci 25:5502-5510.

Newpher TM, Ehlers MD (2009) Spine microdomains for postsynaptic signaling and plasticity. Trends Cell Biol 19:218-227.

Nielsen S, Nagelhus EA, Amiry-Moghaddam M, Bourque C, Agre P, Ottersen OP (1997) Specialized membrane domains for water transport in glial cells: high-resolution immunogold cytochemistry of aquaporin-4 in rat brain. J Neurosci 17:171-180.

Niermann H, Amiry-Moghaddam M, Holthoff K, Witte OW, Ottersen OP (2001) A novel role of vasopressin in the brain: modulation of activity-dependent water flux in the neocortex. J Neurosci 21:3045-3051.

Nimmerjahn A, Kirchhoff F, Kerr JN, Helmchen F (2004) Sulforhodamine 101 as a specific marker of astroglia in the neocortex in vivo. Nat Methods 1:31-37.

Nishiyama H, Knopfel T, Endo S, Itohara S (2002) Glial protein S100B modulates long-term neuronal synaptic plasticity. Proc Natl Acad Sci U S A 99:4037-4042.

Niwa R, Nagata-Ohashi K, Takeichi M, Mizuno K, Uemura T (2002) Control of actin reorganization by Slingshot, a family of phosphatases that dephosphorylate ADF/cofilin. Cell 108:233-246.

Okabe S, Miwa A, Okado H (2001) Spine formation and correlated assembly of presynaptic and postsynaptic molecules. J Neurosci 21:6105-6114.

Orkand RK, Nicholls JG, Kuffler SW (1966) Effect of nerve impulses on the membrane potential of glial cells in the central nervous system of amphibia. J Neurophysiol 29:788-806.

Panatier A, Theodosis DT, Mothet JP, Touquet B, Pollegioni L, Poulain DA, Oliet SH (2006) Glia-derived D-serine controls NMDA receptor activity and synaptic memory. Cell 125:775-784.

Pantaloni D, Boujemaa R, Didry D, Gounon P, Carlier MF (2000) The Arp2/3 complex branches filament barbed ends: functional antagonism with capping proteins. Nat Cell Biol 2:385-391.

Parri HR, Crunelli V (2003) The role of Ca2+ in the generation of spontaneous astrocytic Ca^{2+} oscillations. Neuroscience 120:979-992.

Parri HR, Gould TM, Crunelli V (2001) Spontaneous astrocytic Ca^{2+} oscillations in situ drive NMDAR-mediated neuronal excitation. Nat Neurosci 4:803-812.

Pascual O, Casper KB, Kubera C, Zhang J, Revilla-Sanchez R, Sul JY, Takano H, Moss SJ, McCarthy K, Haydon PG (2005) Astrocytic purinergic signaling coordinates synaptic networks. Science 310:113-116.

Pasti L, Volterra A, Pozzan T, Carmignoto G (1997) Intracellular calcium oscillations in astrocytes: a highly plastic, bidirectional form of communication between neurons and astrocytes in situ. J Neurosci 17:7817-7830.

Perea G, Araque A (2005) Properties of synaptically evoked astrocyte calcium signal reveal synaptic information processing by astrocytes. J Neurosci 25:2192-2203.

Petravicz J, Fiacco TA, McCarthy KD (2008) Loss of IP3 receptor-dependent Ca^{2+} increases in hippocampal astrocytes does not affect baseline CA1 pyramidal neuron synaptic activity. J Neurosci 28:4967-4973.

Piet R, Jahr CE (2007) Glutamatergic and purinergic receptor-mediated calcium transients in Bergmann glial cells. J Neurosci 27:4027-4035.

Pollard TD, Blanchoin L, Mullins RD (2001) Actin dynamics. J Cell Sci 114:3-4.

Pontrello CG, Ethell IM (2009) Accelerators, Brakes, and Gears of Actin Dynamics in Dendritic Spines. Open Neurosci J 3:67-86.

Poopalasundaram S, Knott C, Shamotienko OG, Foran PG, Dolly JO, Ghiani CA, Gallo V, Wilkin GP (2000) Glial heterogeneity in expression of the inwardly rectifying K^+ channel, Kir4.1, in adult rat CNS. Glia 30:362-372.

Porter JT, McCarthy KD (1995) GFAP-positive hippocampal astrocytes in situ respond to glutamatergic neuroligands with increases in $[Ca^{2+}]_i$. Glia 13:101-112.

Porter JT, McCarthy KD (1996) Hippocampal astrocytes in situ respond to glutamate released from synaptic terminals. J Neurosci 16:5073-5081.

Porter JT, McCarthy KD (1997) Astrocytic neurotransmitter receptors in situ and in vivo. Prog Neurobiol 51:439-455.

Prezeau L, Gomeza J, Ahern S, Mary S, Galvez T, Bockaert J, Pin JP (1996) Changes in the carboxyl-terminal domain of metabotropic glutamate receptor 1 by alternative splicing generate receptors with differing agonist-independent activity. Mol Pharmacol 49:422-429.

Racz B, Weinberg RJ (2006) Spatial organization of cofilin in dendritic spines. Neuroscience 138:447-456.

Ransom CB, Ransom BR, Sontheimer H (2000) Activity-dependent extracellular K^+ accumulation in rat optic nerve: the role of glial and axonal Na+ pumps. J Physiol 522 Pt 3:427-442.

Roche KW, Tu JC, Petralia RS, Xiao B, Wenthold RJ, Worley PF (1999) Homer 1b regulates the trafficking of group I metabotropic glutamate receptors. J Biol Chem 274:25953-25957.

Romano C, Sesma MA, McDonald CT, O'Malley K, Van den Pol AN, Olney JW (1995) Distribution of metabotropic glutamate receptor mGluR5 immunoreactivity in rat brain. J Comp Neurol 355:455-469.

Rose CR, Ransom BR (1996) Intracellular sodium homeostasis in rat hippocampal astrocytes. J Physiol 491 (Pt 2):291-305.

Rosenberg PA, Aizenman E (1989) Hundred-fold increase in neuronal vulnerability to glutamate toxicity in astrocyte-poor cultures of rat cerebral cortex. Neurosci Lett 103:162-168.

Roth BJ, Yagodin SV, Holtzclaw L, Russell JT (1995) A mathematical model of agonist-induced propagation of calcium waves in astrocytes. Cell Calcium 17:53-64.

Rothstein JD, Martin L, Levey AI, Dykes-Hoberg M, Jin L, Wu D, Nash N, Kuncl RW (1994) Localization of neuronal and glial glutamate transporters. Neuron 13:713-725.

Rothstein JD, Dykes-Hoberg M, Pardo CA, Bristol LA, Jin L, Kuncl RW, Kanai Y, Hediger MA, Wang Y, Schielke JP, Welty DF (1996) Knockout of glutamate transporters reveals a major role for astroglial transport in excitotoxicity and clearance of glutamate. Neuron 16:675-686.

Rust MB, Gurniak CB, Renner M, Vara H, Morando L, Gorlich A, Sassoe-Pognetto M, Banchaabouchi MA, Giustetto M, Triller A, Choquet D, Witke W (2010) Learning, AMPA receptor mobility and synaptic plasticity depend on n-cofilin-mediated actin dynamics. EMBO J 29:1889-1902.

Sarmiere PD, Bamburg JR (2004) Regulation of the neuronal actin cytoskeleton by ADF/cofilin. J Neurobiol 58:103-117.

Scemes E (2000) Components of astrocytic intercellular calcium signaling. Mol Neurobiol 22:167-179.

Scemes E, Giaume C (2006) Astrocyte calcium waves: what they are and what they do. Glia 54:716-725.

Schummers J, Yu H, Sur M (2008) Tuned responses of astrocytes and their influence on hemodynamic signals in the visual cortex. Science 320:1638-1643.

Segal M (2005) Dendritic spines and long-term plasticity. Nat Rev Neurosci 6:277-284.

Serrano A, Haddjeri N, Lacaille JC, Robitaille R (2006) GABAergic network activation of glial cells underlies hippocampal heterosynaptic depression. J Neurosci 26:5370-5382.

Shankar GM, Bloodgood BL, Townsend M, Walsh DM, Selkoe DJ, Sabatini BL (2007) Natural oligomers of the Alzheimer amyloid-beta protein induce reversible synapse loss by modulating an NMDA-type glutamate receptor-dependent signaling pathway. J Neurosci 27:2866-2875.

Shao Y, McCarthy KD (1993) Quantitative relationship between alpha 1-adrenergic receptor density and the receptor-mediated calcium response in individual astroglial cells. Mol Pharmacol 44:247-254.

Shelton MK, McCarthy KD (2000) Hippocampal astrocytes exhibit Ca2+-elevating muscarinic cholinergic and histaminergic receptors in situ. J Neurochem 74:555-563.

Sheppard CA, Simpson PB, Sharp AH, Nucifora FC, Ross CA, Lange GD, Russell JT (1997) Comparison of type 2 inositol 1,4,5-trisphosphate receptor distribution and subcellular Ca^{2+} release sites that support Ca^{2+} waves in cultured astrocytes. J Neurochem 68:2317-2327.

Shi Y, Pontrello CG, DeFea KA, Reichardt LF, Ethell IM (2009) Focal adhesion kinase acts downstream of EphB receptors to maintain mature dendritic spines by regulating cofilin activity. J Neurosci 29:8129-8142.

Shigemoto R, Nakanishi S, Mizuno N (1992) Distribution of the mRNA for a metabotropic glutamate receptor (mGluR1) in the central nervous system: an in situ hybridization study in adult and developing rat. J Comp Neurol 322:121-135.

Shirao T, Hayashi K, Ishikawa R, Isa K, Asada H, Ikeda K, Uyemura K (1994) Formation of thick, curving bundles of actin by drebrin A expressed in fibroblasts. Exp Cell Res 215:145-153.

Shuai JW, Jung P (2003) Optimal ion channel clustering for intracellular calcium signaling. Proc Natl Acad Sci U S A 100:506-510.

Simpson PB, Russell JT (1997) Role of sarcoplasmic/endoplasmic-reticulum Ca2+-ATPases in mediating Ca^{2+} waves and local Ca^{2+}-release microdomains in cultured glia. Biochem J 325 (Pt 1):239-247.

Sjoblom B, Salmazo A, Djinovic-Carugo K (2008) Alpha-actinin structure and regulation. Cell Mol Life Sci 65:2688-2701.

Smart FM, Halpain S (2000) Regulation of dendritic spine stability. Hippocampus 10:542-554.

Steinhauser C, Berger T, Frotscher M, Kettenmann H (1992) Heterogeneity in the Membrane Current Pattern of Identified Glial Cells in the Hippocampal Slice. Eur J Neurosci 4:472-484.

Stout CE, Costantin JL, Naus CC, Charles AC (2002) Intercellular calcium signaling in astrocytes via ATP release through connexin hemichannels. J Biol Chem 277:10482-10488.

Straub SV, Bonev AD, Wilkerson MK, Nelson MT (2006) Dynamic inositol trisphosphate-mediated calcium signals within astrocytic endfeet underlie vasodilation of cerebral arterioles. J Gen Physiol 128:659-669.

Tada T, Sheng M (2006) Molecular mechanisms of dendritic spine morphogenesis. Curr Opin Neurobiol 16:95-101.

Takumi T, Ishii T, Horio Y, Morishige K, Takahashi N, Yamada M, Yamashita T, Kiyama H, Sohmiya K, Nakanishi S, et al. (1995) A novel ATP-dependent inward rectifier potassium channel expressed predominantly in glial cells. J Biol Chem 270:16339-16346.

Thomas D, Lipp P, Tovey SC, Berridge MJ, Li W, Tsien RY, Bootman MD (2000) Microscopic properties of elementary Ca^{2+} release sites in non-excitable cells. Curr Biol 10:8-15.

Tian GF, Azmi H, Takano T, Xu Q, Peng W, Lin J, Oberheim N, Lou N, Wang X, Zielke HR, Kang J, Nedergaard M (2005) An astrocytic basis of epilepsy. Nat Med 11:973-981.

Trachtenberg JT, Chen BE, Knott GW, Feng G, Sanes JR, Welker E, Svoboda K (2002) Long-term in vivo imaging of experience-dependent synaptic plasticity in adult cortex. Nature 420:788-794.

Tu JC, Xiao B, Yuan JP, Lanahan AA, Leoffert K, Li M, Linden DJ, Worley PF (1998) Homer binds a novel proline-rich motif and links group 1 metabotropic glutamate receptors with IP3 receptors. Neuron 21:717-726.

Vajda Z, Pedersen M, Fuchtbauer EM, Wertz K, Stodkilde-Jorgensen H, Sulyok E, Doczi T, Neely JD, Agre P, Frokiaer J, Nielsen S (2002) Delayed onset of brain edema and mislocalization of aquaporin-4 in dystrophin-null transgenic mice. Proc Natl Acad Sci U S A 99:13131-13136.

Van Calker D, Muller M, Hamprecht B (1978) Adrenergic alpha- and beta-receptors expressed by the same cell type in primary culture of perinatal mouse brain. J Neurochem 30:713-718.

van den Pol AN, Romano C, Ghosh P (1995) Metabotropic glutamate receptor mGluR5 subcellular distribution and developmental expression in hypothalamus. J Comp Neurol 362:134-150.

Ventura R, Harris KM (1999) Three-dimensional relationships between hippocampal synapses and astrocytes. J Neurosci 19:6897-6906.

Verkhratsky A, Orkand RK, Kettenmann H (1998) Glial calcium: homeostasis and signaling function. Physiol Rev 78:99-141.

Volterra A, Steinhauser C (2004) Glial modulation of synaptic transmission in the hippocampus. Glia 47:249-257.

Waldo GL, Ricks TK, Hicks SN, Cheever ML, Kawano T, Tsuboi K, Wang X, Montell C, Kozasa T, Sondek J, Harden TK (2010) Kinetic scaffolding mediated by a phospholipase C-beta and Gq signaling complex. Science 330:974-980.

Walz W (2000) Controversy surrounding the existence of discrete functional classes of astrocytes in adult gray matter. Glia 31:95-103.

Walz W, Hinks EC (1985) Carrier-mediated KCl accumulation accompanied by water movements is involved in the control of physiological K^+ levels by astrocytes. Brain Res 343:44-51.

Wang P, DeFea KA (2006) Protease-activated receptor-2 simultaneously directs beta-arrestin-1-dependent inhibition and Galphaq-dependent activation of phosphatidylinositol 3-kinase. Biochemistry 45:9374-9385.

Wang X, Lou N, Xu Q, Tian GF, Peng WG, Han X, Kang J, Takano T, Nedergaard M (2006) Astrocytic Ca^{2+} signaling evoked by sensory stimulation in vivo. Nat Neurosci 9:816-823.

Wang Y, Shibasaki F, Mizuno K (2005) Calcium signal-induced cofilin dephosphorylation is mediated by Slingshot via calcineurin. J Biol Chem 280:12683-12689.

Weerth SH, Holtzclaw LA, Russell JT (2007) Signaling proteins in raft-like microdomains are essential for Ca^{2+} wave propagation in glial cells. Cell Calcium 41:155-167.

Wolosker H, Blackshaw S, Snyder SH (1999) Serine racemase: a glial enzyme synthesizing D-serine to regulate glutamate-N-methyl-D-aspartate neurotransmission. Proc Natl Acad Sci U S A 96:13409-13414.

Wu H, Parsons JT (1993) Cortactin, an 80/85-kilodalton pp60src substrate, is a filamentous actin-binding protein enriched in the cell cortex. J Cell Biol 120:1417-1426.

Xiao K, Sun J, Kim J, Rajagopal S, Zhai B, Villen J, Haas W, Kovacs JJ, Shukla AK, Hara MR, Hernandez M, Lachmann A, Zhao S, Lin Y, Cheng Y, Mizuno K, Ma'ayan A, Gygi SP, Lefkowitz RJ (2010) Global phosphorylation analysis of beta-arrestin-mediated signaling downstream of a seven transmembrane receptor (7TMR). Proc Natl Acad Sci U S A 107:15299-15304.

Yagodin S, Holtzclaw LA, Russell JT (1995) Subcellular calcium oscillators and calcium influx support agonist-induced calcium waves in cultured astrocytes. Mol Cell Biochem 149-150:137-144.

Yagodin SV, Holtzclaw L, Sheppard CA, Russell JT (1994) Nonlinear propagation of agonist-induced cytoplasmic calcium waves in single astrocytes. J Neurobiol 25:265-280.

Yang N, Higuchi O, Ohashi K, Nagata K, Wada A, Kangawa K, Nishida E, Mizuno K (1998) Cofilin phosphorylation by LIM-kinase 1 and its role in Rac-mediated actin reorganization. Nature 393:809-812.

Yang Y, Ge W, Chen Y, Zhang Z, Shen W, Wu C, Poo M, Duan S (2003) Contribution of astrocytes to hippocampal long-term potentiation through release of D-serine. Proc Natl Acad Sci U S A 100:15194-15199.

Ye ZC, Wyeth MS, Baltan-Tekkok S, Ransom BR (2003) Functional hemichannels in astrocytes: a novel mechanism of glutamate release. J Neurosci 23:3588-3596.

Yin HL, Stossel TP (1979) Control of cytoplasmic actin gel-sol transformation by gelsolin, a calcium-dependent regulatory protein. Nature 281:583-586.

Zhou M, Schools GP, Kimelberg HK (2006) Development of GLAST(+) astrocytes and NG2(+) glia in rat hippocampus CA1: mature astrocytes are electrophysiologically passive. J Neurophysiol 95:134-143.

Zhou Q, Homma KJ, Poo MM (2004) Shrinkage of dendritic spines associated with long-term depression of hippocampal synapses. Neuron 44:749-757.

Ziv NE, Smith SJ (1996) Evidence for a role of dendritic filopodia in synaptogenesis and spine formation. Neuron 17:91-102.

Ziv NE, Garner CC (2004) Cellular and molecular mechanisms of presynaptic assembly. Nat Rev Neurosci 5:385-399.

Zoudilova M, Min J, Richards HL, Carter D, Huang T, DeFea KA (2010) beta-Arrestins scaffold cofilin with chronophin to direct localized actin filament severing and membrane protrusions downstream of protease-activated receptor-2. J Biol Chem 285:14318-14329.

Zur Nieden R, Deitmer JW (2006) The role of metabotropic glutamate receptors for the generation of calcium oscillations in rat hippocampal astrocytes in situ. Cereb Cortex 16:676-687.

Chapter 2: Effects of action potential-driven synaptic activity and miniature neurotransmitter release on spontaneous astrocytic Gq GPCR signaling domains

2.1 Abstract

Astrocytes express numerous Gq-protein coupled receptors (Gq GPCRs) that couple to increases in cytoplasmic Ca^{2+} concentration. Previous research has indicated the presence of three primary astrocytic Gq GPCR signaling domains: 1) microdomain, 2) whole-cell, and 3) intercellular. Astrocyte Ca^{2+} "microdomains" are discrete regions of astrocyte processes that exhibit asynchronous Ca^{2+} elevations in basal conditions. It is still not clear what processes drive active astrocyte signaling microdomains. Furthermore, the role of Ca^{2+} microdomains in astrocyte physiology and pathology is still not well elucidated. Understanding these processes will be critical to our understanding of astrocyte function and the purpose of neuron-to-astrocyte communication in the brain. To study the mechanisms behind spontaneous astrocytic Gq GPCR signaling domains, we set out to determine: 1) Whether spontaneous astrocytic Gq GPCR microdomains are driven by action potential-mediated neuronal synaptic transmission, 2) Whether spontaneous astrocytic Gq GPCR microdomains are driven by miniature neurotransmitter release, 3) Whether spontaneous astrocyte Gq GPCR microdomains are group I metabotropic glutamate receptor ($mGluR_{1/5}$) dependent. These questions were addressed using patch-clamp electrophysiology combined with confocal imaging techniques in CA1 stratum radiatum astrocytes in acute hippocampal slices. Our approach was to increase external K^+ concentration to 5.0 mM to globally elevate neuronal action potential firing rates. Our data revealed no corresponding increase in the frequency of microdomain Ca^{2+}

oscillations with increased neuronal action potentials relative to baseline $[K^+]_o$ of 2.5 mM. We also examined the effects caused by blocking miniature neurotransmitter release on spontaneous microdomain Ca^{2+} oscillations. Frequency of microdomain Ca^{2+} oscillations was significantly decreased when miniature neurotransmitter release was blocked in the presence of Bafilomycin A1, suggesting that astrocyte Gq GPCR microdomains are driven in part by miniature quantal release of neurotransmitter. Finally, we tested whether these spontaneous events are $mGluR_{1/5}$ dependent by comparing the frequency of microdomain Ca^{2+} oscillations before and after $mGluR_{1/5}$ antagonists were applied. Within-cell comparison showed no significant frequency change of spontaneous microdomain Ca^{2+} oscillations in the presence of $mGluR_{1/5}$ antagonists compared to baseline, suggesting that other types of neurotransmitter receptors are involved in triggering these spontaneous events.

2.2 Introduction

Astrocytes exhibit spontaneous, asynchronous microdomain Ca^{2+} oscillations within small compartments of their fine processes in conditions lacking any user-evoked stimulation, a phenomenon that has been observed in cell culture (Fatatis and Russell, 1992; Charles, 1994; Harris-White et al., 1998), in slices (Parri et al., 2001; Aguado et al., 2002; Nett et al., 2002) , and *in vivo* (Hirase et al., 2004; Nimmerjahn et al., 2004; Wang et al., 2006). The majority of these spontaneous Ca^{2+} oscillations are not mediated by voltage-gated calcium channels (Wang et al., 2006) or ryanodine receptors (Parri and Crunelli, 2003; Wang et al., 2006). Based on findings showing that these spontaneous astrocytic Ca^{2+} events were markedly abolished under the treatment of IP_3 receptor antagonist Heparin (Nett et al., 2002) or when astrocyte IP_3 receptors were knocked out (Petravicz et al., 2008), it has been widely accepted that these spontaneous astrocyte Ca^{2+} events are mainly due to activation of G protein-coupled receptors (Gq GPCRs) and depend on IP_3-triggered Ca^{2+} release from internal stores (Agulhon et al., 2008). Therefore, recording astrocyte Ca^{2+} activity using Ca^{2+} indicator dyes and confocal microscopy provides a real-time readout of astrocytic Gq GPCR activity. It has been shown that, for astrocytes in the hippocampus, spontaneous whole-cell Ca^{2+} oscillations still occur in the presence of tetrodotoxin (TTX), which inhibits action potential generation (Parri et al., 2001; Aguado et al., 2002; Nett et al., 2002; Parri and Crunelli, 2003), suggesting that whole-cell astrocytic Ca^{2+} events occur independent of neuronal activity. Mechanisms intrinsic to astrocytes, such as constitutive Gq GPCR activity which occurs in the absence of agonist (de Ligt et al., 2000; Hermans and Challiss, 2001), could

play essential roles in driving these spontaneous astrocytic Ca^{2+} elevations. Interestingly, however, in another report the frequency of astrocytic Ca^{2+} activity was elevated when low concentrations of mGlu Gq GPCR agonists were present, raising the possibility that some microdomain Ca^{2+} activity can be driven by local glutamate spill over from neuronal synaptic transmission (Zur Nieden and Deitmer, 2006). This hypothesis, if proven, would imply that astrocytic Ca^{2+} microdomains are driven by glutamate release from individual synapses, which would change the current view of how neurons signal to astrocytes. Furthermore, this would open the door to future studies examining plasticity of neuron-to-astrocyte signaling microdomains based on changes in local synaptic strength. Plasticity of astrocytic Gq GPCR signaling microdomains has not been studied, and could provide a basis for changes in glial investiture of active neuronal synapses, as well as plasticity of critical astrocytic functions including K^+ and glutamate uptake.

In this study, we performed experiments to test the hypothesis that spontaneous astrocytic Gq GPCR microdomain activity is driven by neuronal activity. This question was addressed by filling a single astrocyte with Ca^{2+} indicator dye using the whole-cell patch-clamp technique, combined with laser scanning confocal microscopy to record changes in local Ca^{2+} activity. To ensure there was effect or photo damage caused by laser light, we first performed a series of control experiments to measure the effects of laser power and exposure time over the recording period on astrocytes. We then globally increased hippocampal neuronal firing by doubling the extracellular K^+ concentration from 2.5 mM to 5 mM, a concentration still within the physiological range which effectively depolarizes neurons by approximately 10 mV and enhances CA3 neuronal

firing rates (Xie, 2011). The sodium channel blocker tetrodotoxin (TTX, 1 μM) was then bath applied in order to block any action potential-driven astrocyte Ca^{2+} activity. To our surprise, we found no significant change in spontaneous astrocytic Ca^{2+} activity in conditions when neuronal activity was globally increased or inhibited, suggesting that spontaneous astrocytic Gq GPCR microdomains are not driven by action potential-mediated neurotransmitter release.

In basal conditions without any action potential-driven events, packets or quanta of neurotransmitters are spontaneously released. This "miniature" release from presynaptic terminals produces miniature excitatory postsynaptic currents (mEPSCs) in neurons, which is thought to play a role in synaptic maintenance (McKinney et al., 1999; Sutton et al., 2006). It has been shown that Bafilomycin A1, an H-ATPase that inhibits acidification of synaptic vesicles and prevents neurotransmitter from being re-loaded into vesicles, blocks miniature neurotransmitter release and mEPSCs (Araque et al., 2000; Zhou et al., 2000). Previous studies indicated that blocking miniature neurotransmitter release using Bafilomycin A1 had no significant effect on spontaneous astrocytic Ca^{2+} oscillations recorded from the cell bodies of astrocytes (Nett et al., 2002; Parri and Crunelli, 2003). These findings suggested that spontaneous whole-cell astrocytic Ca^{2+} activity does not rely on neuronal vesicular release of neurotransmitters, but is driven by mechanisms "intrinsic" to the astrocyte, probably through constitutive Gq GPCR signaling activity (de Ligt et al., 2000; Hermans and Challiss, 2001). However, the methods employed at the time only allowed Ca^{2+} loading in the astrocyte cell bodies so that Gq GPCR activity could not be recorded in astrocyte microdomains. Therefore,

changes occurring in local fine processes might have been overlooked in this study. In the current study, individual astrocytes were filled with a high-affinity Ca^{2+} indicator (Oregon Green BAPTA-1 or OGB-1) via patch pipette, which allowed for maximum visibility of astrocyte processes. Surprisingly, microdomain astrocyte Ca^{2+} elevations were significantly reduced, although not abolished, when slices were pre-incubated in 4 μM Bafilomycin A1 for ≥ 2 hours, suggesting that a significant portion of astrocyte microdomain Gq GPCR activity is driven by miniature release of neurotransmitter. This was surprising based on our initial experiments demonstrating the lack of effect of elevating and blocking neuronal action potentials on the frequency of astrocyte Gq GPCR microdomains.

We also attempted to identify which astrocytic Gq GPCRs were involved in the generation of spontaneous microdomain Ca^{2+} oscillations. Based on previous *in situ* and *in vivo* studies, the neuronal activity-elicited astrocytic Ca^{2+} responses were largely blocked by group I mGluR antagonists (Porter and McCarthy, 1996; Wang et al., 2006). Moreover, the spontaneous astrocytic Ca^{2+} elevations were reported to be reduced or suppressed by MCPG, a group I and II mGluR antagonist, indicating a correlation between mGluRs and spontaneous Ca^{2+} oscillations in astrocytes (Zur Nieden and Deitmer, 2006). However, studies done by another research group revealed no significant change in spontaneous astrocyte Ca^{2+} oscillations when MCPG was applied (Aguado et al., 2002). As both studies used bulk-loading techniques that only reliably fill the astrocyte soma with Ca^{2+} indicator, activity occurring in smaller astrocyte compartments went unmeasured. To solve this problem, we used whole-cell patch-clamp to fill

astrocytes with Ca^{2+} indicator as it allows loading of Ca^{2+} indicator in the astrocyte microdomains while also providing unequivocal identification of the filled cells as astrocytes based on their passive electrophysiological properties. Our results revealed no significant change in spontaneous astrocyte Ca^{2+} oscillations after $mGluR_{1/5}$ antagonists (CPCCOEt, 100 μM and MPEP, 20 μM) were bath-applied. These results suggest that other types of astrocytic Gq GPCRs might be involved in generation of spontaneous astrocytic Ca^{2+} elevations.

2.3 Materials and methods

***Preparation of hippocampal slices*.**

All mice were housed in the animal facility at the University of California, Riverside in accordance with Institutional Animal Care and Use Committee guidelines. Parasagittal hippocampal slices (300 μm thick) were prepared from 12- to 18-day-old C57BL/6J (Jackson Laboratory, Bar Harbor, ME) wild-type mice using a Leica VT1200s Vibratome (Bannockburn, IL). Slices were prepared in ice-cold, nominally Ca^{2+}-free saline containing (in mM): 125 NaCl, 2.5 KCl, 3.8 $MgCl_2$, 1 NaH_2PO_4, 26.6 $NaHCO_3$, and 25 glucose, bubbled with 5% CO_2-95% O_2. Subsequently, slices were incubated for 45 min at 35°C in oxygenated artificial cerebrospinal fluid (ACSF) containing (in mM) 125 NaCl, 2.5 KCl, 2.5 $CaCl_2$, 1.3 $MgCl_2$, 1 NaH_2PO_4, 26.6 $NaHCO_3$, and 25 glucose, bubbled with 5% CO_2-95% O_2. Following the incubation period at physiological temperature, slices were given 15 min to cool to room temperature and then transferred to a recording chamber (Warner Instrument), continuously superfused with oxygenated, room temperature ACSF.

***Patch clamp of passive astrocytes*.**

Pipettes were pulled from borosilicate glass on a Narishige (Tokyo, Japan) PP-83 two-stage vertical pipette puller and not fire-polished. Pipettes were pulled to 7-8MΩ when filled with (in mM): 130 K-gluconate, 4 $MgCl_2$, 10 HEPES, 10 glucose, 1.185 Mg-ATP, 10.55 phosphocreatine, and 0.1315 mg/ml creatine phosphokinase, pH 7.3 by KOH (standard internal solution). The Ca^{2+}-indicator dye Oregon green BAPTA-1 (OGB-1; from Invitrogen; 200 μM) was also included. Whole-cell patch-clamp recordings of astrocytes were performed at room temperature using a Multiclamp 700B amplifier and PCLAMP 10.2 software (Axon Instruments, Union City, CA), or a EPC 10 dual patch amplifier and Patchmaster software (HEKA, Germany). After whole-cell configuration was obtained, passive astrocytes were verified by their electrophysiological properties (Fiacco and McCarthy, 2004). Passive Astrocytes typically rest at -85 mV with low input resistances of 10 MΩ. They exhibit passive currents when stepped from -180 mV to +80 mV in 20 mV increments. A test pulse of -5 mV was included after each voltage step in order to monitor changes in access resistance. Astrocyte current signals were low-pass filtered at 2 kHz and digitized at 100 kHz via a DigiData 1440 (Axon Instruments) interfaced to a personal computer. A smooth, stable off-cell and formation of an outside-out patch was used as an indicator of minimal damage to the cell membrane during the patch procedure. After pipette withdrawal, a recovery time of 10 min was allowed before recording astrocytic Ca^{2+} activity. During astrocyte recordings, solutions were switched using an electronic valve controller (Warner Instrument, Hamden CT).

***Confocal imaging*.**

Hippocampal CA1 stratum radiatum was visualized using an Olympus BX61 WI upright microscope equipped with UMPLFLN 10X (N.A 0.3) and LUMFLN 60X (N.A. 1.1) water-immersion objective lenses and differential interference contrast (DIC) optics. Astrocytes in CA1 stratum radiatum were first identified by their characteristic morphology and size using DIC visualization. After loading with OGB-1 Ca^{2+} indicator dye, the fluorescence intensity in astrocytes was recorded over time on a fixed focal plane of 4.127 μm optical thickness, 1.2 sec scanning interval and 2X zoom-in factor. Changes in fluorescence intensity indicated a Ca^{2+} elevation (criteria described in next section). The microscope was set up for FITC detection to visualize green indicator under the specific detection channel. For all experiments, only a single (field of) astrocyte(s) was recorded per slice to prevent effects caused by multiple electrical stimulations and/or agonist applications. Laser power was generally kept at 0.3% or lower to prevent phototoxicity-induced spontaneous Ca^{2+} oscillations (Wang et al., 2006; see also Fig. 2.2 for control experiment). The group I mGluR agonist (*S*)-3,5-Dihydroxyphenylglycine (DHPG) or an agonist cocktail (containing 10 μM each of histamine, carbachol, and 2Na-ATP, agonists for histamine H1 receptors [H1R], muscarinic acetylcholine receptors [mAchR], and purinergic receptors [P2YR], respectively) were always applied at the end of the experiment as a positive control to verify intact astrocytic Gq GPCR signaling pathways. Astrocytes that failed to respond to the positive control were excluded from further analysis. Solutions were switched using an electronic valve controller during the course of the experiments (Warner Instrument, Hamden CT).

Bafilomycin incubation

Slices were incubated in ACSF containing 4 μm Bafilomycin (LC Laboratorys) for ≥ 2 hours before starting the experiment. Slices in the control group were simultaneously incubated in ACSF (without Bafilomycin) for nearly the same amount of time.

Data analysis.

Square-shaped regions of interest (ROI) of a size ranging from 9.6 - 17.3 μm^2 were placed over the astrocyte cell body and visible processes using Olympus Fluoview 1000 software. For each ROI, fluorescence increases of at least two successive scanning points with values ≥three standard deviations above 30 s of mean baseline signal were defined as Ca^{2+} elevations (Honsek et al., 2012). Spontaneous Ca^{2+} elevations that covered < 75% of the planar area of the astrocyte were defined as "microdomain" Ca^{2+} events, whereas those spanning > 75% of the planar area were defined as "whole cell" Ca^{2+} events. Neighboring ROIs with Ca^{2+} transients at the same time (< 10 s time interval) were grouped together as a single Gq GPCR signaling domain (illustrated in Fig. 2.1). ROIs increasing fluorescence intensity at the same time but with at least one intervening ROI that did not increase in intensity were considered separate microdomains occurring at the same time. Student's independent t-test was used to determine statistical significance among conditions or between control and treatment groups. P value ≤ 0.05 was considered significant.

2.4 Results

2.4.1. Measurement of astrocytic microdomain Ca^{2+} oscillations under increasing laser power intensity

A previous study has revealed a laser light-induced artifact on spontaneous astrocytic Ca^{2+} elevations (Wang et al., 2006). Given that this critical issue could greatly impact our experimental results, we performed a series of control experiments to test the contribution of confocal laser light, if any, to astrocyte Ca^{2+} activity. The effects of laser power intensity were examined by recording spontaneous astrocytic Ca^{2+} activity at 0.2%, 0.5%., 1%, 2%, 5%, 10%, and 20% laser power, each for 5 min (Fig. 2.2C). A significant increase in Ca^{2+} elevation frequency was observed at 5% and 10% laser powers, while elevations gradually diminished at 20% (n = 4 cells). An agonist cocktail composed of histamine, carbachol and 2Na-ATP was then applied to test the cell's viability. No Ca^{2+} response was evoked by the agonist cocktail, suggesting that the astrocyte has been damaged by the laser intensity protocol. These data provided us with an indication of acceptable levels of laser power (< 2%) that were acceptable to use for subsequent experiments. In all experiments agonist cocktail is applied at the end of the recording to verify that the cell remained responsive to stimulation of its Gq GPCRs.

2.4.2. Effects of imaging time at fixed 0.2% laser power on spontaneous astrocyte microdomains

We next attempted to determine the effects of imaging time at fixed laser power on spontaneous astrocytic Ca^{2+} activity. Astrocytic Ca^{2+} elevations were continuously monitored using confocal microscopy at 0.2% laser power for 60 min (Fig. 2.3).

Recording was broken down into three windows, 20 min for each. Frequency of Ca^{2+} elevations was compared among these three intervals. The results showed no significant changes in astrocyte Ca^{2+} elevations frequency among these three time windows (Fig. 2.3D; n = 4 cells, $p > 0.1$), suggesting that the frequency of astrocyte Ca^{2+} activity is not affected by long-term exposure to 0.2% laser light. Based on these findings, all subsequent experiments were performed using 0.2% laser output power.

2.4.3 Global increase followed by inhibition of neuronal firing does not result in significant changes in size or frequency of spontaneous astrocytic Gq GPCR activity

Since increased frequency of astrocytic Ca^{2+} activity was observed in the presence of low-level mGlu Gq GPCR agonists, (Zur Nieden and Deitmer, 2006), the possibility that some astrocytic Gq GPCR activity can be driven by local glutamate spill over from synaptic transmission was tested in this study. To determine if spontaneous astrocyte Gq GPCR signaling domains are driven by action-potential mediated synaptic transmission, neuronal firing frequency was first elevated, and then blocked, during recording of spontaneous astrocyte Ca^{2+} transients. Elevated extracellular K^+ from 2.5 to 5.0 mM was used to increase neuronal firing frequencies, after which TTX was applied to block action potentials (Fig. 2.4). Surprisingly, no significant difference was found in the frequency of microdomain or whole-cell astrocyte Ca^{2+} elevations when synaptic transmission was globally increased or inhibited compared to basal conditions (Fig. 2.5A, n = 8 cells from 8 slices). It is possible that action potentials result in stronger stimulation of astrocytic Gq GPCRs, leading to larger areas of astrocyte Ca^{2+} domains. To test this, the area of propagation of each Ca^{2+} transient was compared by breaking down microdomain

oscillations into small (less than 100 μm^2), medium (between 100 and 500 μm^2) and large (more than 500 μm^2) areas. There was no significant difference in microdomain area in 5.0 mM K^+ or in 5.0 mM K^+ + TTX compared to the baseline 2.5 mM K^+ condition. (Fig. 2.5B). These data suggest that neuronal action potentials are not responsible for producing whole-cell or microdomain spontaneous astrocyte Gq GPCR activity.

2.4.4 Blockade of miniature neurotransmitter release results in significant changes in frequency of spontaneous astrocytic Ca^{2+} activity

Previous studies indicated that spontaneous astrocytic Ca^{2+} activity was unaffected when miniature vesicular neurotransmitter release was blocked (Nett et al. 2002; Parri and Crunelli, 2003). As these studies only examined somatic Ca^{2+} activity in astrocytes, it has remained unclear whether Ca^{2+} activity in local astrocyte processes can be affected by blockade of miniature neurotransmitter release. To address this possibility, we applied Bafilomycin A1, a vacuolar type H^+-ATPase inhibitor which blocks neurotransmitter loading into synaptic vesicles, to deplete miniature neurotransmitter release. In the experimental condition, slices were incubated in Bafilomycin A1 for at least two hours prior to the recording. In the control condition, slices were incubated in regular ACSF without Bafilomycin A1 for at least two hours. To ensure full block of neurotransmitter release, slices were also incubated in TTX for 30-60 min prior to recording Ca^{2+} activity. After 12 min baseline recording, an agonist cocktail composed of histamine, carbachol and 2Na-ATP was bath-applied as a positive control for astrocytic Gq GPCR responsiveness. Compared to control slices, astrocytes in slices incubated in Bafilomycin A1 exhibited a significantly reduced frequency of spontaneous Gq GPCR

activity (Fig. 2.6C; n = 7 cells for control group; n = 8 cells for bafilomycin group; $p < 0.05$). Interestingly, however, the spontaneous microdomain Ca^{2+} activity was not fully depleted in the presence of Bafilomycin A1, suggesting that some of the microdomain Ca^{2+} transients are due to basal or constitutive Gq GPCR signaling activity. Taken together, these data suggest that a significant proportion of the spontaneous astrocytic microdomain Gq GPCR activity is driven by miniature neurotransmitter release.

2.4.5 Blockade of group I mGluRs does not result in significant changes in frequency of spontaneous astrocytic Ca^{2+} activity

It has been well established that group I mGluRs are the major Gq GPCRs involved in astrocytic Ca^{2+} responses evoked by Schaffer Collateral (SC) stimulation *in situ* or by sensory stimulation *in vivo* (Porter and McCarthy, 1996; Wang et al., 2006; Panatier et al., 2011; Honsek et al., 2012). However, the astrocytic Gq GPCRs responsible for spontaneous astrocytic Ca^{2+} elevations are still not fully elucidated. To investigate the role played by group I mGluRs in the generation of spontaneous astrocytic Ca^{2+} elevations, we compared astrocytic Ca^{2+} elevation frequency for 10 min before and after application of the group I mGluR antagonists CPCCOEt (100 μM) and 20 μM MPEP (20 μM). The group I mGluR agonist DHPG was also applied at the end of the experiment as a control to verify that the group I mGluR antagonists were effectively blocking Group I mGluRs. No Ca^{2+} response was evoked by DHPG, confirming functional blockade of group I mGluRs by CPCCOEt and MPEP. This was followed by application of agonist cocktail as a positive control to determine the cell's responsiveness to stimulation of Gq GPCRs (Fig. 2.7 A,B). Overall, there was no significant change in

the frequency of spontaneous astrocytic Ca^{2+} activity while group I mGluR were blocked, suggesting that Group I mGluRs are not responsible for the generation of spontaneous Ca^{2+} activity in astrocytes (Fig. 2.7 C). These findings suggest that other types of astrocytic Gq GPCRs stimulated by miniature vesicular release of neurotransmitter are involved in triggering spontaneous astrocytic Ca^{2+} events.

2.5 Discussion

The mechanisms underlying spontaneous astrocytic Ca^{2+} elevations have remained mysterious. They may represent activity "intrinsic" to the astrocyte due to constitutive or basal signaling of Gq GPCRs in the absence of agonist, or alternatively they could be activity dependent, driven by local neurotransmitter release. Previous work has indicated that spontaneous Ca^{2+} oscillations in the astrocyte soma occur independent of neuronal activity, supporting the idea that this activity is intrinsic (Aguado et al 2002; Nett et al. 2002). However, these studies recorded activity restricted to the astrocyte soma, leaving open the possibility that spontaneous Ca^{2+} activity in astrocyte fine processes is neuronally-driven. Each astrocyte is thought to encompass a volume corresponding to over 100,000 synapses (Bushong et al., 2002). As it is known that astrocytes are important for regulating neuronal excitability by uptake of potassium and glutamate, local stimulation of astrocytic Gq GPCRs would redefine domains of neuron-to-astrocyte communication and open the door to synapse specific modulation of potassium and glutamate uptake by astrocytes. Therefore, we set out to determine: a) the role of neuronal action potentials; and b) the role of miniature or quantal vesicular release, in the

generation of astrocyte microdomain Gq GPCR activity. We were surprised to find that manipulation of neuronal action potentials had no effect on the frequency or size (area of propagation) of astrocyte microdomain Ca^{2+} activity. We first increased neuronal firing rates by doubling the extracellular K^+ from 2.5 to 5.0 mM. As extracellular K^+ is a primary determinant of cellular resting membrane potential, neurons depolarized by 10.09 mV and increased their firing frequency by 0.268 Hz following this manipulation (Xie, 2011). Then in the same recording neuronal action potentials were blocked by TTX. Neither manipulation affected astrocytic Ca^{2+} microdomains. These data indicated that spontaneous astrocytic microdomain Ca^{2+} elevations occur independently of neuronal action potentials, suggesting that spontaneous astrocyte Gq GPCR activity is intrinsic to the astrocyte, at least as far as neuronal action potentials are concerned, which is in agreement with previous studies (Nett et al., 2002; Aguado et al., 2002). However, as a previous study indicated that high-frequency SC stimulation evoked astrocyte whole-cell Ca^{2+} responses (Porter and McCarthy, 1996), our findings do not exclude the possibility that some Ca^{2+} microdomain activity can be evoked by low intensity SC stimulation, which is the focus of Chapter 3. Furthermore, if the frequency of baseline intrinsic spontaneous astrocyte Ca^{2+} activity is very high, it could potentially obscure any possible Ca^{2+} transients evoked by elevated neuronal activity. Due to this caveat, direct low intensity SC stimulation may reveal astrocytic Gq GPCR responses. By gradually bringing down SC stimulation intensity, it will allow us to determine whether astrocytes are capable of responding to neuronal activity with Ca^{2+} elevations at the microdomain level.

Application of TTX will only block action potential driven neurotransmitter release, leaving open the possibility that miniature or quantal release of neurotransmitter is responsible for spontaneous astrocyte Ca^{2+} microdomains. To test this possibility we compared the spontaneous astrocyte Ca^{2+} activity in slices incubated in Bafilomycin A1 to control incubated slices. Surprisingly, our data indicated a significant reduction in spontaneous astrocyte Ca^{2+} transients when Bafilomycin was present, a result contradicting earlier findings in the astrocyte soma made by Nett et al. in 2002. A major difference between Nett et al.'s experimental approach and ours is the method to load Ca^{2+} indicator. In their study the traditional bulk-loading technique was used to study the Bafilomycin effect rather than using patch clamp to fill the astrocyte small compartments with Ca^{2+} indicator as we have used. An additional drawback of the bulk-loading technique is that only cells close to the slice surface can take up the dye. This prevents analysis of Ca^{2+} activity from astrocytes deeper in the slice, which are usually healthier than those near the surface. Another main difference we have noticed between Nett's study and ours, that we have difficulty in reconciling, is the frequency of Ca^{2+} activity recorded from the soma. Nett et al. found a very high frequency of astrocyte soma Ca^{2+} transients with regular periodicity, leading these researchers to refer to these events as "oscillations". Based on our own data, most of the spontaneous astrocyte Ca^{2+} transients are restricted to microdomains, are not oscillatory, and rarely propagate to the cell body (Fig. 2.5 D). These differences could be due in part to differences in cell health or incubation chambers used.

Bafilomycin A1 did not fully block spontaneous astrocyte Ca^{2+} elevations in our

studies. Therefore, the data suggest that the majority of spontaneous astrocyte Gq GPCR activity is governed by quantal vesicular release, while the remaining events are driven by mechanisms solely "intrinsic" to the cells, namely constitutive Gq GPCR activity. Our findings in comparison to those of Nett et al. raise the possibility that, if the cells do not maintain full health, they may no longer be under proper control by neuronal activity, leading toward a shift in favor of "intrinsic" mechanisms. In such circumstances, any effect caused by Bafilomycin would never be detectable anymore.

If miniature vesicular release of neurotransmitter is responsible for a large proportion of microdomain astrocyte Ca^{2+} activity, which astrocytic Gq GPCRs are responsible? Multiple reports point to a role for astrocytic group I mGluRs in neuronally-driven astrocyte Ca^{2+} activity. Surprisingly, we found no significant effects of group I mGluR antagonists on spontaneous microdomain Ca^{2+} elevations in astrocytes, an observation contradicting previous studies (Zur Nieden and Deitmer, 2006). This is surprising given that evoked astrocyte Ca^{2+} responses are driven largely by group I mGluRs. Since astrocytes exhibit numerous types of Gq GPCRs (Porter and McCarthy, 1997; Shelton and McCarthy, 2000), future work will be needed to determine which neurotransmitter and which astrocytic receptor(s) are responsible for this activity, and what its physiological purpose is. Candidate neurotransmitters include ATP, acetylcholine, GABA, and cannabinoids, all of which have been shown to stimulate astrocyte Ca^{2+} responses (Araque et al., 2002; Oka et al., 2006; Navarrete and Araque, 2008). The most straightforward approach to test this is to apply an antagonist cocktail containing blockers of P2YRs, mAchRs, $GABA_B$Rs and CB1Rs in the presence of TTX. If spontaneous Ca^{2+}

activity in astrocytes is largely abolished by this treatment, then different combinations of antagonists can be applied until the most essential receptor is identified.

2.6 References

Aguado F, Espinosa-Parrilla JF, Carmona MA, Soriano E (2002) Neuronal activity regulates correlated network properties of spontaneous calcium transients in astrocytes in situ. J Neurosci 22:9430-9444.

Agulhon C, Petravicz J, McMullen AB, Sweger EJ, Minton SK, Taves SR, Casper KB, Fiacco TA, McCarthy KD (2008) What is the role of astrocyte calcium in neurophysiology? Neuron 59:932-946.

Araque A, Li N, Doyle RT, Haydon PG (2000) SNARE protein-dependent glutamate release from astrocytes. J Neurosci 20:666-673.

Araque A, Martin ED, Perea G, Arellano JI, Buno W (2002) Synaptically released acetylcholine evokes Ca^{2+} elevations in astrocytes in hippocampal slices. J Neurosci 22:2443-2450.

Bushong EA, Martone ME, Jones YZ, Ellisman MH (2002) Protoplasmic astrocytes in CA1 stratum radiatum occupy separate anatomical domains. J Neurosci 22:183-192.

Charles AC (1994) Glia-neuron intercellular calcium signaling. Dev Neurosci 16:196-206.

de Ligt RA, Kourounakis AP, AP IJ (2000) Inverse agonism at G protein-coupled receptors: (patho)physiological relevance and implications for drug discovery. Br J Pharmacol 130:1-12.

Fatatis A, Russell JT (1992) Spontaneous changes in intracellular calcium concentration in type I astrocytes from rat cerebral cortex in primary culture. Glia 5:95-104.

Fiacco TA, McCarthy KD (2004) Intracellular astrocyte calcium waves in situ increase the frequency of spontaneous AMPA receptor currents in CA1 pyramidal neurons. J Neurosci 24:722-732.

Harris-White ME, Zanotti SA, Frautschy SA, Charles AC (1998) Spiral intercellular calcium waves in hippocampal slice cultures. J Neurophysiol 79:1045-1052.

Hermans E, Challiss RA (2001) Structural, signalling and regulatory properties of the group I metabotropic glutamate receptors: prototypic family C G-protein-coupled receptors. Biochem J 359:465-484.

Hirase H, Qian L, Bartho P, Buzsaki G (2004) Calcium dynamics of cortical astrocytic networks in vivo. PLoS Biol 2:E96.

Honsek SD, Walz C, Kafitz KW, Rose CR (2012) Astrocyte calcium signals at Schaffer collateral to CA1 pyramidal cell synapses correlate with the number of activated synapses but not with synaptic strength. Hippocampus 22:29-42.

McKinney RA, Capogna M, Durr R, Gahwiler BH, Thompson SM (1999) Miniature synaptic events maintain dendritic spines via AMPA receptor activation. Nat Neurosci 2:44-49.

Navarrete M, Araque A (2008) Endocannabinoids mediate neuron-astrocyte communication. Neuron 57:883-893.

Nett WJ, Oloff SH, McCarthy KD (2002) Hippocampal astrocytes in situ exhibit calcium oscillations that occur independent of neuronal activity. J Neurophysiol 87:528-537.

Nimmerjahn A, Kirchhoff F, Kerr JN, Helmchen F (2004) Sulforhodamine 101 as a specific marker of astroglia in the neocortex in vivo. Nat Methods 1:31-37.

Oka M, Wada M, Wu Q, Yamamoto A, Fujita T (2006) Functional expression of metabotropic GABAB receptors in primary cultures of astrocytes from rat cerebral cortex. Biochem Biophys Res Commun 341:874-881.

Panatier A, Vallee J, Haber M, Murai KK, Lacaille JC, Robitaille R (2011) Astrocytes are endogenous regulators of basal transmission at central synapses. Cell 146:785-798.

Parri HR, Crunelli V (2003) The role of Ca^{2+} in the generation of spontaneous astrocytic Ca^{2+} oscillations. Neuroscience 120:979-992.

Parri HR, Gould TM, Crunelli V (2001) Spontaneous astrocytic Ca^{2+} oscillations in situ drive NMDAR-mediated neuronal excitation. Nat Neurosci 4:803-812.

Petravicz J, Fiacco TA, McCarthy KD (2008) Loss of IP3 receptor-dependent Ca^{2+} increases in hippocampal astrocytes does not affect baseline CA1 pyramidal neuron synaptic activity. J Neurosci 28:4967-4973.

Porter JT, McCarthy KD (1996) Hippocampal astrocytes in situ respond to glutamate released from synaptic terminals. J Neurosci 16:5073-5081.

Porter JT, McCarthy KD (1997) Astrocytic neurotransmitter receptors in situ and in vivo. Prog Neurobiol 51:439-455.

Shelton MK, McCarthy KD (2000) Hippocampal astrocytes exhibit Ca^{2+}-elevating muscarinic cholinergic and histaminergic receptors in situ. J Neurochem 74:555-563.

Sutton MA, Ito HT, Cressy P, Kempf C, Woo JC, Schuman EM (2006) Miniature neurotransmission stabilizes synaptic function via tonic suppression of local dendritic protein synthesis. Cell 125:785-799.

Wang X, Lou N, Xu Q, Tian GF, Peng WG, Han X, Kang J, Takano T, Nedergaard M (2006) Astrocytic Ca^{2+} signaling evoked by sensory stimulation in vivo. Nat Neurosci 9:816-823.

Xie X (2011) Long-term plasticity of astrocytic metabotropic neurotransmitter receptors driven by changes in neuronal activity in hippocampal slices. Ph.D. Thesis--University of California, Riverside.

Zhou Q, Petersen CC, Nicoll RA (2000) Effects of reduced vesicular filling on synaptic transmission in rat hippocampal neurones. J Physiol 525 Pt 1:195-206.

Zur Nieden R, Deitmer JW (2006) The role of metabotropic glutamate receptors for the generation of calcium oscillations in rat hippocampal astrocytes in situ. Cereb Cortex 16:676-687.

Figure Legends

Figure 2.1 Determining Gq GPCR signaling domains in an astrocyte.

Left: A single astrocyte patch-clamped with OGB-1 Ca^{2+} indicator dye. Numbered ROIs over astrocyte compartments match fluorescence intensity over time traces at right.

Right: 10 min baseline recording of spontaneous astrocytic Ca^{2+} activity. As stated in the "Materials and Methods" section, spontaneous Ca^{2+} elevations were identified using the three standard deviations criteria (Honsek et al., 2012). Adjacent ROIs with Ca^{2+} transients with intervals < 10 s were grouped together as a single Gq GPCR signaling domain. ROIs increasing fluorescence intensity at the same time but with at least one intervening ROI that did not increase in intensity were considered separate domains occurring at the same time. In this representative example, ten Gq GPCR signaling domains (A-J) were identified.

Figure 2.2 Effects of increasing laser output power on spontaneous astrocytic Ca^{2+} elevations.

(A) A single astrocyte was patch-clamped with OGB-1 Ca^{2+} indicator dye. Colored boxes (ROIs) were placed over all visible astrocyte compartments, each with a particular number that matches the number of each fluorescence intensity over time trace in (C).

(B) The astrocyte's membrane potential was stepped from -180 mV to +80 mV in 20 mV increments. This voltage-step protocol induced passive currents in the astrocyte. Following each voltage step was a -5 mV test pulse to monitor changes in access resistance.

(C) Ca^{2+} elevations from ROIs were recorded from the astrocyte over increasing intensities of laser power: 0.2 %, 0.5 %, 1 %, 2 %, 5 %, 10 %, 20 %, each for 5 min. A Gq GPCR agonist cocktail composed of 10 μM ea. of histamine, carbachol, and ATP was applied at the end of the recording to test the viability of the cell. The arrowheads represent focus-adjusted (FA) points to compensate for "slice drift". (n = 4).

Figure 2.3 Effects of exposure to 0.2% confocal laser light over time on astrocytic Ca^{2+} activity.

(A) A single astrocyte was patch-clamped with OGB-1 Ca^{2+} indicator dye. Colored boxes (ROIs) were placed over all visible astrocyte compartments, each with a particular number that matches the number in the fluorescence intensity over time trace in (C).

(B) The cell's membrane potential was stepped from -180 mV to +80 mV in 20 mV increments. This voltage-step protocol produced passive currents, unequivocally identifying the cell as an astrocyte. Following each voltage step was a -5 mV test pulse to monitor changes in access resistance.

(C) Ca^{2+} activity was recorded from an astrocyte over 60 min with 0.2 % laser output power. The arrowheads represent focus-adjusted (FA) points to compensate for "slice drift".

(D) The frequency of microdomain astrocytic Ca^{2+} activity did not change over the three 20 min time periods ($n = 4$, $p > 0.1$).

Figure 2.4 Microdomain astrocyte Ca^{2+} activity under conditions of 2.5 mM K^+ (control), 5 mM K^+ and 5 mM K^++TTX.

(A) A single astrocyte filled with OGB-1 Ca^{2+} indicator dye via patch clamp. Colored ROIs match fluorescence intensity over time traces in (C).

(B) The cell exhibited a passive current profile to a voltage-step protocol (-180 to +80 mV in 20 mV increments), identifying it as an astrocyte.

(C) Gq GPCR activity recorded from an astrocyte. Slices were bathed in regular ACSF for 20 min while the baseline recording was obtained, at which time the medium was switched to ACSF containing 5.0 mM K^+. After an additional 20 min, TTX was bath applied and remained in solution for another 20 min. At the end of the experiment, the group I mGluR agonist DHPG (50 µM) was applied to confirm that the astrocyte has intact mGluR responses. Arrowheads represent focus-adjusted (FA) points to compensate for "slice drift".

Figure 2.5 Frequency and size distribution of spontaneous astrocytic Ca^{2+} elevations following elevated or blocked neuronal firing.

(A) Frequency of total elevations, microdomain elevations and whole-cell elevations recorded under the conditions of 2.5 mM K^+ (control), 5.0 mM K^+ or 5.0 mM K^+ +TTX. Overall, there were no significant effects produced by increasing neuronal firing rates or blocking neuronal firing in TTX compared to the control condition ($n = 8$, $p > 0.1$).

(B) Size distribution of spontaneous microdomain Ca^{2+} elevations in 2.5 mM K^+(control), 5.0 mM K^+ or 5.0 mM K^+ +TTX. Overall, the area of propagation of microdomain astrocytic Ca^{2+} elevations was not affected by neuronal action potentials ($n = 8$, $p > 0.1$).

Figure 2.6 Spontaneous astrocytic Ca^{2+} elevations following blockade of quantal vesicular release of neurotransmitters.

(A) Top: A single astrocyte in the control condition (incubation in ACSF without Bafilomycin A1) patch-clamped with OGB-1 Ca^{2+} indicator dye. Colored ROIs placed over individual astrocytic compartments match numbered fluorescence intensity over time traces, below. Bottom: Astrocyte Ca^{2+} activity was recorded throughout the astrocyte for a minimum of 10 min, after which time agonist cocktail (histamine, carbachol and ATP, 10 μM ea.) was applied as a positive control to evoke a whole-cell Gq GPCR response. TTX was applied during the entire period to block any potential effects caused by action potentials.

(B) Top: A single astrocyte after minimum 2 hr. incubation in Bafilomycin A1 (experimental condition) patch-clamped with OGB-1 Ca^{2+} indicator dye. Numbered ROIs in astrocyte compartments match fluorescence intensity over time traces below. Bottom: Astrocytic Ca^{2+} activity was recorded for a minimum of 10 min, after which agonist cocktail was applied as a positive control to evoke a whole-cell astrocyte Gq GPCR response. TTX was applied during the entire period to block any possible effects caused by action potentials. Arrowheads represent focus-adjusted (FA) points to compensate for "slice drift".

(C) Frequency of spontaneous Ca^{2+} elevations was compared between control and Bafilomycin-treated astrocytes. A markedly reduced frequency of spontaneous Ca^{2+} elevations was observed in Bafilomycin-treated astrocytes compared to the untreated astrocytes. ($n = 7$ in control group; $n = 8$ in Bafilomycin group; $*p < 0.05$).

(D) Percentage of spontaneous astrocytic Ca^{2+} elevations including the soma *versus* events that did not include the soma was compared for both control and Bafilomycin groups. Both groups showed a higher percentage of Ca^{2+} elevations occurring in restricted domains of astrocyte processes that did not propagate to the soma ($n = 7$ for both groups, $*p < 0.05$)

Figure 2.7 Spontaneous astrocytic Ca^{2+} activity before and after block of group I mGluRs.

(A) Left: A single astrocyte patch-clamped with OGB-1 Ca^{2+} indicator dye. Numbered ROIs over astrocyte compartments match fluorescence intensity over time traces at right. Right: Following 10 min baseline recording of spontaneous astrocytic Ca^{2+} activity, the group I mGluR antagonists CPCCOEt (100 μM) and MPEP (20 μM) were bath applied for 10 min. The group I mGluR agonist DHPG (50 μM) was then applied as a control to ensure that group 1 mGluRs were indeed blocked by MPEP+ CPCCOEt. At the end of the recording, agonist cocktail containing histamine, carbachol and 2Na-ATP (10 μM ea.) was applied as a positive control to evoke a whole-cell astrocyte Gq GPCR response.

(B) The frequency of spontaneous astrocytic Ca^{2+} elevations in the presence of group I mGluR antagonists was compared to 10 min. of baseline activity. These data suggest that spontaneous astrocytic Gq GPCR activity is not driven by neuronal glutamate stimulating astrocytic mGluRs ($n = 4$, $p > 0.1$).

Figure 2.1

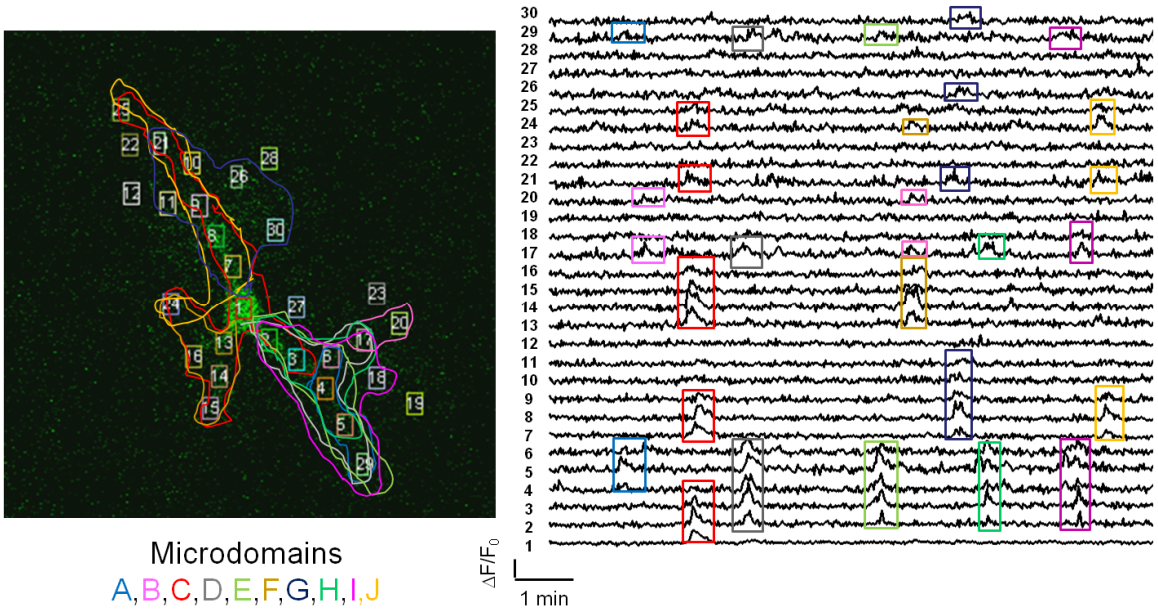

Figure 2.2

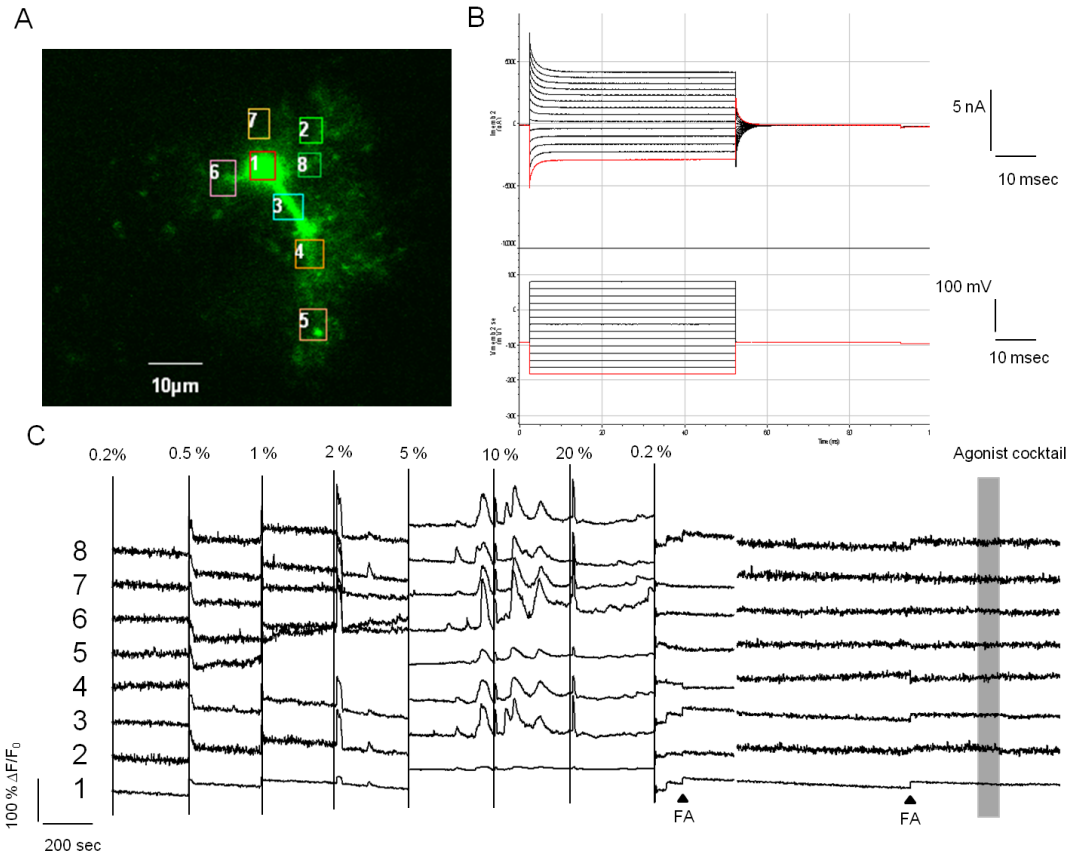
A
B
C
10µm
5 nA
10 msec
100 mV
10 msec
0.2%
0.5 %
1 %
2 %
5 %
10 %
20 %
0.2 %
Agonist cocktail
8
7
6
5
4
3
2
1
100 % ΔF/F0
200 sec
FA
FA

Figure 2.3

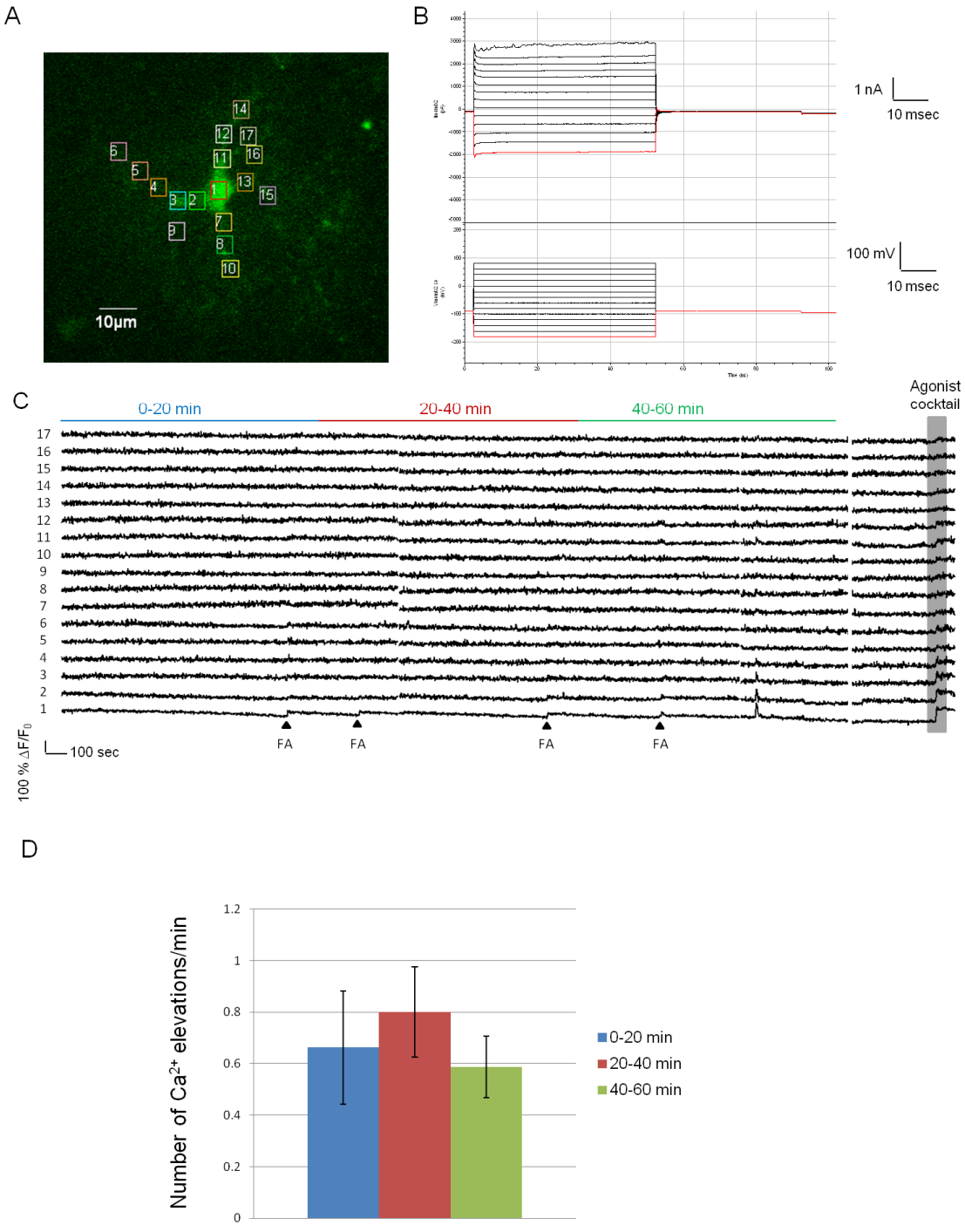
A
B
C
D
10µm
1 nA
10 msec
100 mV
10 msec
0-20 min
20-40 min
40-60 min
Agonist cocktail
100 % ΔF/F0
100 sec
FA
FA
FA
FA
Number of Ca2+ elevations/min
0-20 min
20-40 min
40-60 min

Figure 2.4

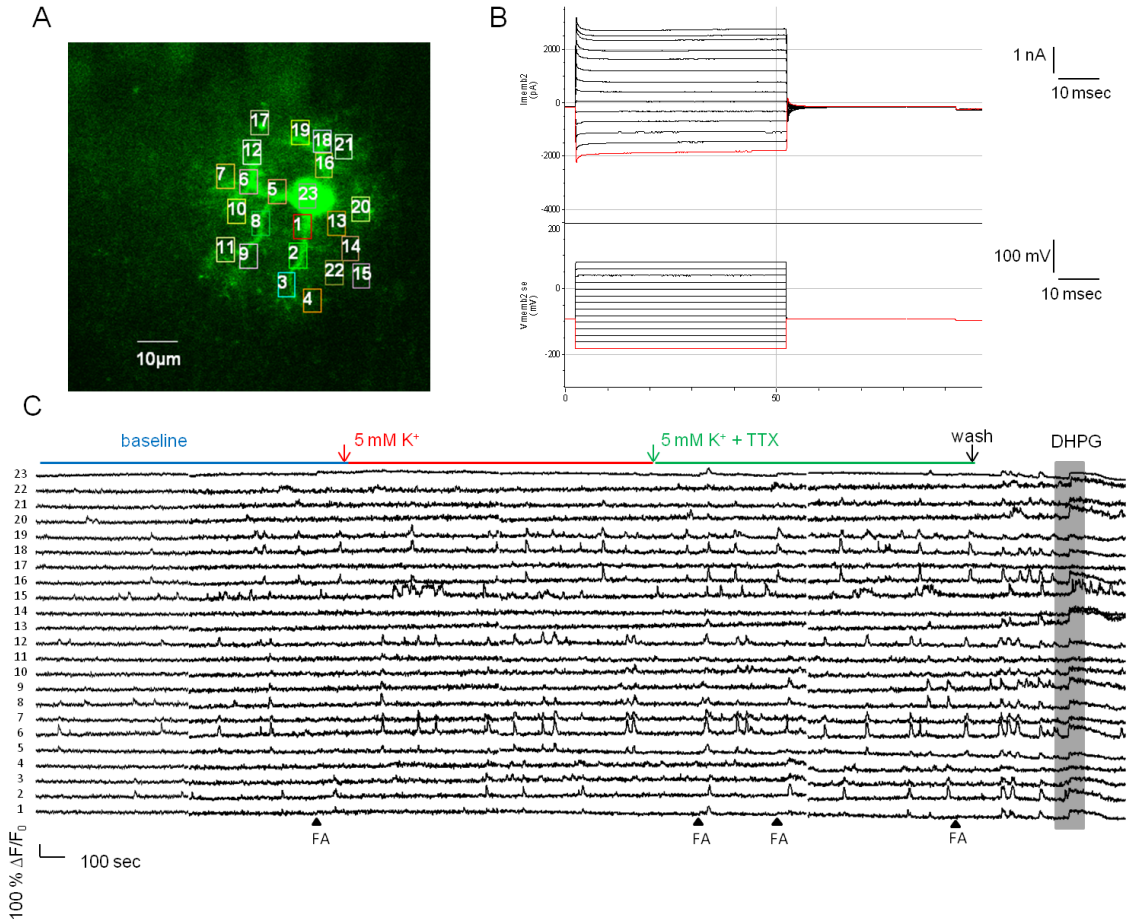
A
B
C
10µm
1 nA
10 msec
100 mV
10 msec
baseline
5 mM K+
5 mM K+ + TTX
wash
DHPG
FA
FA
FA
FA
100 sec
100 % ΔF/F0

Figure 2.5

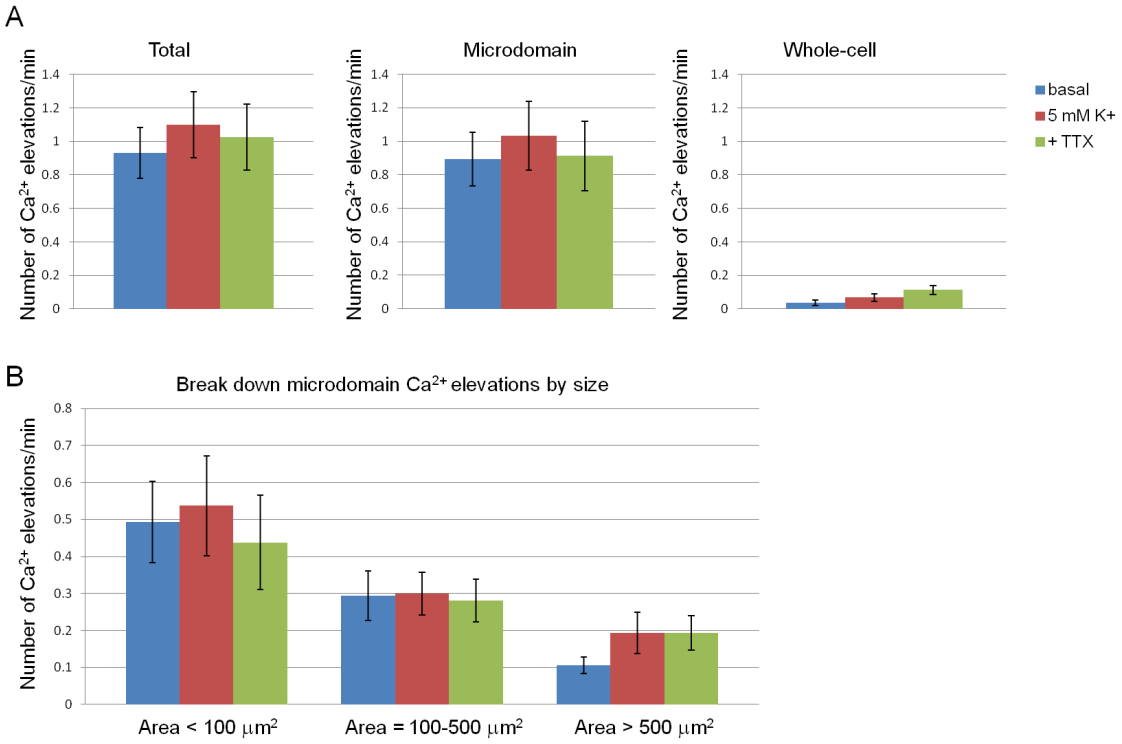
A
Total
Microdomain
Whole-cell
Number of Ca2+ elevations/min
basal
5 mM K+
+ TTX
B
Break down microdomain Ca2+ elevations by size
Number of Ca2+ elevations/min
Area < 100 μm2
Area = 100-500 μm2
Area > 500 μm2

Figure 2.6

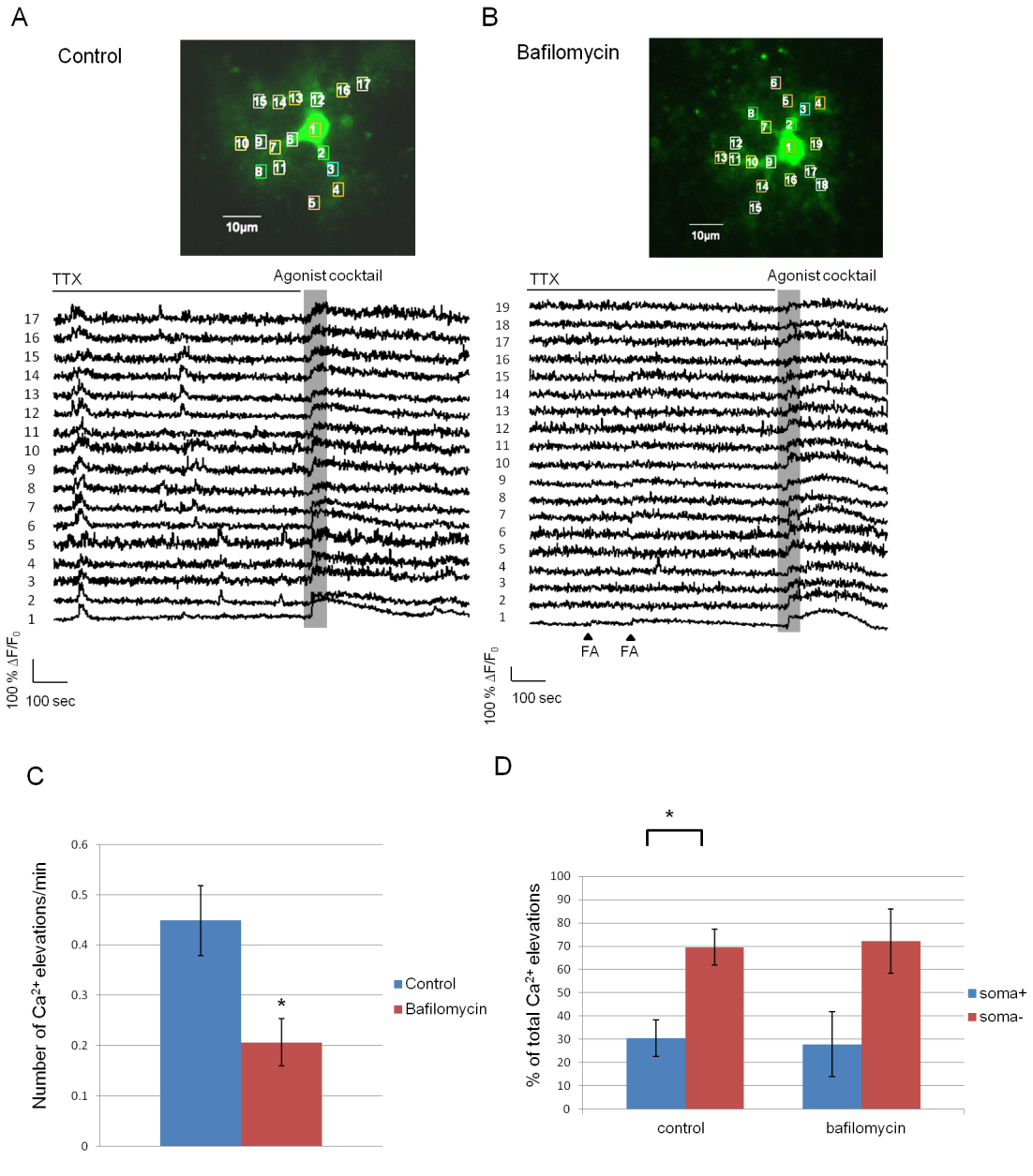
A
Control
10μm
TTX
Agonist cocktail
100 % ΔF/F0
100 sec
B
Bafilomycin
10μm
TTX
Agonist cocktail
FA
FA
100 % ΔF/F0
100 sec
C
Number of Ca2+ elevations/min
Control
Bafilomycin
*
D
% of total Ca2+ elevations
*
soma+
soma-
control
bafilomycin

Figure 2.7

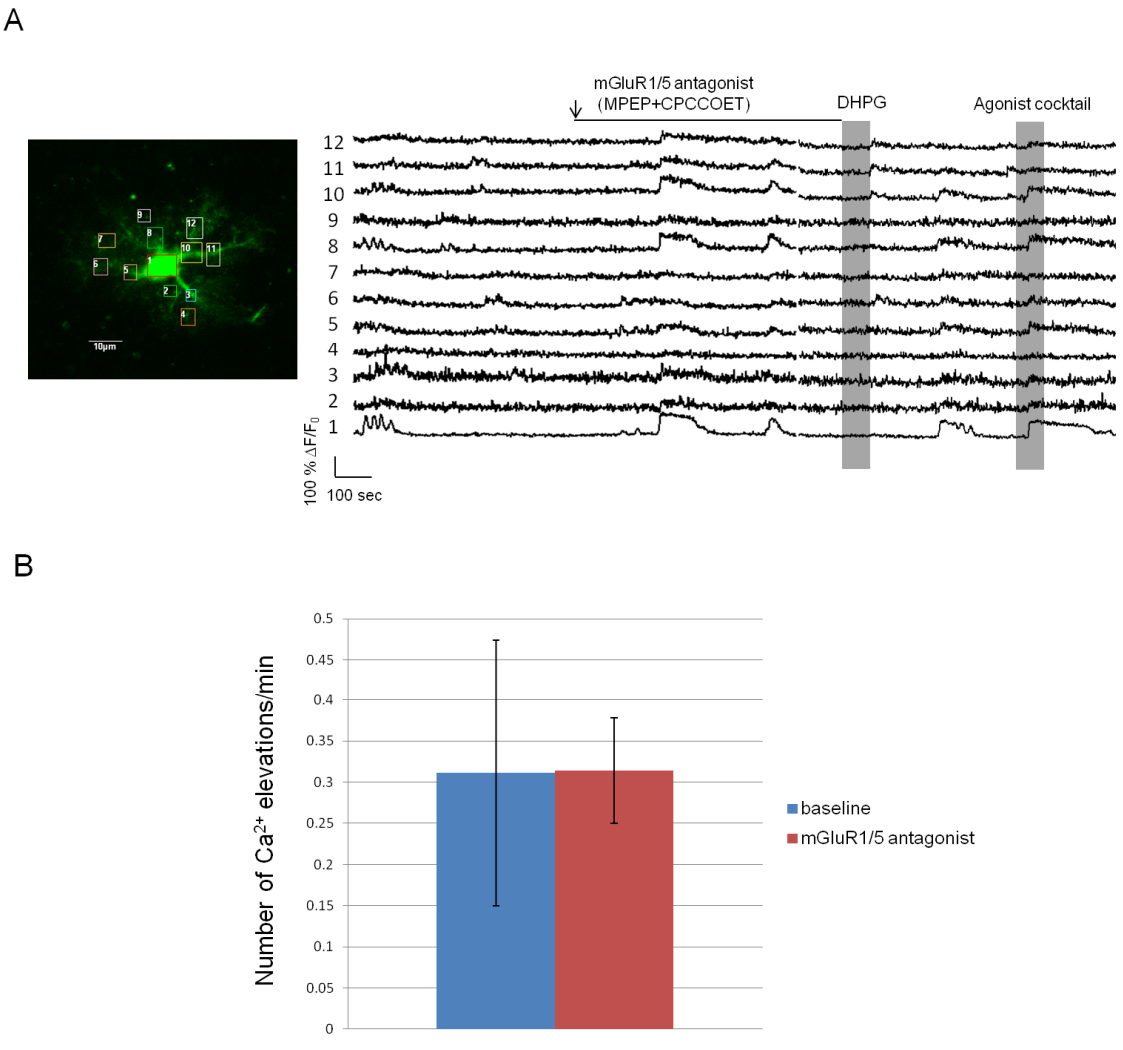
A
mGluR1/5 antagonist
(MPEP+CPCCOET)
DHPG
Agonist cocktail
12
11
10
9
8
7
6
5
4
3
2
1
100 % ΔF/F0
100 sec
B
Number of Ca2+ elevations/min
0.5
0.45
0.4
0.35
0.3
0.25
0.2
0.15
0.1
0.05
0
baseline
mGluR1/5 antagonist

Chapter 3: Assaying for Gq GPCR signaling domains of neuron-to-astrocyte communication using low intensity Schaffer Collateral stimulation

3.1 Abstract

It has been well established that neurons can stimulate astrocytic Gq subtype G protein coupled receptors (Gq GPCRs), resulting in Ca^{2+} elevations that propagate throughout the astrocyte and its processes. It remains unclear, however, the level of neuronal activity required to elicit an astrocytic Gq GPCR response. In stratum radiatum (*s.r.*) of the hippocampus, high-frequency stimulation (HFS, 50 pulses for 1 second) of Schaffer Collaterals (SC) evokes astrocytic group I metabotropic glutamate receptor (mGluR)-mediated Ca^{2+} elevations in the astrocyte soma, raising the possibility that low-level SC stimulation might be capable to evoke astrocyte Ca^{2+} elevations only in microdomains. There were two interesting questions derived from this hypothesis: 1) What is the threshold of neuronal activity required to elicit an astrocytic Gq GPCR response; and 2) Once this threshold is reached, do astrocytes respond in a microdomain or whole-cell manner? To address these questions, we first tested whether astrocytes can respond to various levels of low intensity SC stimulation, ranging from single pulses or 3 pulses to the Schaffer collaterals, to evoking a defined number of action potentials in a single neuron. Astrocytes in CA1 *s.r.* of acute mouse hippocampal slices were identified with Sulforhodamine 101 (SR101) staining and bolus-loading with Oregon Green BAPTA-1 (OGB-1) AM Ca^{2+} indicator dye. Ca^{2+} elevations were monitored using confocal microscopy. Application of three pulses to SCs (ranging from 25-150 μA) evoked astrocytic Ca^{2+} responses detected within a consistent time interval. Interestingly,

these evoked Ca^{2+} transients always included the cell soma, and were larger in size compared to spontaneous Ca^{2+} microdomains, which were most often restricted to a local area without propagating to the cell body (See Chapter 2). This finding suggests that these two events are qualitatively different, despite the observation that the responses often did not include the entire astrocyte. Following this observation, we modified a few parameters in the stimulation protocol and applied single pulse SC stimulation to examine the possibility of evoking local Ca^{2+} microdomains in astrocytes. Application of single pulses to SCs (ranging from 7-120 μA) evoked astrocytic Ca^{2+} responses with a more variable latency. Interestingly, even though most of these evoked Ca^{2+} transients included the cell soma, some were indeed restricted to a local area without propagating to the cell body. Surprisingly, antagonists of group I metabotropic glutamate Gq GPCR receptor mGluRs only partially reduced astrocyte Gq GPCR responses to single pulse SC stimulation, suggesting that other types of astrocytic Gq GPCRs contribute to these evoked events. Finally, we applied stimulation to single neurons by injecting current via whole-cell patch clamp to evoke a defined number of action potentials while recording Gq GPCR responses in astrocytes adjacent to visible synaptic boutons from the stimulated neuron. This approach, while powerful, turned out to be technically challenging, and more advanced methods will be needed to address this issue conclusively.

3.2 Introduction

Studies over the past ten years have introduced a new concept, the tripartite synapse, which includes astrocytes as an active participant in synaptic communication (Ben Barres 2011). It is now well-established that astrocytes can respond to elevated levels of neuronal activity with Ca^{2+} elevations, resulting from the activation of Gq GPCRs and IP_3-mediated Ca^{2+} release from intracellular stores. In CA1 *s.r.* of the hippocampus, high-frequency stimulation (50 pulses for 1 second) of Schaffer Collaterals evokes astrocytic group I mGluR-mediated Ca^{2+} elevations that propagate throughout the cell (Porter and McCarthy, 1996). Moreover, in an *in vivo* study in rats, astrocytes in barrel cortex were able to respond to whisker stimulation with whole-cell or global Ca^{2+} elevations (Wang et al., 2006). As already discussed in Chapter 2, astrocytes are also known to exhibit spontaneous microdomain Ca^{2+} transients independent of any experimental stimulation. A hypothesis derived from these findings is that astrocytes could potentially respond to lower levels of SC stimulation with local Ca^{2+} elevations restricted in their processes and without propagating to the soma area. The capability of astrocytes to respond to lower levels of SC stimulation has been indicated recently, during the same time we were conducting our studies (Honsek et al., 2012). However, the precise manner in which astrocytes responded to low level SC stimulation was not fully elucidated. Specifically, the two main questions we set out to address - the astrocyte response threshold and the characteristics of the astrocytic responses once threshold was reached - were not addressed in this study. Therefore, we first confirmed that CA1 *s.r.* astrocytes respond to SC stimulation at intensities lower than the high-frequency

stimulation models used thus far. Our *in situ* recording results from acute mouse hippocampal brain slices demonstrate that multiple astrocytes bolus-loaded with OGB-1 Ca^{2+} indicator dye responded to three pulses of SC stimulation (intensities ranging from 25-150 μA) with whole-cell Ca^{2+} elevations detected within a consistent time interval. Moreover, 87.7 % of the responses included the astrocyte soma, whereas only 22.5 % of spontaneous Ca^{2+} elevations in the same recordings during the 10 minute baseline prior to stimulation propagated to the cell body. These data suggest that astrocytes respond with a Ca^{2+} elevation to SC stimulation intensities much lower than what has been described previously, but that these responses, by including the astrocyte soma, are qualitatively different than spontaneous astrocyte microdomain Gq GPCR activity.

These findings left unanswered a very interesting question – Can we evoke local astrocytic Gq GPCR responses restricted to processes without propagating to the cell body? To test this possibility, we applied single pulse SC stimulation and modified the experimental approach. First, control experiments were performed to demonstrate that voltage-gated Ca^{2+} channels are not expressed by astrocytes. Results from these experiments eliminated the possibility that direct depolarization of astrocytes by the locally placed stimulating electrode evoked astrocytic Ca^{2+} responses by an alternative mechanism - VGCCs. Our data indicate that astrocytes indeed respond to single pulse SC stimulation, and some of these Gq GPCR responses are restricted to a local area without propagating to the cell body.

We also attempted to determine the main astrocytic Gq GPCRs responsible for the single pulse SC stimulation-evoked astrocyte Ca^{2+} responses. Surprisingly, blocking

group I mGluRs did not result in a complete reduction in astrocytic Ca^{2+} responses. These data suggest, contrary to other published reports, that other types of astrocytic Gq GPCRs are important for locally evoked astrocytic Ca^{2+} elevations. The identity of these receptors remains to be determined and is the focus of future studies.

Stimulation of SCs typically depolarizes a variable number of afferents from multiple neurons. It is possible that true astrocyte microdomains are evoked by single neuronal action potentials or a short train of temporally summated APs. To test this possibility we injected current via whole-cell patch clamp into individual CA1 or CA3 pyramidal neurons while recording Ca^{2+} activity in astrocytes located adjacent to visibly identified synaptic boutons along the neuronal axon. Due to technical problems, however, we were unable to determine if astrocytes can respond to a defined number of APs evoked in a single neuron. Thus, this question has not yet been fully answered and is still awaiting further investigation.

3.3 Materials and methods

Preparation of hippocampal slices.

All mice were housed in the animal facility at the University of California, Riverside in accordance with Institutional Animal Care and Use Committee guidelines. Parasagittal hippocampal slices (300 μm thick) were prepared from 12- to 18-day-old C57BL/6J (Jackson Laboratory, Bar Harbor, ME) wild-type mice using a Leica VT1200s Vibratome (Bannockburn, IL). Slices were prepared in ice-cold, nominally Ca^{2+}-free saline containing (in mM): 125 NaCl, 2.5 KCl, 3.8 $MgCl_2$, 1 NaH_2PO_4, 26.6 $NaHCO_3$,

and 25 glucose, bubbled with 5% CO_2-95% O_2. Subsequently, slices were incubated for 45 min at 35°C in oxygenated artificial cerebrospinal fluid (ACSF) containing (in mM) 125 NaCl, 2.5 KCl, 2.5 $CaCl_2$, 1.3 $MgCl_2$, 1 NaH_2PO_4, 26.6 $NaHCO_3$, and 25 glucose, bubbled with 5% CO_2-95% O_2. Following the incubation period at physiological temperature, slices were given 15 min to cool to room temperature and then transferred to a recording chamber (Warner Instrument), continuously superfused with oxygenated, room temperature ACSF.

Bolus-loading of passive astrocytes with Ca^{2+} indicator.

Slices were prepared as described above, except that they were incubated for 20 min at 35°C in low-Ca^{2+} (0.5 mM) ACSF consisting of 10 μM sulforhodamine-101 (SR101; Sigma), 10 min in low-Ca^{2+} ACSF, and then transferred to regular ACSF in room temperature 15 min prior to imaging. A bolus-loading pipette containing OGB-1 (Invitrogen) dissolved in 0.07% pluronic acid (Invitrogen) in ACSF (final DMSO concentration: 0.4%) was used for loading astrocytes 40 μm from the surface of the tissue.

Patch clamp of passive astrocytes.

Pipettes were pulled from borosilicate glass on a Narishige (Tokyo, Japan) PP-83 two-stage vertical pipette puller and not fire-polished. Pipettes were pulled to 7-8MΩ when filled with (in mM): 130 K-gluconate, 4 $MgCl_2$, 10 HEPES, 10 glucose, 1.185 Mg-ATP, 10.55 phosphocreatine, and 0.1315 mg/ml creatine phosphokinase, pH 7.3 by KOH (standard internal solution). The Ca^{2+}-indicator dye Oregon green BAPTA-1 (OGB-1 from Invitrogen; 200 μM) was also included. Whole-cell patch-clamp recordings of astrocytes were performed at room temperature using either a Multiclamp 700B amplifier

and PCLAMP 10.2 software (Axon Instruments, Union City, CA), or a EPC 10 dual patch amplifier and Patchmaster software (HEKA, Germany). After whole-cell configuration was obtained, passive astrocytes were verified by their electrophysiological properties (Fiacco and McCarthy, 2004). Passive Astrocytes typically rest at - 85 mV with low input resistances of 10 MΩ. They exhibit passive currents when stepped from -180 mV to +80 mV in 20 mV increments. A test pulse of -5 mV was included after each voltage step in order to monitor changes in access resistance. Astrocyte current signals were low-pass filtered at 2 kHz and digitized at 100 kHz via a DigiData 1440 (Axon Instruments) interfaced to a personal computer. A smooth, stable off-cell and formation of an outside-out patch was used as an indicator of minimal damage to the cell membrane during the patch procedure. During astrocyte recordings, solutions were switched using an electronic valve controller (Warner Instrument, Hamden CT).

Low level afferent stimulation of Schaffer collaterals.

For experiments using three pulse SC stimulation, a 2-3 μm tip diameter monopolar glass stimulating electrode was placed 75-80 μm away from the center of a field of OGB-1 bolus-loaded astrocytes (typically 3-5 astrocytes). Ca^{2+} activity was recorded in multiple astrocytes for 10 min as a baseline, after which low-level SC stimulation (three pulses at 50 Hz, 0.2 ms duration, intensity ranging from 25-150 μA) was generated and delivered via a stimulus isolator (World Precision Instruments A360) to SC fibers at 5 min intervals. Stimulation of the same intensity was applied twice in attempt to verify an astrocyte Ca^{2+} elevation as a response to stimulation. For experiments using single pulse SC stimulation, a 2-3 μm tip diameter monopolar glass

stimulating electrode was placed 20-40 μm from the edge of an individual astrocyte boundary defined by the limit of the cell's processes filled by patch-clamp with OGB-1. Astrocytic Ca^{2+} activity was recorded for a 5 min baseline, and low-level SC stimulation (single pulses of 0.2 ms duration, intensities ranging from 7-120 μA) was generated and delivered via a stimulus isolator (World Precision Instruments A360) to SC fibers at 5 min intervals. In both three pulse and single pulse SC stimulation experiments, TTX (1 μM) was used as a negative control to limit the potential of evoking astrocytic Ca^{2+} responses via direct depolarization of presynaptic afferents by the stimulating electrode.

For the single fiber stimulation experiments, A CA3 neuron was filled with Alexa 568 dye (Invitrogen), and after 15-30 min., the course of its axon and en passant boutons was followed through a field of stratum oriens (*s.o.*) or *s.r.* astrocytes bolus-loaded with OGB-1 Ca^{2+} indicator dye. Single and multiple neuronal action potentials were evoked in the neurons by injection of a brief depolarizing current of variable intensity and duration while in current clamp mode.

***Confocal imaging*.**

Hippocampal CA1 stratum radiatum was visualized using an Olympus BX61 WI upright microscope equipped with UMPLFLN 10X (N.A 0.3) and LUMFLN 60X (N.A. 1.1) water-immersion objective lenses and differential interference contrast (DIC) optics. Astrocytes in CA1 stratum radiatum were first identified by their characteristic morphology and size using DIC visualization. After loading with OGB-1 Ca^{2+} indicator dye, the fluorescence intensity in astrocytes was recorded over time on a fixed focal plane of 4.127 μm optical thickness, 1.2 sec scanning interval and 2X zoom-in factor. Changes

in fluorescence intensity indicated a Ca^{2+} elevation (criteria described in next section). The microscope was set up for FITC and rhodamine detection to visualize green or red indicators under separate detection channels. For all experiments, only a single (field of) astrocyte(s) was recorded per slice to prevent effects caused by multiple electrical stimulations and/or agonist applications. For bolus-loading experiments, laser power was used at 1.2 % or below, and for patch-clamp experiments, laser power was used at 0.3% or lower to prevent phototoxicity-induced spontaneous Ca^{2+} oscillations (Wang et al., 2006; see also chapter 2, Fig. 2.1 for control experiment). The group I mGluR agonist (*S*)-3,5-Dihydroxyphenylglycine (DHPG) or an agonist cocktail (containing 10 μM each of histamine, carbachol, and Na2-ATP, agonists for histamine H1 receptors [H1R], muscarinic acetylcholine receptors [mAchR], and purinergic receptors [P2YR], respectively) were always applied at the end of the experiment as a positive control to verify intact astrocytic Gq GPCR signaling pathways. Astrocytes that failed to respond to the positive control were excluded from further analysis. Solutions were switched using an electronic valve controller during the course of the experiments (Warner Instrument, Hamden CT).

Data analysis.

Square-shaped regions of interest (ROI) of a size ranging from 9.6 - 17.3 μm^2 were placed over the astrocyte cell body and visible processes using Olympus Fluoview 1000 software. For each ROI, fluorescence increases of at least two scanning points with values ≥ three standard deviations (S.D.) above 30s of average baseline fluorescence were defined as Ca^{2+} transients (Honsek et al., 2012). Spontaneous Ca^{2+} elevations that

covered < 75% of the planar area of the astrocyte were defined as “microdomain” Ca^{2+} events, whereas those spanning > 75% of the planar area were defined as “whole cell” Ca^{2+} events. Neighboring ROIs with Ca^{2+} transients at the same time (< 10 s time interval) were grouped together as a single Gq GPCR signaling domain. ROIs increasing fluorescence intensity at the same time but with at least one intervening ROI that did not increase in intensity were considered separate microdomains occurring at the same time. Student’s independent t-test was used to determine statistical significance between control and treatment groups. P values ≤ 0.05 were considered significant.

3.4 Results

3.4.1 Astrocytes respond to three pulse SC stimulation with either whole-cell or microdomain Ca^{2+} elevations

It has been well established that astrocytes respond to high frequency SC stimulation with somatic Ca^{2+} elevations. The threshold of evoking astrocytic Ca^{2+} elevations, however, has not yet been fully investigated. A previous study has revealed that astrocytes respond to three pulse SC stimulation with Ca^{2+} elevations (Honsek et al., 2012), indicating that astrocytes can respond to SC stimulation at intensities much lower than what has been described previously. However, it was not fully addressed whether the responses were global, involving the entire cell, or restricted to a microdomain. Furthermore, the threshold level of stimulation intensity required to evoke an astrocyte response was not determined. To elucidate these issues, we performed experiments applying three pulses of SC stimulation and monitoring astrocytic Ca^{2+} activity following

different intensities of stimulation. A 50 μA, 100 Hz (1s) train of pulses was also applied in the experiment as a positive control to evoke whole-cell astrocytic Ca^{2+} responses. Our data showed no detectable Ca^{2+} elevations following the first single pulse stimulation. However, when three pulses of stimulation (ranging from 25-150 μA) was applied the first time, multiple astrocytes responded with Ca^{2+} elevations detected within a consistent time interval (27.8 ± 11.2 s., Fig. 3.1A,B). To avoid any Ca^{2+} responses resulting from direct depolarization of presynaptic terminals or astrocytes, we applied a 50 μA, 100 Hz train in the presence of TTX at the end of each experiment as a negative control. Data were discarded if astrocytes gave responses in the presence of TTX. . To our surprise, results from a recent control experiment indicate that astrocytes can respond to three pulse stimulation of higher intensity (150-200 μA), but not to a 50 Hz train of lower intensity (50 μA), in the presence of TTX (Fig. 3.2D). These data suggest that the amplitude or intensity of the stimulation is critical for direct depolarization of synaptic terminals, not the frequency of stimulation. Therefore, to ensure that only the astrocytic Ca^{2+} responses evoked by action potential-triggered neurotransmitter release were selected, only three pulse stimulations of intensities ≤ 50 μA were included in subsequent analyses.

Most astrocytic Ca^{2+} responses to 3-pulse SC stimulation occurred at the whole-cell level (> 75% of the entire cell surface area; Fig. 3.1 C,D and Fig. 3.2, red area for 25-50 μA). Interestingly, a second stimulation of the same intensity resulted in Ca^{2+} responses at the microdomain level (Fig. 3.2 A, yellow area for 25-50 μA), while 50 μA, 100 Hz trains always evoked whole-cell Ca^{2+} responses both times. Also, as the three-

pulse stimulation intensity increased from 25-50 μA, an area that didn't respond to 25 μA was responding to 50 μA and the 50 Hz trains (Fig. 3.2A, red arrowhead), while another area that didn't respond to either 25 or 50 μA was responding to the trains (Fig. 3.2A, white arrowhead). These observations suggest that the area of the astrocyte responding is directly related to the number of SC afferent fibers stimulated; since additional afferents are recruited as the stimulation intensity is increased. The data also indicate that the global astrocyte Ca^{2+} responses are due to a combination of temporal and spatial summation of neurotransmitter release over a larger area of the astrocyte.

We also compared the areas of the Ca^{2+} responses to the different types of stimulation to the spontaneous Ca^{2+} events occurring over the baseline period. Interestingly, evoked Ca^{2+} elevations have significantly larger areas and higher probability of including the cell soma, while spontaneous events encompass much smaller areas and often occur in restricted regions of the astrocyte processes without propagating to the cell body (Fig. 3.2B, C). These data suggest that evoked astrocyte Ca^{2+} elevations, even involving 3 pulses of low intensity stimulation, are qualitatively different from spontaneous microdomain Gq GPCR activity, even though they can encompass < 75% of the astrocyte area.

Taken together, these results suggest that astrocytes can respond to three pulses of SC stimulation with either microdomain or whole-cell Ca^{2+} elevations, and the evoked Ca^{2+} elevations are qualitatively different from the spontaneous Ca^{2+} events.

3.4.2 Astrocytes do not respond to direct membrane depolarization with Ca^{2+} elevations

An important issue that comes along with SC stimulation is the possibility of directly depolarizing either synaptic terminals or astrocytes by the stimulating electrode. As described above, TTX was used to control for direct depolarization of synaptic terminals. Separate experiments were performed to control for effects that could be due to direct depolarization of astrocytes, namely activation of astrocytic VGCCs by depolarization. A previous study reported that astrocytes do not express voltage-gated Ca^{2+} channels *in situ* (Carmignoto et al., 1998). To confirm this in our experiments, we patch-clamped an astrocyte and left the patch pipette in the whole-cell configuration to directly depolarize the cell membrane potential by applying trains of depolarizing current (-90 to 0 mV at 1 Hz for 10 s) via the pipette electrode. During this depolarization, 83% (5 out of 6) astrocytes showed no Ca^{2+} responses (Fig 3.3). After an additional 5 min baseline recording, another depolarizing train was applied at 1 Hz for 50 s, and still, no Ca^{2+} responses were detected (Fig.3.3). However, both before and after the depolarization protocol, the astrocytes responded to Gq GPCR agonist cocktail with Ca^{2+} responses, indicating that the patch pipette was not interfering with the ability to observe an astrocyte Ca^{2+} response. This result confirmed the idea that astrocytes do not express voltage-gated Ca^{2+} channels and thus would not be able to respond with Ca^{2+} elevations to direct membrane depolarization caused by the stimulating electrode.

3.4.3 Astrocytes respond to single pulse SC stimulation with either whole-cell or microdomain Ca^{2+} elevations

To further identify the threshold of evoking astrocytic Gq GPCR-driven Ca^{2+} elevations, we performed experiments using a single pulse SC stimulation protocol. In this set of experiments, astrocytes were filled with OGB-1 Ca^{2+} indicator dye via a patch pipette to enhance the resolution of visualized processes. The stimulating electrode was placed closer to individual astrocytes (20-40 μm) to increase the likelihood of stimulating single SC fibers (Raastad et al., 1992; Panatier et al., 2011). Stimulating a single fiber may evoke astrocyte microdomains of the same size and location as spontaneously occurring astrocyte microdomains. When single pulse SC stimulation (ranging from 7-120 μA) was applied, astrocytes showed varying response patterns. Some astrocytes responded to lower stimulation intensities with a wide range of latencies (Fig. 3.4A-C), while other astrocytes did not respond to single pulse SC stimulation until intensities above a certain level were applied (Fig. 3.4D-F). Due to the inconsistent time interval between a stimulus and a putative Ca^{2+} response, it was difficult based on observation alone to determine if an astrocyte Ca^{2+} elevation occurred due to stimulation or was rather a spontaneously occurring coincidental Ca^{2+} transient. As a first approach to address this issue, only the first Ca^{2+} elevation occurring after stimulation with a latency shorter than 80 s was considered a putative response. Further analyses were performed (discussed below) to better differentiate true responses from spontaneously occurring astrocyte microdomain Ca^{2+} transients. The average delay time to a putative response following single pulse SC stimulation was longer (46.3 ± 23.3 s; Fig. 3.5A) compared to

that from the three pulse SC stimulation protocol (27.8 ± 11.2 s; Fig. 3.5A), presumably because the lower amount of glutamate released from fewer fibers takes longer to reach an effective concentration to activate astrocytic Gq GPCRs.

We also compared the areas of propagation of the evoked astrocytic Ca^{2+} elevations to spontaneous events occurring over the baseline period prior to stimulation. Once again, evoked Ca^{2+} elevations had significantly larger areas and a higher probability of propagating to the cell body, while spontaneous events were much smaller in size and occurred in a restricted territory without involving the soma (Fig. 3.5B,C). The amplitudes of the astrocytic Ca^{2+} elevations, however, were not significantly different between both groups (Fig. 3.5D). These findings suggest that the spontaneous astrocytic Ca^{2+} elevations are driven by mechanisms other than local AP-mediated release of neurotransmitter, such as miniature vesicular release or constitutive GPCR signaling activity (see Chapter 2).

Interestingly, however, although most astrocytic Ca^{2+} responses to single pulse SC stimulation involved larger areas of the cell, there were occasionally some "putative" Ca^{2+} responses that occurred at local processes without propagating to the cell body (Fig. 3.4F, red arrowheads following 40 μA and 50 μA). These results give rise to the possibility that astrocytic Ca^{2+} responses can be confined to areas similar to spontaneously occurring microdomains when stimulation of single fibers is applied. This possibility has also been tested later in this study (see section 3.4.5).

3.4.4 The astrocytic Ca^{2+} elevations evoked by single pulse SC stimulation cannot be fully blocked by group I mGluR antagonists

It has been shown that a large portion of astrocyte Ca^{2+} responses evoked by high frequency SC stimulation are blocked by group I mGluR antagonists (Porter and McCarthy, 1996). To investigate whether astrocyte Ca^{2+} responses evoked by single pulse SC stimulation are the result of group I mGluR activation, we bath-applied the group I mGluR antagonists CPCCOEt (100 μM) and MPEP (20 μM) for 5 min, followed by single pulse SC stimulation (Fig. 3.6). Our data indicate only a mild reduction in Ca^{2+} response area (Fig. 3.6D), but a significant decrease in response amplitude (Fig. 3.6E). Since astrocyte Ca^{2+} responses were not completely blocked by group I mGluR antagonists, it suggests that other types of astrocytic Gq GPCRs are involved. As a within-recording control, astrocyte Ca^{2+} responses to DHPG were blocked, confirming that the group I mGluR antagonists were working effectively. In the presence of TTX, astrocyte Ca^{2+} responses were not detectable when applying 150 μA SC stimulation (Fig. 3.6C), suggesting that the astrocyte Ca2+ responses were not due to direct depolarization of presynaptic terminals. The astrocyte Ca^{2+} responses to agonist cocktail at the end of the experiment verified the cell's viability and intact Gq GPCR signaling pathways (Fig. 3.6).

3.4.5 Determine whether microdomain astrocyte Ca^{2+} elevations can be driven by glutamate release from single identified CA3 synaptic boutons

To investigate the possibility of evoking local astrocytic Ca^{2+} elevations, we performed experiments controlling the firing pattern of a single CA3 neuron. By

adjusting the amplitude (200-400 pA) and duration (50-200 ms) of the injected current, the number and frequency of evoked action potentials was controlled (Fig. 3.7B). Neurons were also filled with Alexa 568 included in the recording pipette, which enabled labeling of the neuronal axon and its en passant boutons as they coursed through a field of Ca^{2+} dye-loaded astrocytes. Ca^{2+} activity from astrocytes with processes near the visually identified synaptic boutons was recorded during neuronal stimulation (Fig. 3.7A). Astrocytes showed putative responses in processes following single action potential generation. However, the responses could not be re-evoked and were very small in amplitude (Fig. 3.7). To increase the probability of detecting Ca^{2+} responses in astrocytes, neurotransmitter release from axon terminals was enhanced using the potassium channel blocker 4-Aminopyramidine (4-AP) as described previously (Porter and McCarthy, 1996). 4-AP prolongs the duration of neuronal action potentials by blocking the delayed rectifying potassium channel, increasing Ca^{2+} entry into synaptic boutons and therefore enhancing release of neurotransmitter. 4-AP was thus considered as a positive control for the ability of astrocyte microdomains to respond to action potentials evoked in single neurons. However, at 100 µM, 4-AP induced CA3 neuronal bursting with triggered rapid neuronal Ca^{2+} elevations that corresponded to each burst of action potentials (Fig. 3.8B). The neuronal Ca^{2+} spikes were distinguishable from astrocytic Ca^{2+} elevations due to their comparatively fast durations as well as their sensitivity to TTX (Fig. 3.9A). After 4-AP was washed in, we observed a time period prior to burst discharges in which neurons exhibited increased subthreshold EPSPs. Therefore, this time period was considered as a “priming period”, in which release probability and amount of neurotransmitter released

by neurons is enhanced but not yet sufficient to cause bursting. By reducing the concentration of 4 AP from 100 to 25 μM, this priming period was extended (Fig. 3.8A). Furthermore, single neuronal action potentials could then be evoked in 25 μM 4-AP without the confounding variable of spontaneous epileptiform bursting (Fig. 3.8A). However, use of 4-AP even at these reduced concentrations turned out to be problematic. 4-AP itself had a direct effect on astrocytic Ca^{2+} activity, causing a prolonged astrocyte Ca^{2+} response that occurred *prior* to CA3 neuronal burst discharges (Fig. 3.9B). This brought up concerns that any putative astrocyte Ca^{2+} responses evoked by glutamate released from single synaptic boutons would be difficult to differentiate from those caused by 4-AP directly. Therefore, 4-AP was considered an insufficient positive control to determine the link between astrocytic Ca^{2+} elevations and basal neuronal activity. Overall, due to technical difficulties lining up the many variables needed to do these experiments, we have not been able to determine the precise number of action potentials from single synaptic terminals that are capable of stimulating astrocytic Gq GPCR responses.

3.5 Discussion

In this study, we have shown that astrocytes are capable of responding to low level (three pulses or single pulses) SC stimulation with Gq GPCR-driven Ca^{2+} elevations. These Ca^{2+} responses were qualitatively different from spontaneous astrocytic Ca^{2+} transients because they propagated through a significantly larger area of the astrocyte and frequently included the cell soma, whereas the spontaneous events occurred in restricted

areas without involving the soma. Given the differences between these two types of events, we conclude that spontaneous microdomains of astrocyte Ca^{2+} activity are not likely driven by AP-mediated glutamate release. Another way of saying this is that astrocytic Gq GPCR Ca^{2+} events evoked by even single pulses of neuronal afferent stimulation produce large, more global type of astrocyte response. In addition, the SC-evoked events tended to be more plateau-like and thus have larger magnitudes compared to spontaneous activity, most of which appears as single peak, fast-spike like events. One of our future goals is to further quantify these two events by analyzing the magnitude of Ca^{2+} transients in both cases.

While we were testing our hypothesis for this study, another research group published their findings addressing similar questions (Panatier et al., 2011). In this study, astrocytes were able to respond to single-pulse SC stimulation applied to putative single fibers with Ca^{2+} elevations that occurred simultaneously with EPSCs recorded from a neighboring neuron. In addition, the astrocytic Ca^{2+} responses were inhibited completely by the $mGluR_5$ antagonist MPEP. However, there were some concerns with these data. First, the patch pipette was left on the astrocyte over the entire recording period, which has been shown to be capable of dampening the Ca^{2+} signal detected in the cell body. Moreover, their stimulating electrode was placed only 7-15 μm away from the astrocyte process, raising a caveat that the astrocyte Ca^{2+} responses could be due to neurotransmitters released by direct depolarization of neuronal terminals, which was not controlled for. The latency to the astrocyte Ca^{2+} responses was as short as an EPSC, occurring within milliseconds. A previous study done by Fiacco et al. (2004) has

demonstrated that it takes approximately 40 ms to see the astrocyte Ca^{2+} response evoked by uncaging IP_3, which is only one step away from Ca^{2+} release from the internal store (Fiacco and McCarthy, 2004). In the present study, average astrocyte Ca^{2+} response times to single pulses, 3 pulses, and 50 Hz trains to the Schaffer collaterals occurred after 46.3 s, 27.8 s, and 5.1 s, respectively (Fig. 3.5A). The fast astrocyte response times recorded by Panatier et al. therefore raise doubt as to the types of cells they are recording from, as astrocytes do not possess fast sources of activity-evoked Ca^{2+} entry such as VGCCs or ligand-gated ion channels. Based on our results, astrocytic Ca^{2+} responses following single pulse SC stimulation have even longer response latencies on average compared to three pulse SC stimulation experiments. One possible explanation for the difference between Panatier et al's findings and ours could be the different distances of stimulating electrode placement. In Panatier's study, the stimulating electrode was placed much closer to the astrocyte process. We have also tried similar electrode placements with distances of ~ 10-20 μm in some cases. However, even with minimal stimulation intensities of 7 μA, we observed astrocytic Ca^{2+} responses in the presence of TTX, indicating that the responses were caused by direct depolarization of presynaptic terminals. Furthermore, these astrocytic Ca^{2+} responses were blocked by cadmium (100 μM), a voltage-gated Ca^{2+} channel blocker (n = 2 cells, data not shown). The only way we could avoid direct stimulation was to use cadmium combined with TTX as a negative control to figure out a "safe" working distance for electrode placement. Therefore, it is possible that the astrocytic Ca^{2+} responses observed in Panatier's study are due to direct stimulation, which would explain the very short response latencies they observed.

Another important finding in our study is the effect of group I mGluR antagonists on astrocytic Ca^{2+} responses evoked by single pulse SC stimulation. Even though we observed a significantly reduced amplitude following application of group I mGluR antagonists, the astrocytic Ca^{2+} responses were not completely blocked, a similar phenomenon observed by Porter and McCarthy in 1996 (Porter and McCarthy, 1996). These results imply that other types of astrocytic Gq GPCRs contribute to minimal-stimulation evoked astrocyte Ca^{2+} responses. Moreover, this finding is consistent with the antagonist effects we described in Chapter 2, which also suggests essential roles played by other Gq GPCRs including P2YRs, $GABA_B$ receptors, mAchRs and CB1Rs in triggering the generation of astrocytic Ca^{2+} elevations. Therefore, our next step for this study is to combine the potential receptor antagonists in different combinations to investigate their potential to block SC stimulation-evoked astrocytic Ca^{2+} responses.

Our last approach in this study to assay for microdomains of neuron-to-astrocyte Gq GPCR communication at single synapses - failed to provide conclusive results. From this set of experiments we have identified a few caveats to consider in future studies. First, since OGB-1 AM Ca^{2+} indicator delivered by bolus-loading is preferentially taken up by astrocytes compared to neurons (Porter and McCarthy, 1995), we came in with the assumption that all Ca^{2+} activity observed would be occurring only in astrocytes, even within the “background” loading of neuropil which was considered the latticework of fine astrocyte processes. However, we discovered that bolus-loading in fact also fills neuronal components of the neuropil which contaminates the astrocyte Ca^{2+} activity with faster response properties of neurons due to their expression of fast local sources of Ca^{2+} entry

(e.g. ligand-gated ion channels and VGCCs). This prevented us from detecting microdomain Ca^{2+} activity that occurs solely in the very fine astrocytic processes. To deal with this issue, we had considered applying SR101 staining in this experiment as it is a astrocyte-specific marker, and then use an Alexa dye of a different wavelength for neuronal loading. However, this approach still does not solve the problem of detecting Ca^{2+} signals exclusively in astrocytes. The best strategy is to use patch-clamp to deliver Ca^{2+} indicator to single astrocytes surrounding neuronal boutons, as this would enable loading of a specific astrocyte with Ca^{2+} indicator without any confounding factors related to non-specific uptake of dye by neurons. Moreover, it also enhances our ability to detect the microdomain Ca^{2+} activity that occurs in the very fine astrocytic processes due to the high signal-to-background ratio. The only caveat with this strategy is that it is very technically challenging, as neuronal boutons would need to be identified first so that astrocytes surrounding them could then be selected for patch-clamp. Figuring out the course of the axon and its boutons is in itself is a very critical and challenging step in this experiment, for axons have a much narrower diameter compared to dendrites and take longer to fill with dye. Moreover, the patch pipette for the neuron needs to be left on the cell for current injection at a later time point. As one could imagine, when patching adjacent astrocytes, there is a very high chance of losing seals on both the neuron and the astrocyte. Taken together, we still believe this experiment is the most powerful to determine if astrocyte microdomains can be evoked by a defined number and frequency of action potentials from single neurons, but all of these issues would need to be overcome in order to make this study feasible.

3.6 References

Barres BA (2008) The mystery and magic of glia: a perspective on their roles in health and disease. Neuron 60:430-440.

Carmignoto G, Pasti L, Pozzan T (1998) On the role of voltage-dependent calcium channels in calcium signaling of astrocytes in situ. J Neurosci 18:4637-4645.

Fiacco TA, McCarthy KD (2004) Intracellular astrocyte calcium waves in situ increase the frequency of spontaneous AMPA receptor currents in CA1 pyramidal neurons. J Neurosci 24:722-732.

Honsek SD, Walz C, Kafitz KW, Rose CR (2012) Astrocyte calcium signals at Schaffer collateral to CA1 pyramidal cell synapses correlate with the number of activated synapses but not with synaptic strength. Hippocampus 22:29-42.

Nimmerjahn A, Kirchhoff F, Kerr JN, Helmchen F (2004) Sulforhodamine 101 as a specific marker of astroglia in the neocortex in vivo. Nat Methods 1:31-37.

Panatier A, Vallee J, Haber M, Murai KK, Lacaille JC, Robitaille R (2011) Astrocytes are endogenous regulators of basal transmission at central synapses. Cell 146:785-798.

Porter JT, McCarthy KD (1995) GFAP-positive hippocampal astrocytes in situ respond to glutamatergic neuroligands with increases in $[Ca^{2+}]_i$. Glia 13:101-112.

Porter JT, McCarthy KD (1996) Hippocampal astrocytes in situ respond to glutamate released from synaptic terminals. J Neurosci 16:5073-5081.

Raastad M, Storm JF, Andersen P (1992) Putative Single Quantum and Single Fibre Excitatory Postsynaptic Currents Show Similar Amplitude Range and Variability in Rat Hippocampal Slices. Eur J Neurosci 4:113-117.

Wang X, Lou N, Xu Q, Tian GF, Peng WG, Han X, Kang J, Takano T, Nedergaard M (2006) Astrocytic Ca^{2+} signaling evoked by sensory stimulation in vivo. Nat Neurosci 9:816-823.

Figure Legends

Figure. 3.1 Astrocyte Ca^{2+}elevations following three pulse SC stimulation.

(A) Ca^{2+} activity in both the cell soma and major processes of four astrocytes was recorded for 10 min prior to low-level SC stimulation. The first stimulation was a single pulse while the rest were three pulses, ranging from 25-150 μA. A 50 μA, 100 Hz train was applied as a positive control to evoke a whole-cell Ca^{2+} response as has been published previously (Porter and McCarthy, 1996). The 50 μA, 100 Hz train was re-applied in the presence of TTX as a control to test for direct stimulation of astrocytes by the stimulating electrode. The group I mGluR agonist DHPG (50 μM) was applied at the end of the recording as a positive control for the presence of functional group I mGluRs. The first Ca^{2+} elevation following each stimulus is shown by arrowheads marked with a different color to differentiate individual astrocytes.

(B) OGB-1 AM bolus-loaded astrocytes were identified by co-labeling with the astrocyte-specific marker SR101 (Nimmerjahn et al., 2004). Four astrocytes in this field (marked with colored numbers) were assayed for their Ca^{2+} activity with recording traces labeled with colored arrowheads that match the color of numbered astrocytes.

(C) Recording of Ca^{2+} activity in both the cell soma and processes of a single astrocyte. The first Ca^{2+} elevation following each stimulus is shown by red arrowheads.

(D) The OGB-1 AM bolus-loaded astrocyte was identified using the astrocyte-specific marker SR101.

Figure 3.2 Quantitative analysis of astrocyte Ca^{2+}elevations following three pulse SC stimulation.

(A) Area of propagation of Ca^{2+} events under different conditions. For the SC-evoked Ca^{2+} events, the area that was evoked by the first stimulus is marked in red, while the area that was evoked by the second stimulus is marked in yellow. Red arrowhead points to an area of the cell that did not respond to 25 μA pulses but responded to 50 μA pulses and 50 μA, 100 Hz trains; white arrowhead points to another area that did not respond to 25 μA and 50 μA pulses, but responded to 50 μA, 100 Hz pulse trains.

(B) Areas of propagation were compared between spontaneous and evoked Ca^{2+} events. The evoked Ca^{2+} events to different stimulation intensities were grouped together as the "evoked" Ca^{2+} events, and the comparison was made between this group and the group of spontaneous Ca^{2+} events. Overall, the evoked events have significantly larger surface areas compared to the spontaneous events. (*$p < 0.05$, n = 4 cells for spontaneous Ca^{2+} events and 3 cells for evoked Ca^{2+} events).

(C) Percentage of Ca^{2+} events that included the cell soma. Overall, the evoked events have significantly higher chance to propagate to the cell soma compared to the spontaneous events. (**$p < 0.01$, n = 4 cells for spontaneous Ca^{2+} events and 3 cells for evoked Ca^{2+} events).

(D) In the presence of TTX, astrocytes responded with Ca^{2+} elevations to the three pulse SC stimulation protocol with intensities > 50 μA (150-200 μA in this case), but did not respond to the 50 μA, 100 Hz train, suggesting that the intensity of the stimulation is a critical determinant of directly depolarizing synaptic terminals, not the frequency.

Figure 3.3 Recording of astrocytic Ca^{2+} activity following direct cell membrane depolarization.

(A) A single astrocyte filled with OGB-1 Ca^{2+} indicator dye via patch clamp. Colored ROIs match fluorescence intensity over time traces in (C).

(B) The cell exhibited a passive current profile to a voltage-step protocol (-180 to +80 mV in 20 mV increments), identifying it as an astrocyte.

(C) Astrocytic Ca^{2+} activity was recorded while the patch pipette was left on the cell. After 5 min baseline recording, agonist cocktail was applied as a positive control for the ability to record Ca^{2+} elevations while the whole-cell patch pipette is dialyzing the cell. Two depolarizing trains (-90 mV to 0 mV at 1 Hz for 10s and then 50s, respectively) were then applied via the patch pipette, and agonist cocktail (10 µM ea. of histamine, carbachol, and 2Na-ATP) was washed in again at the end of the experiment (n = 6 cells). These data suggest that astrocytes do not express functional voltage-dependent sources of Ca^{2+} elevations.

Figure 3.4 Astrocyte Ca^{2+}elevations following single pulse SC stimulation.

(A) Left: Transmitted light image to indicate the position of the stimulating pipette relative to the recorded cell. Right: A single astrocyte filled with OGB-1 Ca^{2+} indicator dye via patch clamp. Colored ROIs match fluorescence intensity over time traces in (C).

(B) The cell exhibited a passive current profile to a voltage-step protocol (-180 to +80 mV in 20 mV increments), identifying it as an astrocyte.

(C) Spontaneous Ca^{2+} activity in the astrocyte was recorded for 5 min followed by single pulse SC stimulation ranging from 7-120 μA (7-50 μA in this representative trace). TTX was washed in to test for direct depolarization of synaptic terminals using the same or higher stimulation intensities as those used to evoke Ca^{2+} elevations in the absence of TTX (50-75 μA in this case) . Agonist cocktail (10 μM ea. of histamine, carbachol, and 2Na-ATP) was applied at the end of the recording as a positive control for viable Gq GPCR responses to verify the lack of responses in TTX. The first Ca^{2+} elevation following each stimulus is shown by red arrowheads. Note that this astrocyte started to respond to single pulse SC stimulation with whole-cell Ca^{2+} elevations at 7 μA and 25 μA.

(D) Left: Transmitted light image showing the position of the stimulating pipette relative to the recorded astrocyte. Right: A single astrocyte filled with OGB-1 Ca^{2+} indicator dye via patch clamp. Colored ROIs match fluorescence intensity over time traces in (C).

(E) The cell exhibited a passive current profile to a voltage-step protocol (-180 to +80 mV in 20 mV increments), identifying it as an astrocyte.

(F) Spontaneous Ca^{2+} activity was recorded in the astrocyte for 5 min prior to single pulse SC stimulation ranging from 7-120 μA (7-60 μA in this representative trace). TTX

was washed in to test for direct depolarization of synaptic terminals using the same or higher stimulation intensities as those used to evoke Ca^{2+} elevations in the absence of TTX (60 and 75 μA in this case). Agonist cocktail (10 μM ea. of histamine, carbachol, and 2Na-ATP) was applied at the end of the recording as a positive control for functional Gq GPCR responses to verify the effect of TTX. The first Ca^{2+} elevation following each stimulus is shown by red arrowheads. Note that this astrocyte did not respond to single pulse SC stimulation with whole-cell Ca^{2+} elevations until higher stimulation intensities (60 μA) were reached. Instead, it showed local Gq GPCR signaling domains in processes without propagating to the cell body in response to lower stimulation intensities (7 μA, 25 μA, 40 μA and 50 μA).

Figure 3.5 Quantitative analysis of astrocyte Ca^{2+}elevations following single pulse SC stimulation.

(A) Average astrocyte Ca^{2+} response times (latency) to single pulse, 3 pulses, and 50 Hz trains (high frequency stimulation; HFS) of SC stimulation occurred after 46.3 s, 27.8 s, and 5.1 s, respectively. (n = 9 cells for single pulse; n = 3 cells for three pulses; n = 6 cells for HFS)

(B) Areas of propagation were compared between spontaneous and evoked Ca^{2+} events. The Ca^{2+} events to different stimulation intensities were grouped together as the"evoked" Ca^{2+} events, and the comparison was made between this group and the group of spontaneous Ca^{2+} events occurring over the baseline period. Overall, the evoked events have significantly larger surface areas compared to the spontaneous events. (*$p < 0.05$, n = 4 cells for spontaneous Ca^{2+} events and 8 cells for evoked Ca^{2+} events).

(C) Percentage of Ca^{2+} events that included the cell soma. Overall, the evoked events have significantly higher chance to propagate to the cell soma compared to the spontaneous events. (***$p < 0.005$, n = 4 cells for spontaneous Ca^{2+} events and 8 cells for evoked Ca^{2+} events).

(D) Amplitude of Ca^{2+} transients was compared between spontaneous and evoked Ca^{2+} events. Amplitude ($\Delta F/F_0$) of spontaneous and evoked events was compared within each trace/ROI first, and then these ROIs were averaged within each cell. Based on the data, no significant change of amplitude was detected between these two groups. ($p > 0.1$, n = 4 cells for both spontaneous and evoked Ca^{2+} events).

Figure 3.6 Effects of group I mGluR antagonists on astrocytic Ca^{2+} responses following single pulse SC stimulation.

(A) Left: Transmitted light image showing the position of the stimulating pipette relative to the recorded astrocyte. Right: A single astrocyte filled with OGB-1 Ca^{2+} indicator dye via patch clamp. Colored ROIs match fluorescence intensity over time traces in (C).

(B) The cell exhibited a passive current profile to a voltage-step protocol (-180 to +80 mV in 20 mV increments), verifying it as an astrocyte.

(C) Spontaneous Ca^{2+} activity of the astrocyte was recorded over a 5 min baseline period followed by single pulse SC stimulation ranging from 7-120 μA (40-120 μA in this representative trace). Group I mGluR antagonists ($mGluR_1$ antagonist CPCCOEt, 100 μM; $mGluR_5$ antagonist MPEP, 20 μM) were applied to the bath prior to re-stimulating using the peak intensity used prior to antagonist application (120 μA in this case). DHPG was bath-applied afterward to test the effectiveness of the Group I mGluR antagonists. TTX was then applied to test for direct depolarization of synaptic terminals using the same or higher stimulation intensities as those used to evoke Ca^{2+} elevations in the absence of TTX (120 and 150 μA in this case). Agonist cocktail (10 μM ea. of histamine, carbachol, and 2Na-ATP) was applied at the end of the recording as a control to make sure that any absence of responses in TTX were not due to the cell dying. The first Ca^{2+} elevation following each stimulus is shown by red arrowheads. Note that the astrocytic Ca^{2+} responses evoked by single pulse SC stimulation were only partially reduced by group I mGluR antagonists.

(D) Area of propagation of Ca^{2+} responses to SC stimulation were compared before and

after applying group I mGluR antagonists. The evoked Ca^{2+} transients of matching intensity (120 μA in this case) were selected for analysis and comparison ($p > 0.1$, $n = 3$ cells). Data were displayed as percent change in Ca^{2+} response area relative to before group I mGluR antagonist application.

(E) Amplitude of Ca^{2+} transients elicited by SC stimulation was compared before and after applying group I mGluR antagonists. Ca^{2+} transients evoked by a given intensity (120 μA in this case) were selected for analysis and comparison. Amplitude ($\Delta F/F_0$) of spontaneous and evoked events was compared within each trace/ROI first, and then these ROIs averaged within each cell. Data were displayed as percent change in amplitude of Ca^{2+} response relative to before group I mGluR antagonist application. (*$p < 0.05$, $n = 3$ cells).

Figure 3.7 Microdomain astrocytic Ca^{2+} elevations evoked by action potentials in single CA3 pyramidal neurons.

(A) Astrocytes in CA3 s. oriens or s. radiatum were bolus-loaded with OGB-1 Ca^{2+} indicator. A CA3 pyramidal neuron was patch-clamped and infused with Alexa 568 dye, and after 15-30 min., the course of the axon and its en passant boutons was followed through a field of astrocytes in s. oriens.

(B) Left: Ca^{2+} elevations in the cell soma and processes of astrocytes surrounding boutons of the CA3 neuronal axon were recorded. The first Ca^{2+} elevations occurring after stimulation are marked with red arrowheads. The existence of frequent spontaneous astrocyte Ca^{2+} activity together with inconsistency in the delay time between stimulation and the first Ca^{2+} elevation made it difficult to determine if the microdomains were spontaneous events or responses to stimulation. Right: Pattern of action potentials in a CA3 neuron evoked by different amounts of current injection. Higher current amplitudes (400 pA) injected for a longer duration (200 ms) generated a greater frequency or number of action potentials, which reduced the latency to the astrocyte Ca^{2+} elevations in traces #6,7,13 and 14, but not for others. Moreover, the Ca^{2+} elevations from traces #4 and #7 following the first action potential evoked by 200 pA, 50 ms current did not re-occur for the second time following the same stimulation. Overall, the data were inconclusive (n = 6).

Figure 3.8 4-AP effects on microdomain astrocytic Ca^{2+} elevations evoked by single neuronal action potentials.

(A) Astrocytic Ca^{2+} elevations and neuronal firing patterns were recorded simultaneously. Action potentials were evoked by manual current injection (marked as 'stim') to depolarize the neurons (from resting Vm to -38 mV) in current-clamp mode (n = 3). Application of 25 μM 4-AP was used to elevate the level of EPSPs so as to amplify any putative astrocytic Ca^{2+} responses (as in Porter & McCarthy, 1996). DHPG was applied at the end of the recording as a positive control to verify the astrocyte's intact Gq GPCR signaling pathway.

(B) Ca^{2+} elevations (marked with red arrowheads) recorded over Alexa 568 filled boutons were synchronized to each single action potential (marked by gray arrowheads), suggesting that the green Ca^{2+} dye in the neuropil loads primarily neuronal compartments (red arrowheads).

Figure 3.9 Potential problems associated with 4-AP to study astrocytic Ca^{2+} elevations evoked by single neuronal action potentials.

(A) 4-AP (100 µM) evoked neuronal Ca^{2+} oscillations (trace #5) that tightly corresponded to each action potential and were sensitive to TTX. To distinguish between neuronal and astrocytic Ca^{2+} transients, response kinetics were used. Astrocytic Ca^{2+} responses (traces #1-4) are slower and longer lasting compared to the fast, tiny spikes of neuronal Ca^{2+} oscillations (trace #5), and were insensitive to TTX.

(B) Application of 100 µM 4-AP produced astrocytic Ca^{2+} elevations prior to neuronal bursting, suggesting that 4-AP directly evokes astrocyte Ca^{2+} elevations through an unknown mechanism (n = 5 slices). Therefore, it was difficult to differentiate direct effects of 4-AP on astrocyte Ca^{2+} from neuronally-driven astrocytic Ca^{2+} elevations. The arrowhead represents a focus-adjusted (FA) point to compensate for “slice drift”.

Figure 3.1

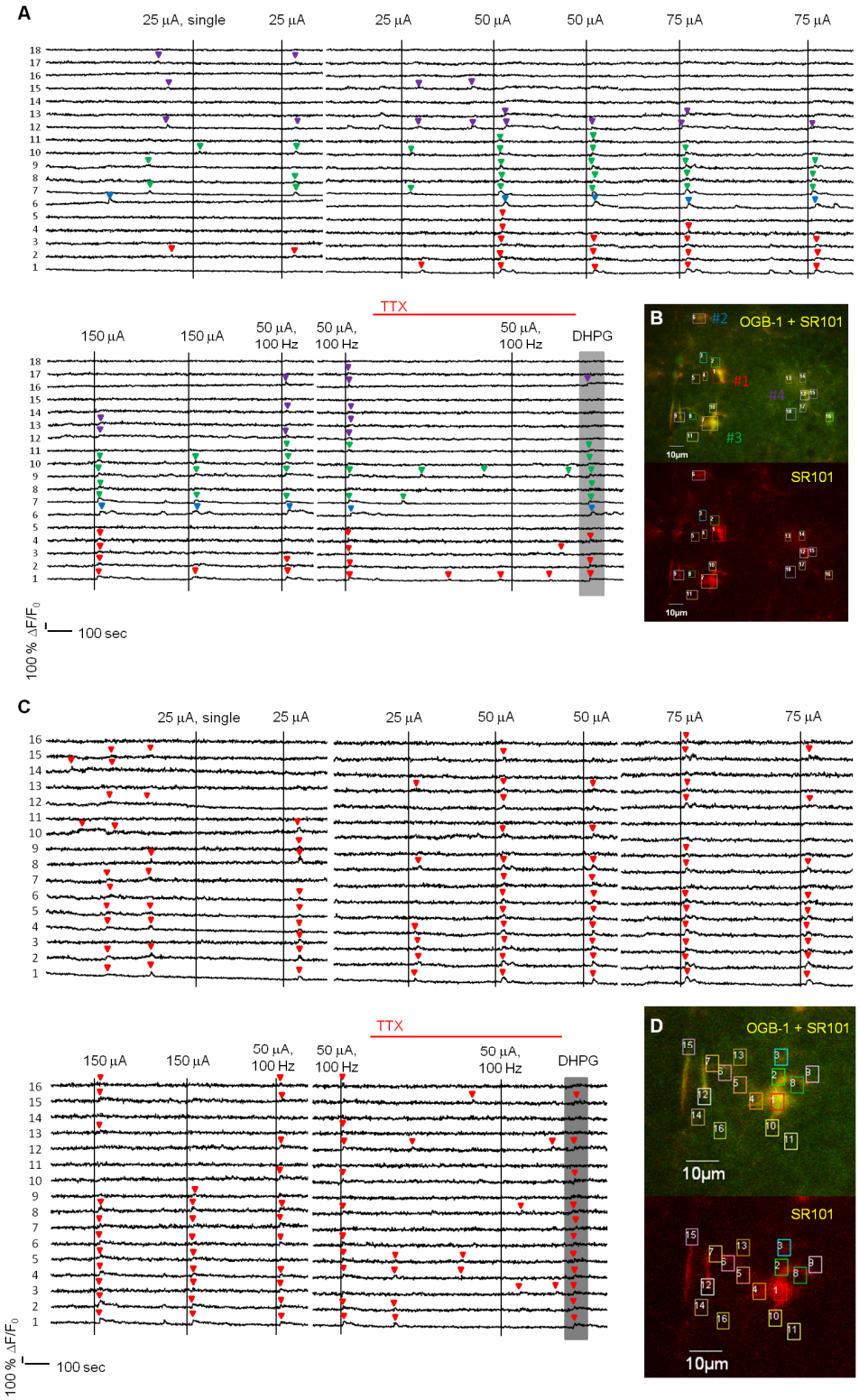
A
25 µA, single
25 µA
25 µA
50 µA
50 µA
75 µA
75 µA
TTX
150 µA
150 µA
50 µA, 100 Hz
50 µA, 100 Hz
50 µA, 100 Hz
DHPG
100 % ΔF/F0
100 sec
B
#2
OGB-1 + SR101
#1
#4
#3
10µm
SR101
10µm
C
25 µA, single
25 µA
25 µA
50 µA
50 µA
75 µA
75 µA
TTX
150 µA
150 µA
50 µA, 100 Hz
50 µA, 100 Hz
50 µA, 100 Hz
DHPG
100 % ΔF/F0
100 sec
D
OGB-1 + SR101
10µm
SR101
10µm

Figure 3.2

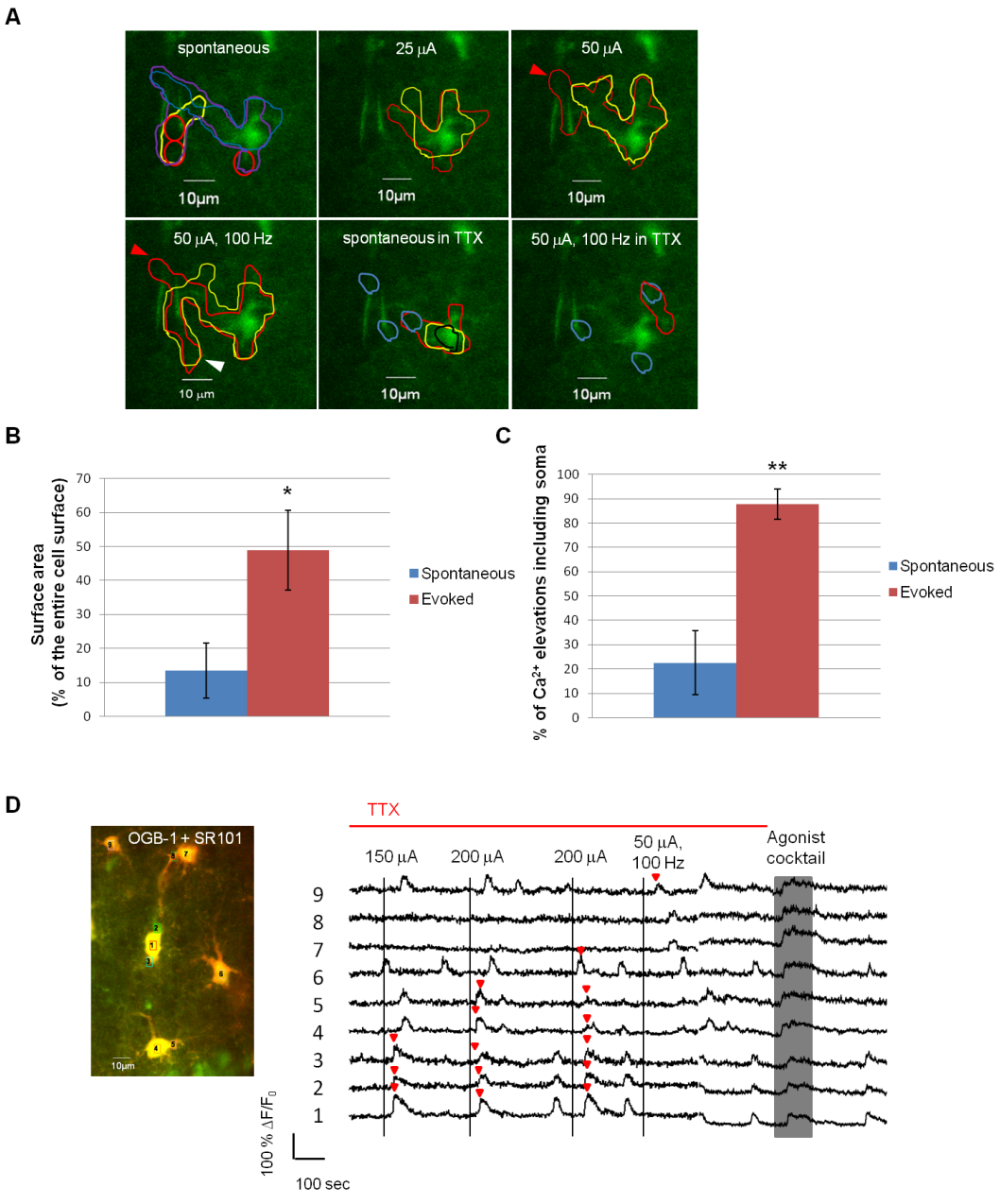
A
spontaneous
25 μA
50 μA
50 μA, 100 Hz
spontaneous in TTX
50 μA, 100 Hz in TTX
10μm
B
Surface area
(% of the entire cell surface)
*
Spontaneous
Evoked
C
% of Ca2+ elevations including soma
**
Spontaneous
Evoked
D
OGB-1 + SR101
TTX
150 μA
200 μA
200 μA
50 μA,
100 Hz
Agonist
cocktail
100 % ΔF/F0
100 sec

Figure 3.3

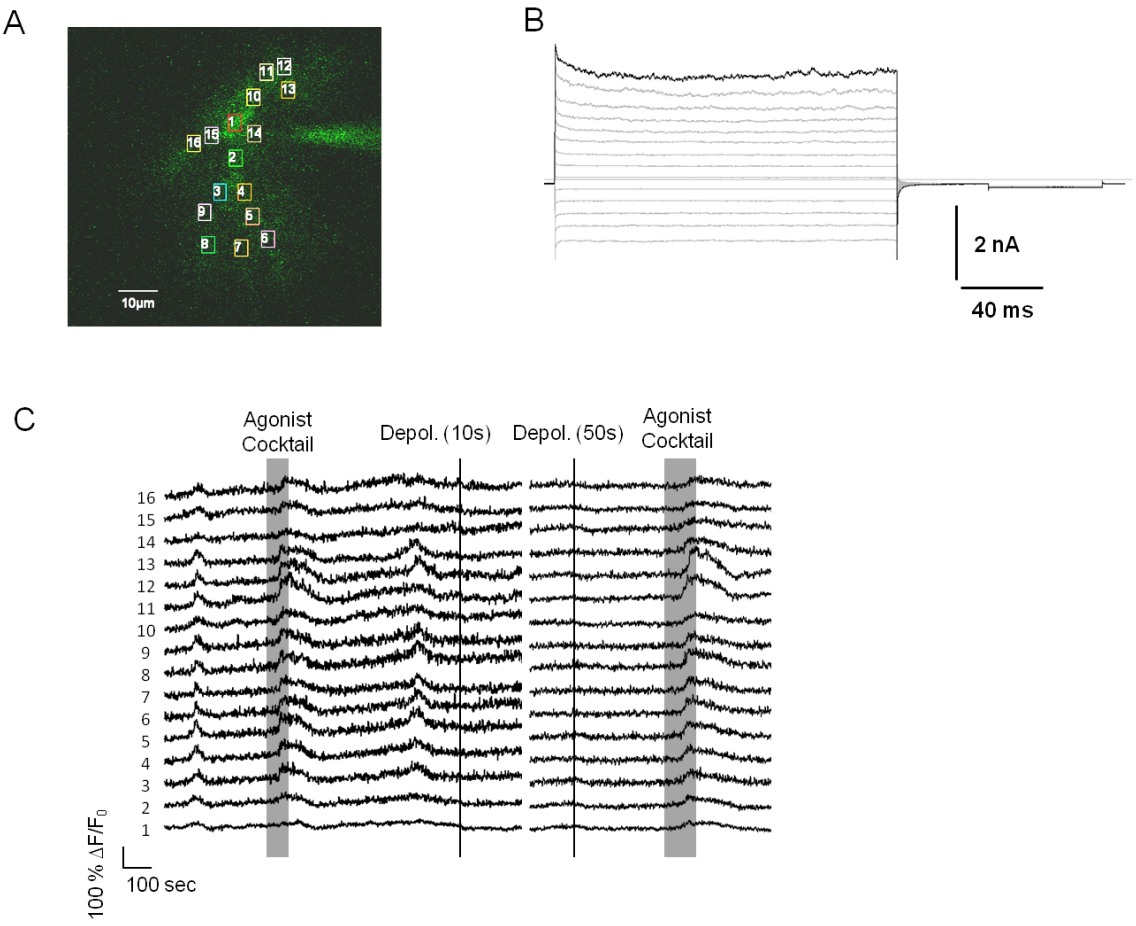
A
B
C
10µm
2 nA
40 ms
Agonist Cocktail
Depol. (10s)
Depol. (50s)
Agonist Cocktail
100 sec
100 % ΔF/F0

Figure 3.4

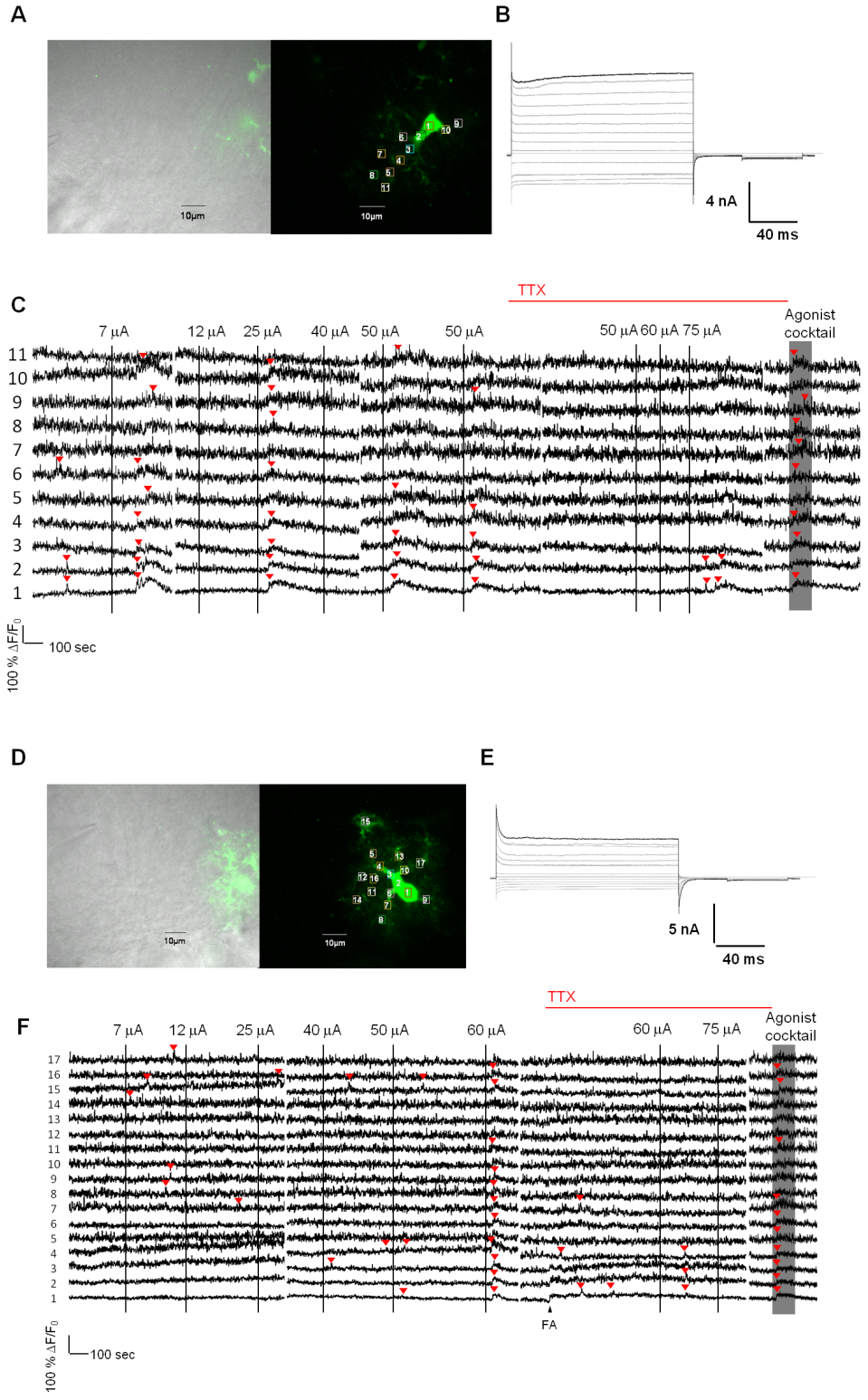
A
B
10µm
10µm
4 nA
40 ms
C
TTX
7 µA
12 µA
25 µA
40 µA
50 µA
50 µA
50 µA
60 µA
75 µA
Agonist cocktail
11
10
9
8
7
6
5
4
3
2
1
100 % ΔF/F0
100 sec
D
E
10µm
10µm
5 nA
40 ms
F
TTX
7 µA
12 µA
25 µA
40 µA
50 µA
60 µA
60 µA
75 µA
Agonist cocktail
17
16
15
14
13
12
11
10
9
8
7
6
5
4
3
2
1
FA
100 % ΔF/F0
100 sec

Figure 3.5

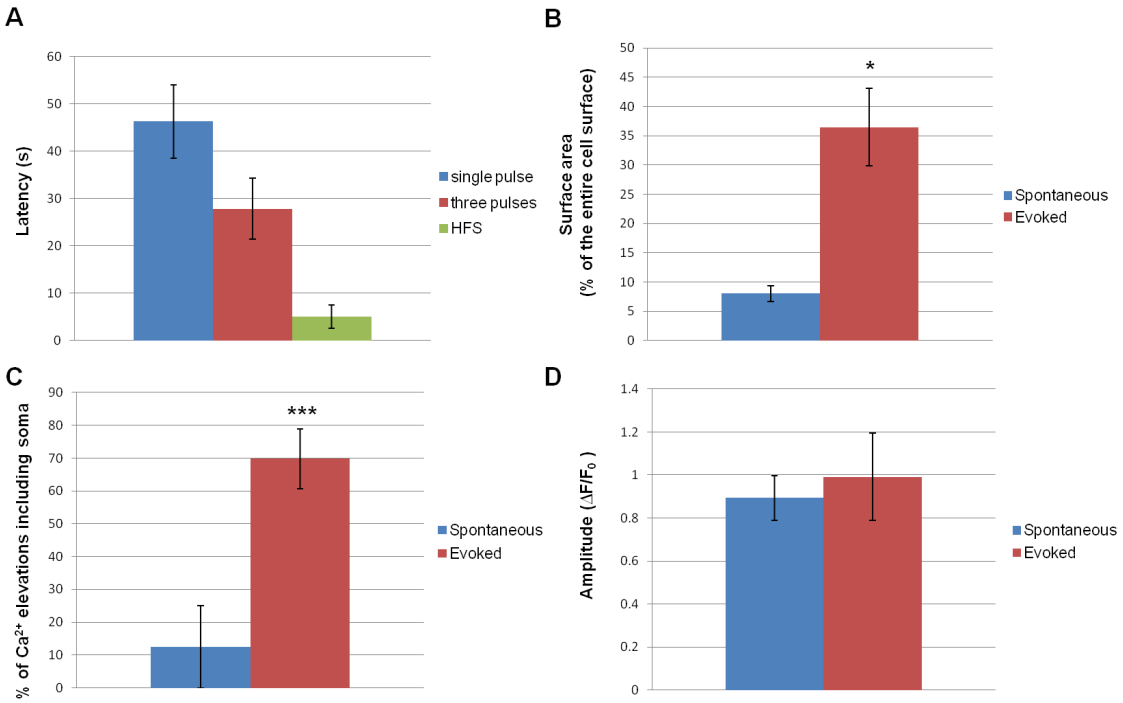
A
Latency (s)
60
50
40
30
20
10
0
single pulse
three pulses
HFS
B
Surface area
(% of the entire cell surface)
50
45
40
35
30
25
20
15
10
5
0
*
Spontaneous
Evoked
C
% of Ca2+ elevations including soma
90
80
70
60
50
40
30
20
10
0
***
Spontaneous
Evoked
D
Amplitude (ΔF/F0)
1.4
1.2
1
0.8
0.6
0.4
0.2
0
Spontaneous
Evoked

Figure 3.6

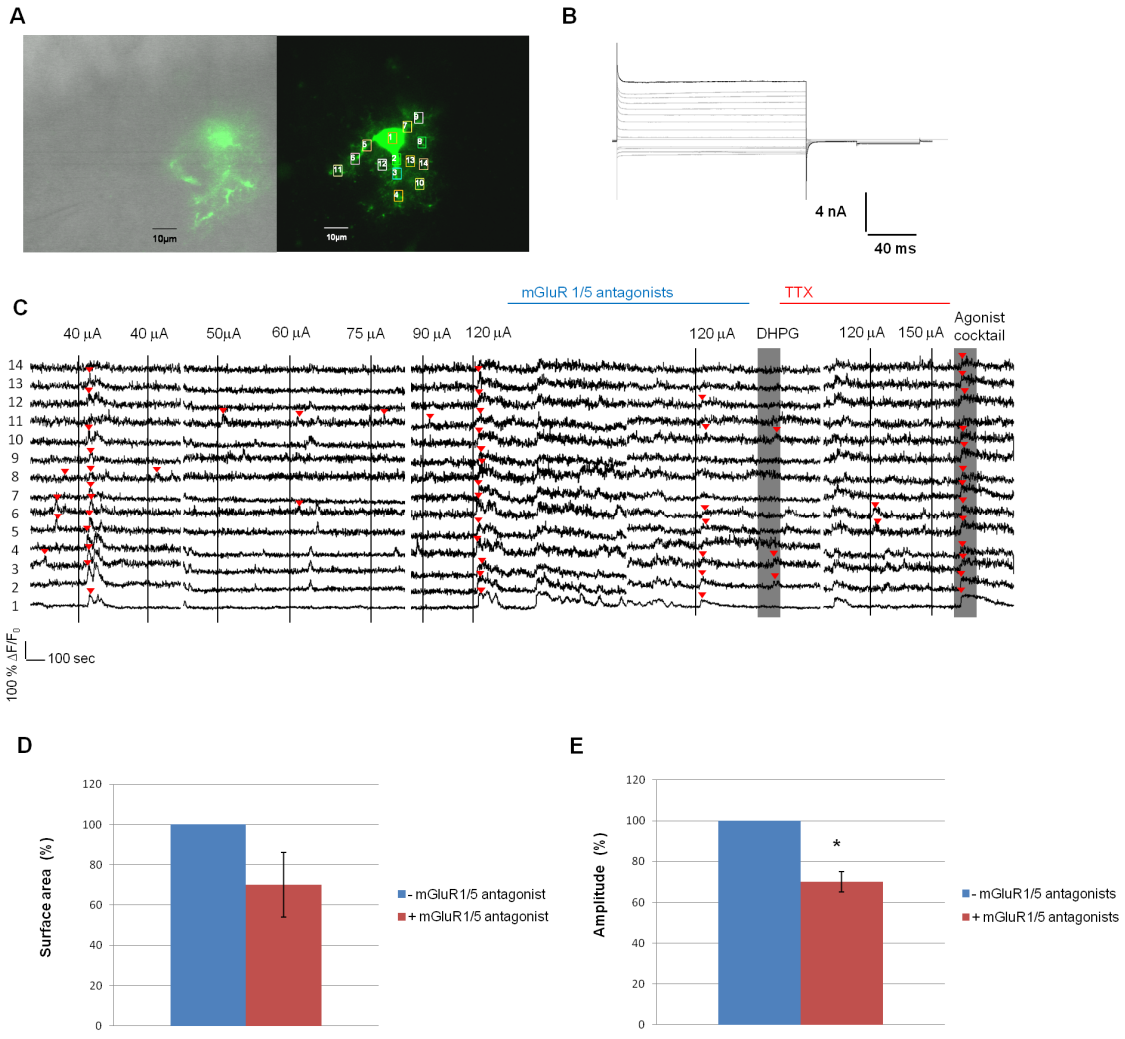
A
B
4 nA
40 ms
C
mGluR 1/5 antagonists
TTX
40 µA
40 µA
50µA
60 µA
75 µA
90 µA
120 µA
120 µA
DHPG
120 µA
150 µA
Agonist cocktail
100 % ΔF/F0
100 sec
D
Surface area (%)
- mGluR1/5 antagonist
+ mGluR1/5 antagonist
E
Amplitude (%)
*
- mGluR1/5 antagonists
+ mGluR1/5 antagonists

Figure 3.7

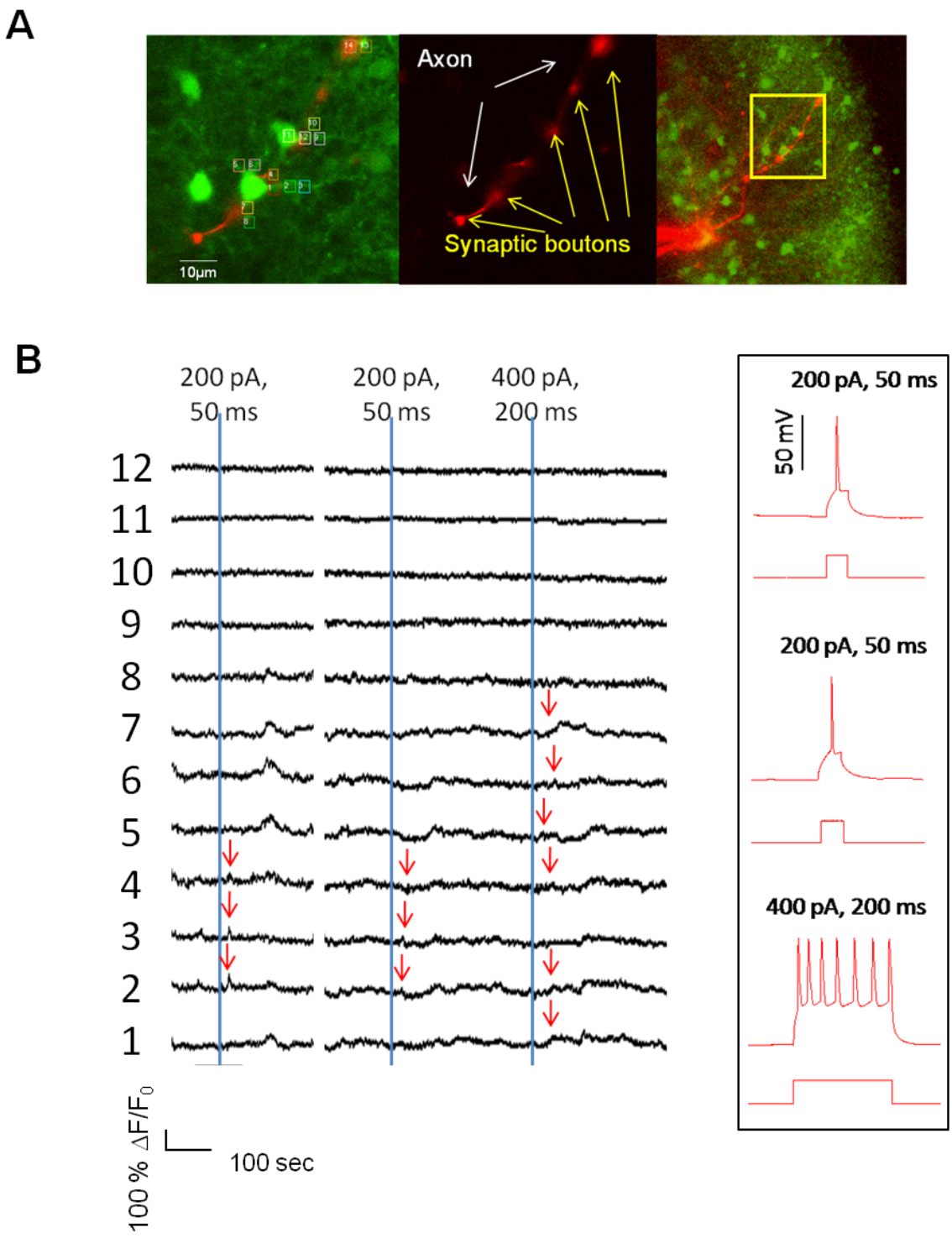
A
Axon
Synaptic boutons
10μm
B
200 pA, 50 ms
200 pA, 50 ms
400 pA, 200 ms
12
11
10
9
8
7
6
5
4
3
2
1
100 % ΔF/F0
100 sec
200 pA, 50 ms
50 mV
200 pA, 50 ms
400 pA, 200 ms

Figure 3.8

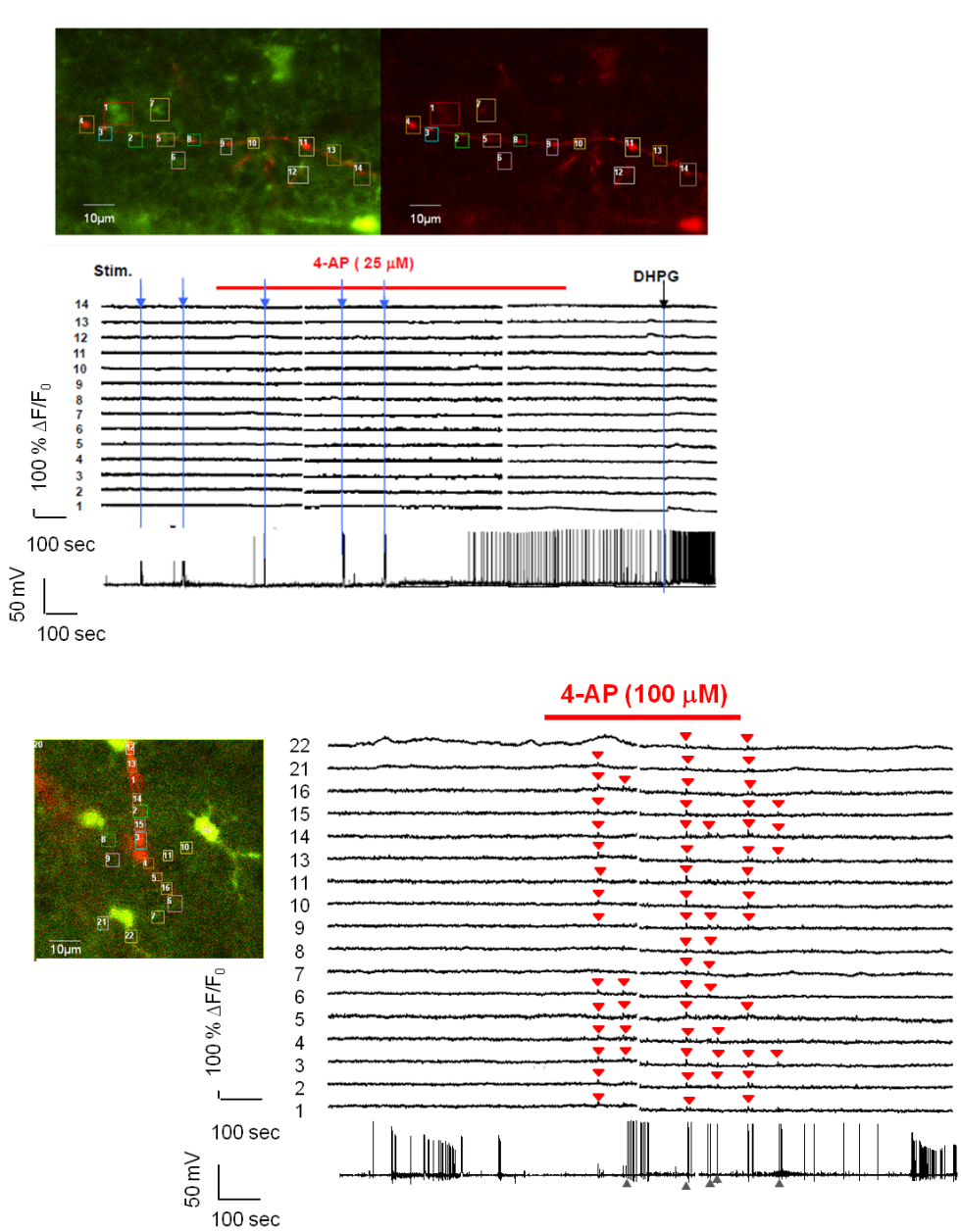
A
10μm
10μm
Stim.
4-AP (25 μM)
DHPG
100 % ΔF/F0
100 sec
50 mV
100 sec
B
4-AP (100 μM)
10μm
100 % ΔF/F0
100 sec
50 mV
100 sec

Figure 3.9

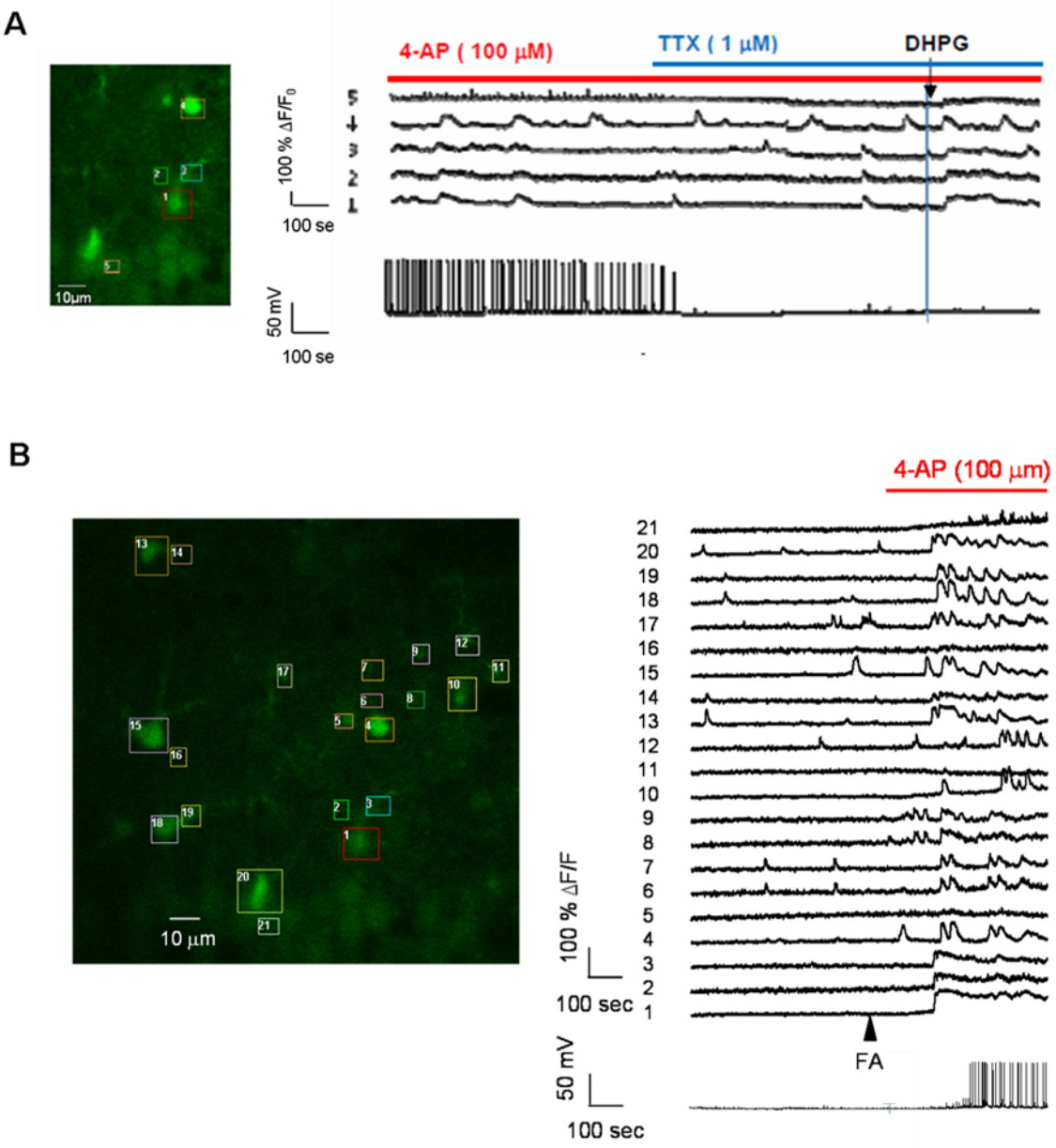
A
4-AP (100 µM)
TTX (1 µM)
DHPG
10µm
100 % ΔF/F0
100 se
50 mV
100 se
B
4-AP (100 µm)
10 µm
100 % ΔF/F
100 sec
50 mV
100 sec
FA

Chapter 4: Exploring the role for β-Arrestin2 in NMDA receptor-dependent long-term potentiation (LTP) and long-term depression (LTD)

4.1 Abstract

Dendritic spines are small protrusions expressed on the postsynaptic neuronal dendrites where they receive neurotransmitters released from excitatory synapses. Their morphology is regulated by filamentous actin (F-actin), whose turnover is accelerated by an actin-binding protein, cofilin, which has been implicated in modulating synaptic plasticity. Dephosphorylation of cofilin by N-methyl-D-aspartate (NMDA) receptor activation makes it functional and able to travel to dendritic spines, where it triggers spine and synapse remodeling. The fact that cofilin trafficking to spines is dependent on β-Arrestin2 suggests a direct involvement of β-Arrestin2 in regulating synaptic plasticity. In this study, we explored the impacts of β-Arrestin2 deficiency on two forms of NMDA receptor-dependent synaptic plasticity: long term potentiation (LTP) and long term depression (LTD), in knockout mice lacking *β-Arrestin2* gene expression. Our results revealed normal LTP, but significantly impaired LTD in mice lacking β-Arrestin2. This finding provides new insight concerning the role of β-Arrestin2 in regulating NMDA receptor-dependent synaptic plasticity.

4.2 Introduction

Dendritic spines, located on neuronal dendrites, are the main postsynaptic sites where numerous excitatory neurotransmitter receptors are expressed. They are small protrusions varying in morphology and are categorized as two immature forms (thin and stubby) and a mature mushroom form (Pontrello and Ethell, 2009). Their structures are rich in filamentous actin (F-actin) and are highly dynamic, exhibiting plasticity that is considered to be the underlying mechanism of learning and memory in the hippocampus (Yuste and Bonhoeffer, 2001). It has been well established that cofilin promotes F-actin turnover via binding and severing actin filaments, allowing the new barbed ends to be generated and reached by other actin monomers (Moriyama et al., 1990; Yahara et al., 1996; Carlier et al., 1997; Lappalainen and Drubin, 1997; Rosenblatt et al., 1997; Bamburg, 1999; Pontrello and Ethell, 2009). The alternation between F-actin depolarization and assembly facilitates spine remodeling and is thought to be regulated by activation of NMDA receptors - one of the ionotropic glutamate receptors involved in excitatory synaptic transmission.

Previous studies suggest that cofilin is dephosphorylated via calcineurin and PI3 kinase pathways in response to NMDAR activation (Wang et al., 2005). The dephosphorylated cofilin is functional and can be delivered to dendritic spines to modulate spine morphology. The translocation of cofilin to spines depends on the assistance from a scaffolding protein, β-Arrestin2 (Zoudilova et al., 2010), suggesting a role for β-Arrestin2 in dendritic spine remodeling. Interestingly, while hippocampal neurons lacking β Arrestin2 have shown normal spine development and maturation both

in vitro and *in vivo*, they lose the ability to undergo spine remodeling when exposed to NMDA (Pontrello 2011). Based on these findings, we proposed a hypothesis that β-Arrestin2 is involved in the two forms of NMDAR-dependent synaptic plasticity: LTP and LTD.

In this study, we tested the hypothesis using β-Arrestin2 knockout (KO) mice as a model system. Effects of LTP and LTD were measured in β-Arrestin2 KO mice hippocampal slices and were compared to those measured from wild-type, littermate control mice. Our results indicated no difference of LTP between both groups, but a significantly impaired LTD was observed in β-Arrestin2 KO mice. This finding suggests an essential role of β-Arrestin2 in regulating NMDAR-dependent LTD by facilitating cofilin-mediated F-actin turnover and spine remodeling.

4.3 Materials and methods

***Preparation of hippocampal slices*.**

All mice were housed in the animal facility at the University of California, Riverside in accordance with Institutional Animal Care and Use Committee guidelines. Mice aged 17-22 postnatal days old were anesthetized by isofluorane inhalation and decapitated. Brains were removed from the skull and immediately immersed in chilled dissection buffer containing the following (in mM): 87 NaCl, 2.5 KCl, 1.25 NaH_2PO_4, 25 $NaHCO_3$, 75 sucrose, 10 dextrose, 1.3 ascorbic acid, 7 $MgCl_2$, and 0.5 $CaCl_2$, bubbled with 95% O_2/ 5% CO_2. Transverse hippocampal slices (400 μm thick) were prepared from β-Arrestin2 KO and wt C57BL/6J mice using a Vibratome (Leica VT1200S). Slices were allowed to recover for 45 min in a 35°C submersion chamber filled with oxygenated

artificial cerebrospinal fluid (ACSF) containing the following (in mM): 125 NaCl, 2.5 KCl, 1.25 NaH_2PO_4, 26 $NaHCO_3$, 15 dextrose, 1.3 $MgCl_2$, and 2.5 $CaCl_2$. Following the incubation period at physiological temperature, slices were allowed to recover for an additional 2 hrs at room temperature and then transferred to a recording chamber, continuously superfused with oxygenated, room temperature ACSF.

Electrophysiology.

For LTP experiments, a previously-described protocol (Agulhon et al., 2010) was used. Briefly, extracellular field excitatory postsynaptic potentials (fEPSPs) were recorded in CA1 stratum radiatum 50 μm below the pyramidal cell layer with glass electrodes (1 MΩ) filled with ACSF. Stimuli were delivered to the commissural/Schaffer collateral afferents with a concentric bipolar electrode positioned parallel to the recording electrode 500 μm away. Input/output curves were generated by stepping the stimulation amplitude from 5 to 80/120 μA. The basal stimulation intensity for our experiments was set at 50% of the intensity that evoked maximal fEPSP amplitude, and was delivered at a frequency of 0.033 Hz. The half maximal intensity of stimulation ranged between 18 (lowest level) to 40 μA (highest level). After 15 min of stable baseline recording (< 5% drift), two trains of 1 sec, 100 Hz pulses were applied to induce LTP. LTP was sampled for 60 min after induction, and potentiation was calculated by dividing the average slope of 45-60 min post-induction responses with the average slope of 0–15 min pre-induction baseline responses. For LTD, a LFS consisting of 900 pairs of stimuli (distance 50 ms) at 1 Hz was used (Rust et al., 2010). LTD was sampled for 60 min after induction, and depression was calculated by dividing the average slope of 45-60 min post-induction

responses with the average slope of 0-15 min pre-induction baseline responses. Student's independent t-test was used to determine statistical significance between littermate control and β-Arrestin2 KO groups. P values ≤ 0.05 were considered significant.

4.4 Results

β-Arrestin2 KO mice exhibit normal LTP, but significantly impaired LTD, in acute hippocampal slices.

Since abnormal NMDAR-mediated dendritic spine plasticity was observed in the β-Arrestin2 KO mice, it raised the possibility that deletion of β-Arrestin2 would result in alteration of long-term synaptic plasticity. To address this hypothesis, we performed LTP and LTD experiments in acute hippocampal slices from littermate control and β-Arrestin2 KO mice. The LTP induction protocol consisted of two 1 s duration 100 Hz tetani of Schaffer collaterals (Agulhon et al., 2010). To our surprise, a potentiation of 150% of the field excitatory postsynaptic potentials (fEPSPs) was found in both groups following 60 minutes of high frequency stimulation, suggesting that β-Arrestin2 KO mice exhibit normal levels of LTP (Fig. 4A,B, $P > 0.1$). There were also no differences observed in input-output (I/O) curves between β-Arrestin2 KO and littermate control mice, an indication that basal pre- and postsynaptic responses are not altered by knockout of β-Arrestin2. (Fig. 4E).

Based on the findings in cultured hippocampal neurons, β-Arrestin2 KO mice failed to respond to NMDA-induced dendritic spine remodeling by exhibiting resistance

to spine head shrinkage, a mechanism that is associated with LTD (Beattie et al., 2000; Zhou et al., 2004). Furthermore, Rust et al. (2010) found in n-cofilin KO mice normal levels of LTP using this induction protocol but significantly altered LTD (Rust et al., 2010). Therefore, we next tested whether LTD is altered in the β-Arrestin2 KO mice using a similar protocol as Rust and coworkers. Paired-pulse low frequency stimulation (PP-LFS) at 1 Hz for 15 minutes was applied to Schaffer collateral-CA1 synapses to evoke LTD in slices from both wild-type and β-Arrestin2 KO groups. Interestingly, LTD was significantly impaired in β-Arrestin2 KO mice as only a 1.2 % depression was detected following 60 minutes of PP-LFS, compared to a 16.1 % depression observed in wild-type mice (Fig. 4C,D; *$p < 0.05$).

4.5 Discussion

Interestingly, significant differences were measured in LTD but not LTP in β-Arrestin2 KO mice compared to littermate controls. These effects on long-term synaptic plasticity were very similar to those observed by Rust et al. (2010) in n-cofilin KO mice. This is significant because data from Pontrello suggest that β-Arrestin2 acts by NMDAR-triggered localization of cofilin to dendritic spines to initiate spine remodeling (Pontrello, 2011). Rust et al. found no change in early-LTP (E-LTP) induced by a single 1 s, 100 Hz tetanus of Schaffer collaterals in acute hippocampal slices from β-Arrestin2 KO mice. Even though β-Arrestin2 KO mice were resistant to NMDA-induced dendritic spine shrinkage, they were still able to exhibit normal LTP, suggesting that alternate mechanisms may compensate for disrupted β-Arrestin2-mediated cofilin trafficking to

dendritic spines during LTP-induced spine remodeling. However, in terms of spine remodeling, generation of LTP is more likely to correlate with spine enlargement and stability (Chen et al., 2007; Bozdagi et al., 2010), whereas LTD tends to associate with spine shrinkage (Beattie et al., 2000; Zhou et al., 2004). This fits very well with our findings of normal LTP but almost completely absent LTD in β-Arrestin2 KO mice. Therefore, the inability of β-Arrestin2 KO mice to exhibit LTD corroborate findings from Pontrello (2011) indicating that β-Arrestin2 is essential for localization of cofilin to dendritic spines during NMDA induced spine remodeling (Pontrello, 2011).

Pontrello also observed deficient long-term spatial learning ability in β-Arrestin2 KO mice, which seems to conflict with our LTP data if LTP is considered the essential mechanism underlying hippocampal-mediated learning and memory (Pontrello et al., 2011). However, many transgenic and knockout mouse models have shown normal LTP effects but altered learning and memory phenotypes (Lee and Silva, 2009). Furthermore, Ge et al. (2010) recently demonstrated that an LTP-blocking NMDAR 2A antagonist had no significant effect on any aspect of spatial memory performance in a Morris water maze task in adult rats, whereas an LTD-blocking NMDAR2B antagonist impaired spatial memory consolidation (Ge et al., 2010). These findings suggest that in the present study, changes in LTD may underlie impaired spatial memory performance in β-Arrestin2 KO mice.

4.6 References

Agulhon C, Fiacco TA, McCarthy KD (2010) Hippocampal short- and long-term plasticity are not modulated by astrocyte Ca^{2+} signaling. Science 327:1250-1254.

Bamburg JR (1999) Proteins of the ADF/cofilin family: essential regulators of actin dynamics. Annu Rev Cell Dev Biol 15:185-230.

Beattie EC, Carroll RC, Yu X, Morishita W, Yasuda H, von Zastrow M, Malenka RC (2000) Regulation of AMPA receptor endocytosis by a signaling mechanism shared with LTD. Nat Neurosci 3:1291-1300.

Bozdagi O, Wang XB, Nikitczuk JS, Anderson TR, Bloss EB, Radice GL, Zhou Q, Benson DL, Huntley GW (2010) Persistence of coordinated long-term potentiation and dendritic spine enlargement at mature hippocampal CA1 synapses requires N-cadherin. J Neurosci 30:9984-9989.

Carlier MF, Laurent V, Santolini J, Melki R, Didry D, Xia GX, Hong Y, Chua NH, Pantaloni D (1997) Actin depolymerizing factor (ADF/cofilin) enhances the rate of filament turnover: implication in actin-based motility. J Cell Biol 136:1307-1322.

Chen LY, Rex CS, Casale MS, Gall CM, Lynch G (2007) Changes in synaptic morphology accompany actin signaling during LTP. J Neurosci 27:5363-5372.

Ge Y, Dong Z, Bagot RC, Howland JG, Phillips AG, Wong TP, Wang YT (2010) Hippocampal long-term depression is required for the consolidation of spatial memory. Proc Natl Acad Sci U S A 107:16697-16702.

Lappalainen P, Drubin DG (1997) Cofilin promotes rapid actin filament turnover in vivo. Nature 388:78-82.

Lee YS, Silva AJ (2009) The molecular and cellular biology of enhanced cognition. Nat Rev Neurosci 10:126-140.

Moriyama K, Matsumoto S, Nishida E, Sakai H, Yahara I (1990) Nucleotide sequence of mouse cofilin cDNA. Nucleic Acids Res 18:3053.

Pontrello CG, Ethell IM (2009) Accelerators, Brakes, and Gears of Actin Dynamics in Dendritic Spines. Open Neurosci J 3:67-86.

Pontrello CG (2011) The regulation of dendritic spine plasticity by EphB and N-methyl-D-aspartate receptors through spatial control over cofilin activity in mature hippocampal neurons. Ph.D. Thesis--University of California, Riverside.

Rosenblatt J, Agnew BJ, Abe H, Bamburg JR, Mitchison TJ (1997) Xenopus actin depolymerizing factor/cofilin (XAC) is responsible for the turnover of actin filaments in Listeria monocytogenes tails. J Cell Biol 136:1323-1332.

Rust MB, Gurniak CB, Renner M, Vara H, Morando L, Gorlich A, Sassoe-Pognetto M, Banchaabouchi MA, Giustetto M, Triller A, Choquet D, Witke W (2010) Learning, AMPA receptor mobility and synaptic plasticity depend on n-cofilin-mediated actin dynamics. EMBO J 29:1889-1902.

Wang Y, Shibasaki F, Mizuno K (2005) Calcium signal-induced cofilin dephosphorylation is mediated by Slingshot via calcineurin. J Biol Chem 280:12683-12689.

Yahara I, Aizawa H, Moriyama K, Iida K, Yonezawa N, Nishida E, Hatanaka H, Inagaki F (1996) A role of cofilin/destrin in reorganization of actin cytoskeleton in response to stresses and cell stimuli. Cell Struct Funct 21:421-424.

Yuste R, Bonhoeffer T (2001) Morphological changes in dendritic spines associated with long-term synaptic plasticity. Annu Rev Neurosci 24:1071-1089.

Zhou Q, Homma KJ, Poo MM (2004) Shrinkage of dendritic spines associated with long-term depression of hippocampal synapses. Neuron 44:749-757.

Zoudilova M, Min J, Richards HL, Carter D, Huang T, DeFea KA (2010) beta-Arrestins scaffold cofilin with chronophin to direct localized actin filament severing and membrane protrusions downstream of protease-activated receptor-2. J Biol Chem 285:14318-14329.

Figure Legends

Figure 4 β-Arrestin2 KO mice exhibit normal baseline synaptic function and LTP, but significantly impaired LTD compared to wild-type mice.

(A) LTP of Schaffer collateral-CA1 synapses evoked by two trains of high-frequency stimulation (HFS, 100 Hz pulses at 1 s duration) was unaltered in β-Arrestin2 KO mice compared to wild-type mice.

(B) Both groups expressed ~40% potentiation at 45-60 min following HFS (n = 7 for wild-type mice and 7 for β-Arrestin2 KO mice, $P > 0.1$).

(C) LTD of Schaffer collateral-CA1 synapses evoked by paired-pulse LFS (PP-LFS) at 1 Hz for 15 min was significantly reduced in β-Arrestin2 KO mice compared to wild-type mice.

(D) β-Arrestin2 KO mice expressed ~1.2 % depression compared to the 16.1% from the wild-type mice at 45-60 min following PP-LFS (n = 9 for wild-type mice and 10 for β-Arrestin2 KO mice, $*p = 0.027$).

(E) Basal synaptic transmission is normal in Schaffer collateral-CA1 synapses of β-Arrestin2 KO mice (n = 17 for wild-type mice and 15 for β-Arrestin2 KO mice).

Figure 4

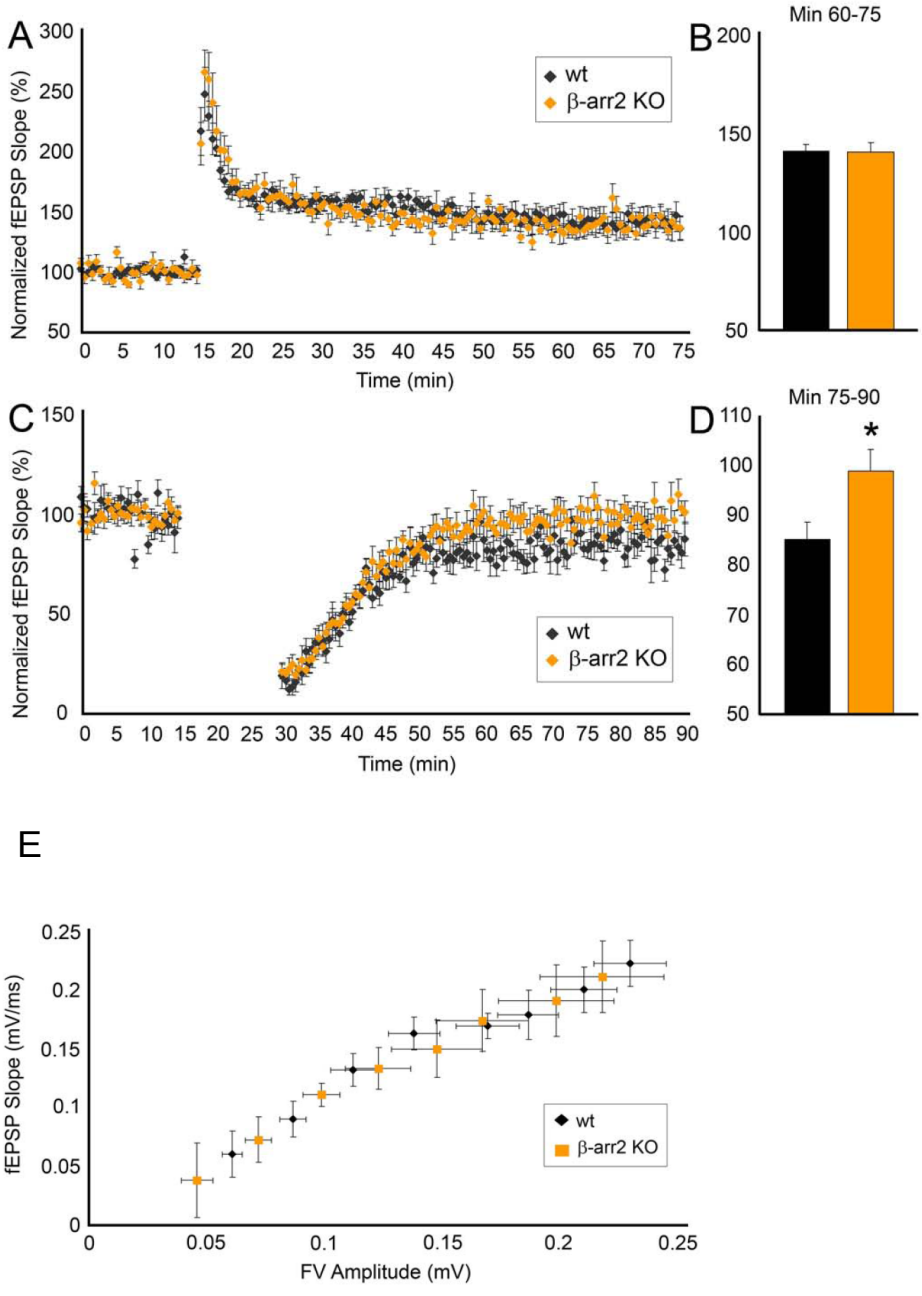
A
Normalized fEPSP Slope (%)
Time (min)
wt
β-arr2 KO
B
Min 60-75
C
Normalized fEPSP Slope (%)
Time (min)
wt
β-arr2 KO
D
Min 75-90
*
E
fEPSP Slope (mV/ms)
FV Amplitude (mV)
wt
β-arr2 KO

Chapter 5: Discussion and Perspective

5.1 The function of astrocyte Gq GPCR activity in neurophysiology

In this study, we have shown that astrocytes exhibit spontaneous Gq GPCR activity, some of which appears to be driven by spontaneous miniature neurotransmitter release (Chapter 2). Moreover, stimulating Schaffer collateral afferents using low levels of intensity (7 - 150 μA) and frequency (single or three pulses) elicits astrocytic Gq GPCR-driven Ca^{2+} elevations, most of which have larger areas compared to spontaneous events and propagate to the cell body (Chapter 3). These data provide clear evidence that "astrocytes listen to neuronal conversation *in situ*" (Agulhon et al., 2008), and astrocytes could be even more sensitive sensors of neuronal signals than previously thought. Our findings give rise to a very interesting question: What is the function of neuron-to-astrocyte Gq GPCR signaling in neurophysiology? A model that has been proposed in recent years is the concept of "gliotransmission", which states that astrocytes talk back to neurons by releasing gliotransmitters in a Ca^{2+}-dependent manner to modulate neuronal activity as well as modify synaptic strength (Agulhon et al., 2008; Barres, 2008; Hamilton and Attwell, 2010). It has been widely observed that astrocytes release transmitters (glutamate, D-serine and ATP, reviewed in Chapter 1) under particular conditions. A recently-proposed theory that seems appealing argues that gliotransmitters are released via a Ca^{2+}-dependent mechanism. This model is supported by studies in hippocampal Schaffer Collateral (SC)-CA1 pyramidal neuron synapses (SC-CA1 synapse) showing that uncaging IP_3 or Ca^{2+} elicits glutamate release from astrocytes, which in turn regulates presynaptic neuronal activity (Fiacco and McCarthy, 2004; Perea and Araque,

2007). Moreover, the SC-evoked astrocytic Ca^{2+} responses have been found to elicit ATP release, which then breaks down to adenosine and binds/activates the presynaptic adenosine receptors (A1Rs), thus suppressing glutamate release from presynaptic terminals (Pascual et al., 2005; Serrano et al., 2006). Furthermore, studies reported that astrocytes *in situ* release glutamate in response to mGluR-mediated Ca^{2+} elevations, which then evoked slow inward currents (SICs) in postsynaptic neurons via activation of extrasynaptic NR2B subtype NMDA receptors (Angulo et al., 2004; Fellin et al., 2004). Based on these findings, astrocyte Ca^{2+} elevations were considered 'necessary and sufficient' to trigger gliotransmitter release from astrocytes, which in turn evokes SICs in postsynaptic neurons (Fellin and Carmignoto, 2004). Moreover, it has been reported that astrocytes release transmitters through mechanisms of Ca^{2+}-dependent vesicular exocytosis, as release of transmitters was blocked in the presence of tetanus toxin (TeNT) or botulinum B (BoNT), two drugs that disrupt vesicle exocytosis (Jourdain et al., 2007; Perea and Araque, 2007).

This model, however, has been challenged by findings that conflict with the results described above. Shigetomi et al in 2008 reported different effects of activating protease-activated receptor 1 (PAR-1) versus P2Y1 purinergic receptors on neuronal activity, even if astrocytic Ca^{2+} responses were elicited in both cases. Activation of PAR-1 resulted in SICs in 60% of CA1 neurons, whereas no SICs were detected following P2Y1 receptor activation (Shigetomi et al., 2008). These findings suggest that increasing astrocytic Ca^{2+} is not guaranteed to modulate neuronal activity. In support of this interpretation were findings from studies using transgenic mouse models. In mice that

express MrgA1 receptors (MrgA1Rs, a type of Gq GPCR) exclusively in astrocytes, selectively eliciting astrocytic Ca^{2+} responses using the ligand for MrgA1Rs did not change the frequency or amplitude of miniature EPSCs (mEPSCs), suggesting unaffected pre-and postsynaptic neuronal activity (Fiacco et al., 2007). Similar to this finding, no effects on SC-CA1 synaptic transmission was observed in mice lacking IP_3R2 expression, in which astrocytic Ca^{2+} activity was fully abolished (Petravicz et al., 2008).

Given the discrepancy arising from previous reports concerning the involvement of astrocytic Ca^{2+} increases in gliotransmission, the underlying mechanisms for astrocytic-mediated gliotransmitter release still remain controversial. In fact, we have found it very difficult to believe that astrocytes behave as similar as neurons in terms of releasing transmitters. Given that astrocytes do not express voltage-gated Ca^{2+} channels (Carmignoto et al., 1998) see also chapter 3), the kinetics of astrocytic Ca^{2+} elevations in response to afferent stimulation are significantly slower compared to neuronal Ca^{2+} elevations. Instead of having a latency in milliseconds such as neuronal iGluR-driven Ca^{2+} elevations (Bloodgood and Sabatini, 2007), astrocyte Ca^{2+} elevations occur with a latency of seconds as shown *in vivo* (Wang et al., 2006; Dombeck et al., 2007; Bekar et al., 2008; Schummers et al., 2008). Our *in situ* study also revealed a significantly longer latency of astrocytic Ca^{2+} responses to SC stimulation compared to astrocytic glutamate transporter currents (GTC) or neuronal fEPSPs (Fig. 5A). A future experiment will be performed by simultaneously recording astrocytic GTCs and Ca^{2+} responses simultaneously within the same astrocyte to further define the slow response times of astrocytic Gq GPCR-driven Ca^{2+} elevations (Fig. 5B).

There is no question that astrocytes release transmitters under certain conditions (reviewed in Agulhon et al., 2008; Hamilton and Attwell, 2010; see also Chapter 1). However, the correlation between activation of astrocytic Gq GPCRs and gliotransmitter release needs to be further elucidated. An alternative possibility would be to consider downstream signaling molecules other than Ca^{2+} to be involved in Gq GPCR-mediated functional regulation of astrocytes. Activation of astrocytic Gq GPCRs results in not only a rise of intracellular Ca^{2+}, but also activation of a vast array of other signaling molecules. The role of protein kinase C (PKC) in modulating astrocyte function in response to neuronal activity should also be considered. It has been found in Purkinje neurons in the cerebellum and cultured astrocytes that PKC activation plays an essential role in regulating the function of glutamate transporters via phosphorylation (Casado et al., 1993; Aronica et al., 2003; Shen and Linden, 2005; Susarla and Robinson, 2008). Therefore, these findings raise the possibility that activation of astrocytic Gq GPCRs modulates astrocyte glutamate uptake via activation of PKC. This hypothesis has indeed been tested and proven in a recent study from our lab, where a marked potentiation in amplitude of glutamate transporter current has been detected following high frequency SC stimulation-evoked astrocytic Gq GPCR activation. This HFS-evoked potentiation of astrocytic glutamate uptake was shown to be group I mGluR-dependent, and was not observed when PKC inhibitor was delivered into the astrocyte (Devaraju, 2011). These findings suggest that activation of astrocytic Gq GPCRs following elevated neuronal activity can modulate astrocyte glutamate uptake, thus removing excess glutamate in the extracellular space. As previous work suggests that neuronal activity regulates expression and activity

of astrocyte glutamate transporters, our findings open up numerous possibilities for how glutamate uptake might be modulated by neuron-to-astrocyte Gq GPCR communication. Miniature release of transmitter might be essential for maintenance of appropriate expression levels of glutamate transporters and uptake by astrocytes, while spatially- and temporally summated neuronal action potentials may be critical for the rapid potentiation of astrocyte glutamate uptake. Modulation of astrocyte glutamate uptake is also very important as it provides a critical role for astrocytes in the progress of certain brain disorders including epilepsy, in which neurons suffer from hyperactivity due to excessive stimulation of glutamatergic receptors.

5.2 Effects of miniature neurotransmitter release on spontaneous astrocytic Ca^{2+} elevations

One of the most interesting findings from Results presented in Chapter 2 is the effect of miniature neurotransmitter release on astrocytic Ca^{2+} elevations. As we have discussed, this finding conflicts with previous findings which demonstrate the persistence of cell soma astrocyte Ca^{2+} oscillations after incubation in Bafilomycin A1 and TTX (Nett et al., 2002; Parri and Crunelli, 2003) see also Chapter 2). An additional experiment to corroborate our findings that Bafilomycin A1 reduces astrocytic microdomain Ca^{2+} activity is to increase vesicular fusion in TTX using high sucrose ACSF. Elevated sucrose is a known secretagogue for increasing fusion of readily releasable vesicles (Rosenmund and Stevens, 1996; Di Castro et al., 2011). This would add strength to our findings by demonstrating that spontaneous astrocytic Gq GPCR activity is bidirectionally regulated by the direction of miniature neurotransmitter release. This result would provide more

convincing evidence demonstrating the effects of miniature neurotransmitter release on spontaneous astrocytic Ca^{2+} elevations, and is high on our list of future experiments.

5.3 Plasticity of astrocytic Gq GPCRs

In Chapter 3, we have shown that astrocytes respond to single or three pulse SC stimulation with Ca^{2+} elevations. During the course of these experiments, we did notice a nonsignificant trend of increased frequency of spontaneous astrocytic Ca^{2+} elevations over time. Interestingly, a similar phenomenon has been reported by Pasti et al. (1997). They observed an increased frequency of astrocyte Ca^{2+} transients over time after repetitive episodes of neuronal stimulation as well as repetitive stimulation with a metabotropic glutamate receptor agonist (Pasti et al., 1997). Based on these results, it raises the possibility that astrocytic Gq GPCRs could potentially exhibit use-dependent plasticity. Plasticity of astrocytic Gq GPCR signaling might be important to ensure sufficient glial coverage of active synapses and uptake of synaptically released glutamate. This hypothesis will be tested in future studies by taking the advantage of the MrgA1R transgenic mice. Since MrgA1Rs are exclusively expressed in astrocytes, and the ligand for MrgA1Rs - FMRF - does not simulate endogenous receptors in brain, Gq GPCR signaling cascades can be selectively activated in astrocytes without directly affecting the activity of nearby neurons. The most appropriate strategy for this experiment is to uncage FMRF in a local area of astrocytic processes to elicit Ca^{2+} responses, and to assay for changes in the amplitude or areas of propagation after repetitive stimulation of the same MrgA1R microdomain. Moreover, it has been shown that each astrocyte displays a unique "Ca^{2+} signature", where the initiation sites of Ca^{2+} elevations are consistent upon

activation of the same or different astrocytic Gq GPCRs (Yagodin et al., 1994; Fiacco et al., 2007); reviewed in Chapter 1). The initiation sites of the Gq GPCR signaling domains - the “hotspots”- are thought to be areas with a higher density of Gq GPCR expression. Therefore, it is very likely that the expression levels of Gq GPCRs can be potentiated or depressed in response to changes in local synaptic strength. One of our future plans is to test this hypothesis by bath-applying FMRF or DHPG to figure out the Ca^{2+} signature for a specific astrocyte. We will then uncage FMRF repetitively over a local area of the astrocyte which initially does not appear to be a hotspot. After this repetitive stimulation, FMRF or DHPG will be bath-applied again to evoke the Ca^{2+} signature for this particular astrocyte, and the pattern of the Ca^{2+} initiation sites will be compared before and after repetitive uncaging of FMRF. These data will help us to determine whether astrocytic Gq GPCRs exhibit plasticity in a synapse-specific manner. This hypothesis, once supported, will provide a better understanding of the plasticity of astrocytic receptors and enrich our understanding of neuron-to-astrocyte communication.

5.4 References

Agulhon C, Petravicz J, McMullen AB, Sweger EJ, Minton SK, Taves SR, Casper KB, Fiacco TA, McCarthy KD (2008) What is the role of astrocyte calcium in neurophysiology? Neuron 59:932-946.

Angulo MC, Kozlov AS, Charpak S, Audinat E (2004) Glutamate released from glial cells synchronizes neuronal activity in the hippocampus. J Neurosci 24:6920-6927.

Aronica E, Gorter JA, Ijlst-Keizers H, Rozemuller AJ, Yankaya B, Leenstra S, Troost D (2003) Expression and functional role of mGluR3 and mGluR5 in human astrocytes and glioma cells: opposite regulation of glutamate transporter proteins. Eur J Neurosci 17:2106-2118.

Barres BA (2008) The mystery and magic of glia: a perspective on their roles in health and disease. Neuron 60:430-440.

Bekar LK, He W, Nedergaard M (2008) Locus coeruleus alpha-adrenergic-mediated activation of cortical astrocytes in vivo. Cereb Cortex 18:2789-2795.

Bloodgood BL, Sabatini BL (2007) Ca^{2+} signaling in dendritic spines. Curr Opin Neurobiol 17:345-351.

Carmignoto G, Pasti L, Pozzan T (1998) On the role of voltage-dependent calcium channels in calcium signaling of astrocytes in situ. J Neurosci 18:4637-4645.

Casado M, Bendahan A, Zafra F, Danbolt NC, Aragon C, Gimenez C, Kanner BI (1993) Phosphorylation and modulation of brain glutamate transporters by protein kinase C. J Biol Chem 268:27313-27317.

Devaraju P (2011) Gq G Protein Coupled Receptor Mediated Potentiation of Astrocytic Glutamate Uptake. Ph.D. Thesis—University of California, Riverside.

Di Castro MA, Chuquet J, Liaudet N, Bhaukaurally K, Santello M, Bouvier D, Tiret P, Volterra A (2011) Local Ca^{2+} detection and modulation of synaptic release by astrocytes. Nat Neurosci 14:1276-1284.

Dombeck DA, Khabbaz AN, Collman F, Adelman TL, Tank DW (2007) Imaging large-scale neural activity with cellular resolution in awake, mobile mice. Neuron 56:43-57.

Fellin T, Carmignoto G (2004) Neurone-to-astrocyte signalling in the brain represents a distinct multifunctional unit. J Physiol 559:3-15.

Fellin T, Pascual O, Gobbo S, Pozzan T, Haydon PG, Carmignoto G (2004) Neuronal synchrony mediated by astrocytic glutamate through activation of extrasynaptic NMDA receptors. Neuron 43:729-743.

Fiacco TA, McCarthy KD (2004) Intracellular astrocyte calcium waves in situ increase the frequency of spontaneous AMPA receptor currents in CA1 pyramidal neurons. J Neurosci 24:722-732.

Fiacco TA, Agulhon C, Taves SR, Petravicz J, Casper KB, Dong X, Chen J, McCarthy KD (2007) Selective stimulation of astrocyte calcium in situ does not affect neuronal excitatory synaptic activity. Neuron 54:611-626.

Hamilton NB, Attwell D (2010) Do astrocytes really exocytose neurotransmitters? Nat Rev Neurosci 11:227-238.

Jourdain P, Bergersen LH, Bhaukaurally K, Bezzi P, Santello M, Domercq M, Matute C, Tonello F, Gundersen V, Volterra A (2007) Glutamate exocytosis from astrocytes controls synaptic strength. Nat Neurosci 10:331-339.

Nett WJ, Oloff SH, McCarthy KD (2002) Hippocampal astrocytes in situ exhibit calcium oscillations that occur independent of neuronal activity. J Neurophysiol 87:528-537.

Parri HR, Crunelli V (2003) The role of Ca^{2+} in the generation of spontaneous astrocytic Ca^{2+} oscillations. Neuroscience 120:979-992.

Pascual O, Casper KB, Kubera C, Zhang J, Revilla-Sanchez R, Sul JY, Takano H, Moss SJ, McCarthy K, Haydon PG (2005) Astrocytic purinergic signaling coordinates synaptic networks. Science 310:113-116.

Pasti L, Volterra A, Pozzan T, Carmignoto G (1997) Intracellular calcium oscillations in astrocytes: a highly plastic, bidirectional form of communication between neurons and astrocytes in situ. J Neurosci 17:7817-7830.

Perea G, Araque A (2007) Astrocytes potentiate transmitter release at single hippocampal synapses. Science 317:1083-1086.

Petravicz J, Fiacco TA, McCarthy KD (2008) Loss of IP3 receptor-dependent Ca^{2+} increases in hippocampal astrocytes does not affect baseline CA1 pyramidal neuron synaptic activity. J Neurosci 28:4967-4973.

Rosenmund C, Stevens CF (1996) Definition of the readily releasable pool of vesicles at hippocampal synapses. Neuron 16:1197-1207.

Schummers J, Yu H, Sur M (2008) Tuned responses of astrocytes and their influence on hemodynamic signals in the visual cortex. Science 320:1638-1643.

Serrano A, Haddjeri N, Lacaille JC, Robitaille R (2006) GABAergic network activation of glial cells underlies hippocampal heterosynaptic depression. J Neurosci 26:5370-5382.

Shen Y, Linden DJ (2005) Long-term potentiation of neuronal glutamate transporters. Neuron 46:715-722.

Shigetomi E, Bowser DN, Sofroniew MV, Khakh BS (2008) Two forms of astrocyte calcium excitability have distinct effects on NMDA receptor-mediated slow inward currents in pyramidal neurons. J Neurosci 28:6659-6663.

Susarla BT, Robinson MB (2008) Internalization and degradation of the glutamate transporter GLT-1 in response to phorbol ester. Neurochem Int 52:709-722.

Wang X, Lou N, Xu Q, Tian GF, Peng WG, Han X, Kang J, Takano T, Nedergaard M (2006) Astrocytic Ca^{2+} signaling evoked by sensory stimulation in vivo. Nat Neurosci 9:816-823.

Yagodin SV, Holtzclaw L, Sheppard CA, Russell JT (1994) Nonlinear propagation of agonist-induced cytoplasmic calcium waves in single astrocytes. J Neurobiol 25:265-280.

Figure Legend

Figure 5 Experimental design for simultaneous recording of astrocytic glutamate transporter currents and Ca^{2+} elevations following high frequency SC stimulation.

(A) Latency of fEPSPs (recorded in CA1 pyramidal neurons following 0.033 Hz SC stim.), astrocyte glutamate transporter currents (Devaraju, 2011) and Ca^{2+} elevations (both recorded in astrocytes following 100-200 Hz SC stim.) are compared (n = 5 cells for each group; ***$p < 0.001$).

(B) With the patch pipette left on an OGB-1 filled astrocyte, glutamate transporter currents and Ca^{2+} responses can be recorded simultaneously following high frequency SC stimulation.

Figure 5

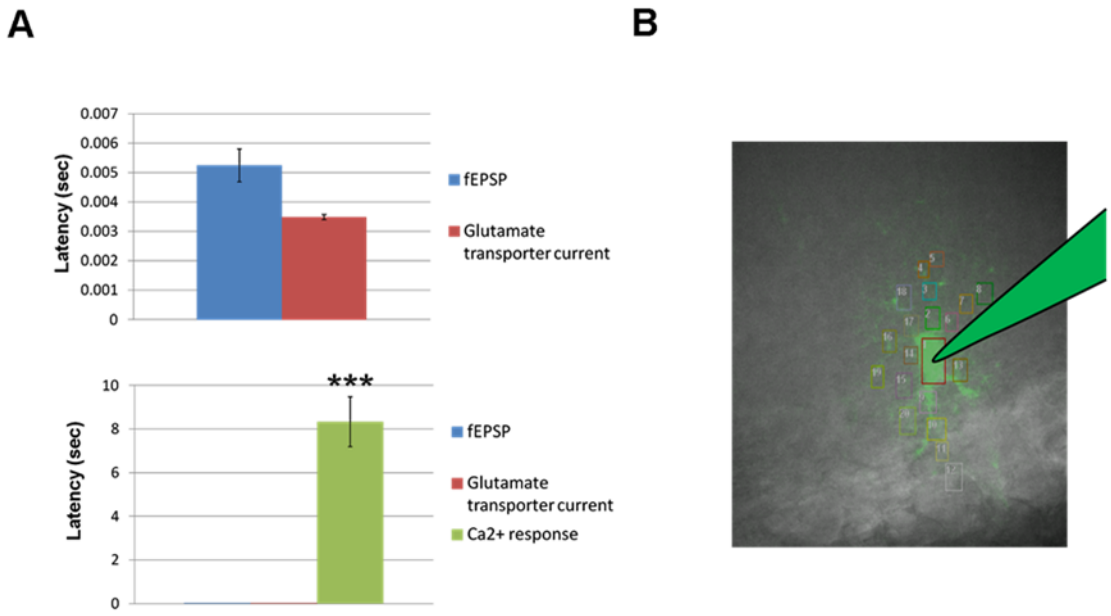
A
B
0.007
0.006
0.005
0.004
0.003
0.002
0.001
0
Latency (sec)
fEPSP
Glutamate transporter current
***
10
8
6
4
2
0
Latency (sec)
fEPSP
Glutamate transporter current
Ca2+ response